

**Woods Hole
Oceanographic
Institution**



***Tidal Circulation and Flushing Characteristics
of the Nauset Marsh System***

Report to the Town of Orleans

by

David G. Aubrey, George Voulgaris, Wayne D. Spencer
and Stephen P. O'Malley

July 1997

Technical Report

Funding was provided by the Town of Orleans, the National Park Service
and the Andrew W. Mellon Foundation

Approved for public release; distribution unlimited.

19970924 028

DTIC QUALITY INSPECTED 4

WHOI-97-11

**Tidal Circulation and Flushing Characteristics
of the
Nauset Marsh System**

**Report to the Town of Orleans
June 1997**

**David G. Aubrey, George Voulgaris, Wayne D. Spencer and
Stephen P. O'Malley**

**Department of Geology and Geophysics
Woods Hole Oceanographic Institution
Woods Hole, MA 02543**


Technical Report

Funding was provided by the Town of Orleans, the National Park Service
and the Andrew W. Mellon Foundation.

Reproduction in whole or in part is permitted for any purpose of the United States Government.
This report should be cited as Woods Hole Oceanographic Inst. Tech. Rept., WHOI-97-11.

Approved for public release; distribution unlimited.

Approved for Distribution



William B. Curry, Chairman
Department of Geology and Geophysics

EXECUTIVE SUMMARY

Various interested bodies (i.e., National Park Service, Cape Cod Commission, and the Town of Orleans) charged with management of the Nauset Marsh system on Cape Cod, MA, commissioned a study of the estuarine circulation within the Nauset system. Recent significant morphological changes in the system have changed mixing processes and residence times for the embayment. This study specifically addressed the differing water circulation and residence times arising from a migrating single inlet (dominant condition) and dual inlet (1992-1996) situations. These residence times are to be used by the Cape Cod Commission to identify nitrogen-sensitive sub-embayments based on various assumptions of build-out and nutrient loading. The Nauset Marsh system has experienced considerable development in recent years; proper management of this resource area requires knowledge of the consequences of such development.

Application of field observations of bathymetry, sea surface elevation, temperature, salinity and currents, leads to better understanding the physics of the system. These data, analyzed in various forms, served as input data for a numerical, two-dimensional circulation model of the embayment. The circulation model provided flow and discharge data with which the residence times were calculated. Bathymetric measurements defined the volumes of the various sub-embayments to be used in the calculation of residence times.

Residence times were calculated for six sub-embayments of the system, defined on the basis of their common hydrodynamic and morphologic characteristics. Two scenarios were evaluated: one for the present single-inlet system, which is near typical for most system states, and one for a dual inlet system such as existed for a period of time from 1992 through 1996.

Residence times were evaluated for twelve cases, to demonstrate the range of residence times that can be defined based on varying assumptions. For instance, residence times can be defined on the basis of mean low water volumes or mean water levels, the latter being the more conservative (yielding a longer residence time). In addition, residence times depend on whether spring tides, neap tides, or average tidal conditions are used. We provide data on all three conditions: the neap tidal case is the most conservative in the sense of providing a longer residence time. This case can serve as the basis for flushing if conservatism is desired. Finally, residence time can be defined based on the amount of time it takes for water to renew itself with water from adjacent sub-embayments, or more conservatively assuming renewal from the offshore waters (which are presumed to be cleaner).

Based on these various inputs, assumptions and calculations, residence times for Salt and Mill ponds under conditions of a single inlet are the longest of the various sub-embayments. Town Cove is still relatively quickly renewed, though not as fast as the main channels serving the system.

Flow pattern under dual-inlet condition does seem to be partitioned well, with the northern inlet serving the northern part of the system and the southern inlet serving the southern part of the system, with little hydrodynamic communication between the two divisions. This

new hydrodynamic behavior results in shorter residence times under dual inlets than under a single inlet.

Calculations indicate that the slowest flushing occurs in Mill and Salt ponds. The main body of the embayment, consisting of narrow channels between well-flushed salt marsh and tidal flats, flushes rapidly. Two-dimensional calculations show that Town Cove also flushes relatively rapidly, on average. However, its greater depth and occasional temperature stratification create conditions which might accumulate nutrients in bottom sediments, which, when released, can cause decrease in water quality (such as plankton blooms). A more sophisticated low-trophic level ecosystem model combined with vertical hydrodynamic structure could clarify the dynamics of this process.

This study provides a defensible basis for evaluating nutrient loading and potential eutrophication arising from development in the watershed around Nauset embayment. However, since morphological changes occur on a rapid basis in this area, the issue of residence time should be re-examined periodically. For instance, rapid onshore migration of the southern barrier beach is threatening closure of the south channel, a condition which could adversely affect water quality in Nauset Harbor in the near future. A process should be established to examine the sensitivity of residence times for rapidly changing morphology.

TABLE OF CONTENTS

	Page Number
Executive Summary	i
List of Figures	iv
List of Tables	vii
Introduction	1
Definition of Residence Time	4
Field Measurements	5
Tide Recordings	6
Bathymetry	9
Conductivity, Temperature, Depth Profiling and ADCP	9
Measurement Results	13
Bathymetry	13
Tidal Analysis and Prediction	13
CTD & ADCP Results	18
Hydrodynamic Modeling	23
Model Identification	23
Model Theory	23
Model Setup	25
Finite Element Grid Development	25
Boundary Conditions	28
Model Calibration Procedures and Results	28
Model Results and Residence Times	33
Hydrodynamics and Water Circulation	33
Residence Times	36
Conclusions and Recommendations	45
Acknowledgments	47
References	48
Appendices	
Appendix I: Results of Harmonic Analyses	50
Appendix II: RMA-2V Governing Equations	58
Appendix III: Vector Diagram Maps for Water Circulation	61
Appendix IV: CTD Profiles	72

LIST OF FIGURES

	Page
Figure 1: General location map for Nauset embayment.	2
Figure 2: Location of tide-gauge stations during the April - May, 1996 deployment. Filled circles indicate gauges having partial data recovery whereas open symbols denote gauges having no data recovery.	7
Figure 3: Location of tide-gauge stations deployed during October-December, 1996. Data from these stations were used for tidal analysis and calibration of the hydrodynamic model. Open symbols (i.e., PTL#4 and PTL#6) denote stations that failed to operate.	8
Figure 4: Location of track lines for bathymetric surveying.	10
Figure 5: Location of tide-gauge stations used for the tidal correction of the bathymetric data. Circles denote stations operational during the bathymetric survey whereas squares denote stations for which tidal elevation data were predicted based on measurements obtained by Aubrey and Speer (1985).	11
Figure 6: Location map of CTD casts and ADCP current measuring stations.	12
Figure 7: Time-series of sea surface elevation as collected during the October - December, 1996 deployment using the PTLC instruments. Elevation is referenced to NGVD of 1927.	14
Figure 8: (a) Time-series of recorded sea surface elevation from Salt Pond tide gauge of the National Park Service. (b) Time-series of predicted sea surface elevation in Salt Pond using the result of the tidal analysis of the raw record (a).	15
Figure 9: Time-series of predicted sea surface elevation at the PTLC deployment locations.	17
Figure 10: Tidal distortion indices as a function of distance into the estuary (abscissa) for the main (solid line, filled symbols) and North channels (dashed line, open symbols), respectively: (a) ratio of amplitudes of the M_4 and the M_2 tidal constituents; (b) tidal amplitude variation for the M_4 (squares) and M_2 (circles) tidal constituents; and (c) phase variation in degrees.	19
Figure 11: Tidal variation of depth-averaged water temperature calculated from the CTD measurements at stations A to F. Bottom panel: predicted oceanic sea surface elevation.	20

	Page
Figure 12: Tidal variation of depth-averaged water salinity calculated from the CTD measurements at stations A to F. Bottom panel: predicted oceanic sea surface elevation.	21
Figure 13: Tidal variation of depth-averaged water density calculated from the temperature (Fig. 11) and salinity (Fig. 12) measurements. Bottom panel: predicted oceanic sea surface elevation.	22
Figure 14: Depth-averaged current speed calculated from ADCP measurements at stations A to F. The predicted ocean sea surface elevation is also shown at the bottom as a reference.	24
Figure 15: Finite element grid for the case of a single inlet. It consists of 4331 nodes and 1320 elements.	26
Figure 16: RMA-2V Finite element grid for the case of dual inlets. It consists of 4483 nodes and 1381 elements.	27
Figure 17: Model Calibration. Sea surface elevations: measured (solid line) versus predicted by the hydrodynamic model (dashed line).	30
Figure 18: Model Calibration. Sea surface elevations: measured (solid line) versus predicted by the hydrodynamic model (dashed line).	31
Figure 19: Intercomparison of depth-averaged current speeds: measured (solid circles) versus predicted by the model (solid line). The forcing tide is also shown for reference.	32
Figure 20: Example of the current velocity results, during the flood stage of the tide, obtained by application of the model. One vector is shown for each node of the finite element grid; the length of the vector represents the magnitude of current velocity (in m/s). Appendix III contains more examples of model simulations.	34
Figure 21: Map showing the sub-embayments into which the Nauset estuary was divided. The solid lines represent the boundaries between adjacent basins where flow rates were calculated for each time step during the numerical simulation. (Note: A second line (dotted line) was defined for separating the North from the Middle Channel basins; this is examined as option 2.)	35
Figure 22a: Water elevation at the tide-gauge stations, predicted by the model for the cases of single (solid line) and dual inlets (dotted line), respectively.	37
Figure 22b: Water elevation at the tide-gauge stations, predicted by the model for the cases of single (solid line) and dual inlets (dotted line), respectively.	38

	Page
Figure 23a: Time-series of flow rates across the sub-embayment boundaries for the case of single (solid line) and dual inlets (dotted line), respectively.	39
Figure 23b: Time-series of flow rates across the sub-embayment boundaries for the case of single (solid line) and dual inlets (dotted line), respectively.	40
Figure 24: Schematic diagram of water circulation in Nauset estuary during the flood and ebb stages of the tide for the case of single and dual inlets respectively.	41

LIST OF TABLES

	Page
Table 1: April-May, 1996, tide-gauge deployment.	6
Table 2: October- November, 1996, tide-gauge deployment.	6
Table 3: Periods of hourly water elevation data used for the tidal analysis.	16
Table 4: Definition of sub-embayments used for calculation of flow rates across their boundaries and residence time (see Fig. 21).	33
Table 5: Volume of water in the various sub-embayments of the Nauset system at Mean High (V_{MHW}), Mean Low (V_{MLW}) and Mean Water Level (V_{MWL}), respectively. The volumes presented here are averaged over a neap-spring tidal cycle (15 days).	42
Table 6: <i>Case: 1 Inlet.</i> "Local" Flushing times (in hours) of the sub-embayments defined in Fig. 21. Flushing times listed are for the smallest neap, largest spring and tidal elevation averaged over a 15-day period. Note: Values shown were calculated using equation (3) with the volume of water (V_i) estimated at Mean Low Water (MLW) and Mean Water Level (MWL), respectively.	42
Table 7: <i>Case: 1 Inlet.</i> Flushing times (in hours) for the whole Nauset system and for the sub-embayments as defined in Fig. 21. Flushing times listed are for the smallest neap, largest spring and tidal elevation averaged over a 15-day period. Note: Values shown were calculated using equation (4) with the volume of water (V_o) estimated at Mean Low Water (MLW) and Mean Water Level (MWL), respectively.	43
Table 8: <i>Case: 2 Inlets.</i> "Local" residence times (in hours) of the sub-embayments defined in Fig. 21. Residence times listed are for the smallest neap, largest spring and tidal elevation averaged over a 15-day period. Note: Values shown were calculated using equation (4) with the volume of water (V_o) estimated at Mean Low Water (MLW) and Mean Water Level (MWL), respectively.	44
Table 9: <i>Case: 2 Inlets.</i> Residence times (in hours) for the whole Nauset estuary and for the sub-embayments as defined in Fig. 21. Residence times listed are for the smallest neap, largest spring and tidal elevation averaged over a 15-day period. Note: Values shown were calculated using equation (4) with the volume of water (V_o) estimated at Mean Low Water (MLW) and Mean Water Level (MWL), respectively.	44

Table 10: *Case: 2 Inlets.* Residence times (in hours) for the Nauset Marsh System assuming the existence of two inlets. The numerical simulation showed that the basin is separated into two parts (northern and southern) with independent hydrodynamic behavior. Flushing times were calculated using equation (4) with the volume of water V_0 being defined as the volume of the northern segment for Salt Pond and North Basin, whereas for the remaining sub-embayments the volume of water of the southern segment was used. Residence times listed are for the smallest neap, largest spring and tidal elevation averaged over a 15-day period. 45

TIDAL CIRCULATION AND FLUSHING CHARACTERISTICS OF THE NAUSET MARSH SYSTEM

David G. Aubrey, George Voulgaris, Wayne D. Spencer and Stephen P. O'Malley

Department of Geology and Geophysics
Woods Hole Oceanographic Institution

INTRODUCTION

The Woods Hole Oceanographic Institution has studied the marine resources within the Towns of Orleans and Eastham extensively during the past 20 years. Studies have been completed on the geological evolution of the nearshore region (Aubrey et al., 1982; Uchupi et al., 1996), the evolution of the barrier beach and adjacent beaches (Speer et al., 1982; Aubrey and Speer, 1983; Aubrey and Speer, 1984; Miller and Aubrey, 1985; and Aubrey and Giese, 1987), tidal behavior and flushing characteristics of Nauset embayment (Aubrey and Speer, 1985; Speer and Aubrey, 1985; Hess and Aubrey, 1985; Aubrey, 1986; Aubrey and Friedrichs, 1988; Friedrichs and Aubrey, 1988; Fry and Aubrey, 1990; Speer et al., 1991), sediment transport (Aubrey, 1986; Fry and Aubrey, 1990; Aubrey and Speer, 1993), tidal inlet migration (Speer et al., 1982; Aubrey and Speer, 1984), water quality in Town Cove (Aubrey and Speer, 1984), and numerical modeling (Aubrey and Speer, 1984; Speer and Aubrey, 1985; Friedrichs and Aubrey, 1989). One study in particular examined in a rudimentary way the flushing in the embayment as a function of inlet location and number of inlets (for the National Park Service; Friedrichs and Aubrey, 1989).

The Nauset embayment, located on Cape Cod, MA (Fig. 1), is a mature salt marsh system having both extensive *Spartina* marshes and unvegetated sand flats. The barrier beach protecting the marsh from the open ocean has a long history of migration, and changes in number and position of tidal inlets servicing it (e.g., Aubrey and Speer, 1984). As the barrier beaches and inlets have migrated, significant changes in tidal sand flats, vegetated flats, and channels have occurred. Prior to the early 1960's, the primary inlet was located nearly continuously according to historical records at the southern end of the system (Nauset Heights). Since the early 1960's, the inlet has migrated primarily in a northward direction, and the barrier beach has breached numerous times. At times, the breaches have evolved into inlets that remain for some period of time (one or more years); at other times, the breaches have closed only to become reactivated by storm surges and waves, through overwash processes.

The flushing rate within Nauset embayment, controlled by the local bathymetry and the number and position of inlets, is of concern to the governing bodies (Orleans, Eastham, National Park Service, Cape Cod Commission) because of declining water quality coupled with the biological sensitivity and importance of the system. Increased rural and urban pressures on the region due to development have increased nitrogen loading to the system. Long sinuous channel geometry has led to poor flushing of the southern segments, particularly as the primary inlet has migrated towards the north. Concern over the viability of multiple inlets present in recent years has increased concern over the flushing. The conundrum persists: is a single inlet or a dual inlet system desirable? What is the "optimal" location for an inlet? What management decisions can be taken to help encourage an optimal tidal flushing action?

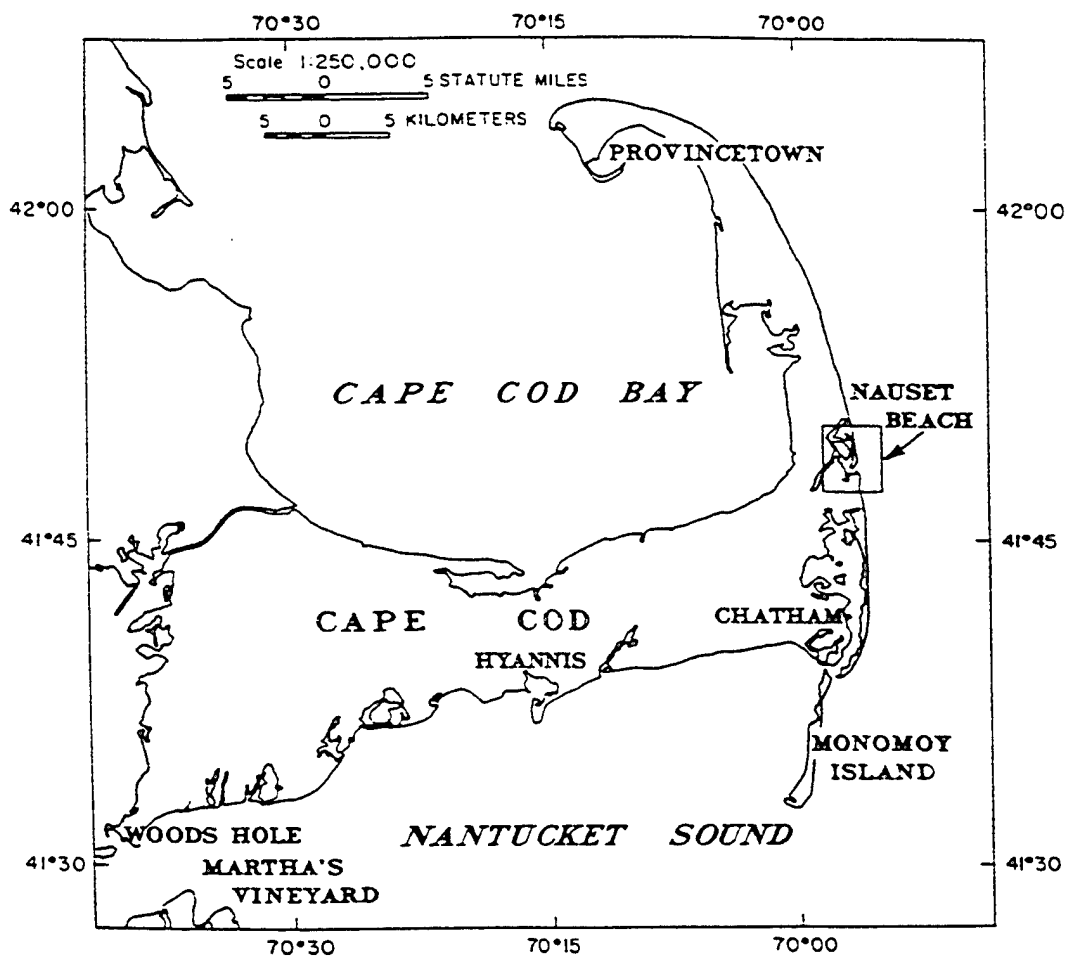


Figure 1: General location map for Nauset embayment.

Inlet position is of concern for a number of reasons:

- flushing and renewal of waters, and hence, water quality;
- stability of coastal bio-resources;
- coastal erosion;
- navigation for small fishing vessels and recreational boats.

In this study, we focus on inlet position as it affects water quality. The residence times obtained during this study will be applied by the Cape Cod Commission for purposes of nitrogen loading estimates and consequent water quality assessment.

The present program consisted of a series of elements:

- field measurement program, to determine accurate bathymetry for the site, and to measure tidal and non-tidal response of the system;
- implementation of a 2-dimensional numerical circulation model for the Nauset embayment
- validation of the 2-dimensional model;
- using output of the numerical model for calculating residence times for water parcels in pre-determined sub-embayments within Nauset;
- assessment of flushing within the estuary for a one-inlet and two-inlet system, for management purposes;
- delivery of the hydrodynamic model, calibrated for present configurations, to the Town of Orleans.

The aim of the study is mainly on water circulation within the estuary and the exchange (flushing) of water between the estuary and the Atlantic Ocean arising from tidal processes. Previous work (Aubrey and Speer, 1985) performed at Nauset embayment has documented the primary importance of tidal action for flushing. Additionally, other factors such as local winds and regional winds can be important for flushing (Geyer, 1997). However, their importance is limited to short time-scales and to estuaries with wide mouths. At longer time-scales the tidal fluctuations are the most important contributors to residence time. We assume a well-mixed water column in this study, though previous studies (e.g., Aubrey and Speer, 1984; Andersen and Stolzenbach, 1989) have shown that stratification can occur in Town Cove, Salt Pond and Mill Pond. However, the extreme shallowness of average depths of channels makes most flow two-dimensional and well-mixed; hence, we ignore the effects of vertical stratification. Stratification reduces the effective depth of a basin by isolating deeper waters from active tidal exchange, therefore, stratification in Town Cove will have the effect of reducing the residence time of nutrient-rich groundwater, which will exchange with the tide at the surface (absent biological processes). However, during a plankton bloom, nutrients will cycle to the bottom waters rapidly, increasing the loading to the bottom waters which will have a longer residence time, and hence reducing water quality. We have not quantified these contrasting processes. To address the biogeochemical issues, we would recommend implementation of a simplified, low trophic level ecosystem model. Numerous ecosystem models applicable to shallow water have been developed recently as a tool complimentary to hydrodynamic models to explore ecosystem relations and biological contributions to water quality.

DEFINITION OF RESIDENCE TIME

In a loose sense, residence time can be defined as the length of time a parcel of water will remain in an estuarine sub-system until it is replaced by waters from outside the sub-system. In more mathematical terms, the general concept of residence time (τ) of an element/pollutant is defined as: the ratio of the quantity of a substance (dissolved or particulate) in a given environmental compartment (water, sediment or biota) divided by the quantity of the compound supplied (or removed) per unit time (Kramer et al., 1994):

$$\tau = \frac{C}{(dC/dt)} \quad (1)$$

where C is the total quantity (or concentration) of the element in suspension or solution, and dC/dt is the time-dependent input (loading) to the system. After the substance is introduced to the system, its concentration C depends on the hydrodynamic regime and in particular on the fresh water discharge and the tidal flushing of the estuary.

The hydrodynamic modeling undertaken in this project provided information used to calculate the residence times of the system. Residence time can also be defined as the time a particular particle of water spends in the system. Long residence times represent stagnant water and often poor quality conditions. However, efficient tidal flushing (low residence times) is not an indication of high water quality if the loading of the system with the pollutant (dC/dt) is higher than the rate of water exchange. Use of the predicted flushing times for planning management should always be applied with care and in relation to the pollutant loading.

Assuming that the volume of the entire system at mean water level (MWL) is V_o , then the residence time of the estuary is defined as (Zimmerman, 1988):

$$\tau_o = \frac{V_o}{\sum Q_f(t)\Delta t} T_{M2} \quad (2)$$

where $Q_f(t)$ is the instantaneous flow rate across the mouth of the estuary during the flood stage of the tidal cycle, calculated at time intervals Δt , and T_{M2} is the period of a full tidal cycle (=12.42 hours for the semi-diurnal tide which is the dominant constituent at Nauset). Q_f also incorporates freshwater inflow to the estuary. This freshwater inflow may come from rivers, streams, or groundwater. At Nauset, this freshwater inflow volume is negligible hydrodynamically, although it does provide the main source of new nutrients. The above defined residence time is the time required for the estuary to replace the entire water volume with water from outside the estuary.

In previous flushing time studies (e.g., Aubrey Consulting, Inc., 1996), the water volume (V_o) in equation (2) has been defined as the volume of water at the mean low water level (V_{MLW}). This latter definition predicts a more conservative residence time than the original one of Zimmerman (1988).

Different parts of an estuary require different times to renew their water volume. These differences are based on the hydrodynamic characteristics and fresh water input to these different areas. Therefore, different sub-embayments (basins) within a given system are usually defined based on the morphological and hydrodynamic characteristics of each basin. Each basin can have one or more boundaries with one another and/or with the open sea. Similar to equation (2), the "local" residence time of each basin can be calculated as:

$$\tau_i = \frac{V_i}{\sum Q_{fi}(t)\Delta t} T_{M2} \quad (3)$$

where V_i is the volume of water of the basin (at mean or low water level) and $Q_{fi}(t)$ is the combined saltwater and freshwater discharge across the boundaries of the basin. The subscript i denotes the index of the basin under investigation. When a basin is defined by more than one boundary, then the discharge (Q_{fi}) is calculated as the algebraic sum of the time-series of the flow rates across each boundary, where the net flow is defined as toward the basin. This "local" residence time, however, defines the "future" of the particle, (i.e., how long the water particle will remain in the basin). Each particle also has a "history" (i.e., the time the particle has been in other parts of the system before it was transported to basin i). Therefore, blind estimation of the local residence times is not necessarily indicative of the water quality since contaminated parcels of water can be replaced by other parcels of water contaminated by another part of the system. An alternative, conservative estimate of the local residence time is obtained by replacing the local volume, V_i , with the water volume of the entire system V_o :

$$\tau_i = \frac{V_o}{\sum Q_{fi}(t)\Delta t} T_{M2} \quad (4)$$

The physical explanation of this latter definition of the residence time is the time that it is required for a basin to replace its entire water volume with clean oceanic water assuming that all the water of the system will pass through this particular basin. In practice, only part of the total water volume will go through the particular basin; thus the residence times estimated with this definition can be considered fairly conservative. Application of the Aubrey Consultants, Inc. (1996) definition for residence time (i.e., V_o = volume of water at mean low water instead of mean water level) will predict more rapid flushing with differences depending upon the relative (volumetric) size of the sub-embayment to the total size of the system. In this report residence times were calculated using both definitions for comparison.

FIELD MEASUREMENTS

In situ measurements are required for setting up (i.e., accurate bathymetric data), calibrating and validating (in instances where more than a single data set is available) the numerical model.

Field operations consisted of three types: (i) tide-gauge deployments, (ii) bathymetric surveying, and (iii) a 12-hour observation of vertical variation of temperature, salinity and velocity. Measurements were obtained between April and December 1996.

Tide Recordings

Tidal data used for numerical model calibration and correction of raw bathymetric data were acquired using internally recording pressure/temperature (PTL) and pressure/temperature/-conductivity (PTLC) loggers. These loggers were deployed at ten different locations in order to document the tidal characteristics throughout the system (Figs. 2 and 3, and Tables 1 and 2). Six-minute sampling intervals provided 240 samples/day. All tide recorders were calibrated at WHOI prior to deployment, allowing a field measurement accuracy for elevation of 1 cm. The instruments were mounted to sub-surface pipes which had been water-jetted vertically into the seabed. Instrument positions were obtained using Differential Global Positioning System (DGPS) referenced to the NAD 1983 horizontal datum. Elevations of the tide recorders were established and referenced to NGVD 1929 by standard land survey techniques utilizing laser-based technology. Pressure readings were reduced to water surface elevations by assuming constant water density of approximately 1.032 g/cm^3 .

Only 3 of the instruments during the April deployment returned 100% data sets (Table 1). Therefore, seven tide recorders were re-deployed during October, 1996. This second deployment provided the sea-surface elevation time-series from 6 out of 7 deployment stations (Table 2). These data were used for the implementation of the numerical model. The failure in the April deployment was due to both hardware (within the power supply units) and software deficiencies.

Table 1: April-May, 1996, Tide-Gauge Deployment.

Location	Position	Instrument	Data Return
Town Cove	41° 47.290'N, 69° 59.106'W	PTLC 5	100%
Albany Creek	41° 48.866'N, 69° 57.634'W	PTLC 1	40%
Stony Island	41° 48.703'N, 69° 57.207'W	PTLC 6	No Data
Priscilla Landing	41° 48.123'N, 69° 56.751'W	PTLC 4	100%
South inlet			
ocean side	41° 49.084'N, 69° 55.860'W	PTLC 3	No Data
inside, south	41° 48.689'N, 69° 56.524'W	PTLC 2	No Data
inside, north	41° 48.984'N, 69° 56.250'W	PTL 5	No data
North inlet	41° 49.730'N, 69° 56.731'W	PTL 1	No data
Salt Pond	41° 49.968'N, 69° 58.031'W	PTL 4	No Data
Marsh, west	41° 49.320'N, 69° 57.670'W	PTL 6	100%

Table 2: October- November, 1996, Tide-Gauge Deployment

Location	Position	Instrument	Data Return
Town Cove	41° 47.290'N, 69° 59.142'W	PTLC 5	100%
Albany Creek	41° 48.880'N, 69° 57.602'W	PTLC 2	100%
Stony Island	41° 48.697'N, 69° 57.218'W	PTL 4	100%
South inlet			
ocean side	41° 48.966'N, 69° 55.849'W	PTL 6	No Data
inside, south	41° 48.615'N, 69° 56.565'W	PTL 3	100%
North inlet	41° 49.594'N, 69° 56.788'W	PTLC 1	100%
Salt Pond	41° 49.959'N, 69° 58.033'W	PTLC 4	100%

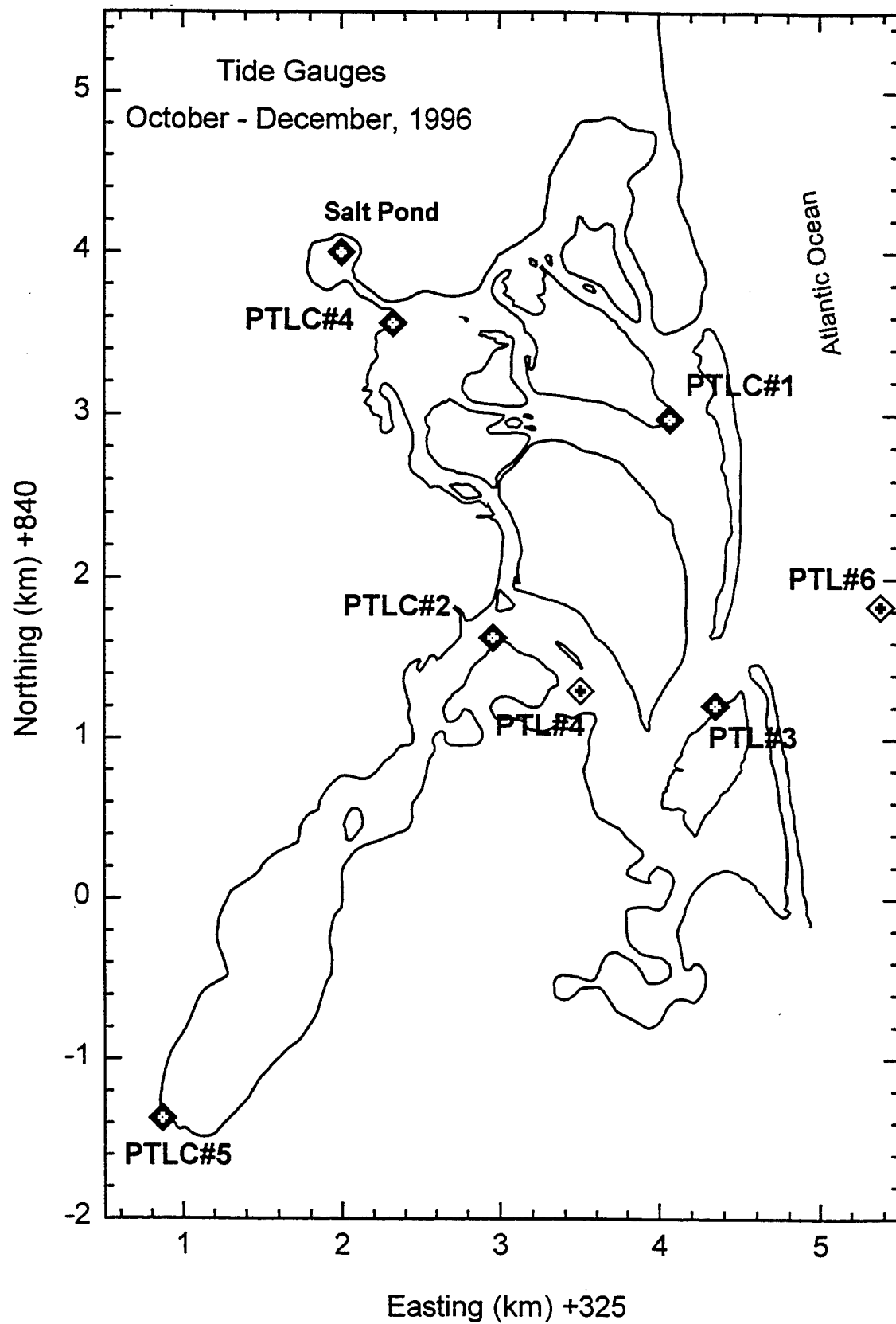


Figure 3: Location of tide-gauge stations deployed during October-December, 1996. Data from these stations were used for tidal analysis and calibration of the hydrodynamic model. Open symbols (i.e., PTL #4 and PTL #6) denote stations that failed to operate.

Bathymetry

Bathymetric survey data were acquired using an integrated hydrographic survey system (Hypack). Positioning of the survey vessel was accomplished using Differential Global Positioning System (DGPS) while soundings were acquired using a dual-frequency, high precision echosounder, calibrated daily. About 500 km of survey lines were run while recording a depth measurement every 3 m (Fig. 4). Only a limited amount of bathymetric data was acquired in the shallow, northern reaches of the system because of lack of sufficient draft for boat operations, whereas in the deeper southern areas, more dense data were taken. These data were processed at WHOI using Hypack software.

Tidal data recorded during the period of the bathymetric survey were used to correct depth sounding to vertical datum. Sea surface elevation values for areas where instruments had failed to record were predicted using the constituents determined by Aubrey and Speer (1985). Because the amplitude and phase of the tidal signature vary strongly throughout the system, it was necessary to sub-divide the survey area into regions in which an appropriate tidal logger could be used to correct the raw depth values. To minimize sharp changes in depth over tidal region boundaries, tide correction data from the two adjacent tide-gauge stations were averaged for approximately 0.5 km on each side of this boundary. The tide gauge stations used for the bathymetric corrections are shown on Fig. 5.

Conductivity, Temperature, and Current (ADCP) Profiles

On 4 May 1996, a 12-hour (0700 to 1900) profiling experiment was conducted. CTD and water velocity profiles were recorded at 8 different stations located between Nauset Inlet and Town Cove (see Fig. 6). Stations were sampled on an average of once every 80 minutes. More frequent sampling was not possible due to the shallow water depths and abundant shoals present in the area that obstruct navigation. In addition, during the course of the bathymetric survey, two profiles were recorded in Mill Pond. A SeaBird CTD SBE-19 equipped with a pump and a fluorometer was used in this survey. It is easily handled by one person as it is light and rugged. The CTD as used at Nauset was installed in a protective stainless steel cage, rectangular and slightly larger than the CTD. The CTD was manually deployed from the WHOI-owned *RV Mytilus*.

A broadband, high-frequency RDI Acoustic Doppler Current Profiler (ADCP) was used to document the water velocity profiles (surface to bottom) at each station. Additional ADCP data were collected along the main channel. The ADCP was mounted on an over-the-side gimbaled mount that allowed it to be brought on-board between stations for high speed running. This high speed running (20-25 knots) between stations during the 12 hour experiment was important in order to increase the temporal resolution of the experiment. These ADCP data are useful in estimating the current flow in the channel at different times of the tidal cycle. However, shallow water depths limited the utility of the ADCP data (the surface and near-bottom bins are not useful due to interference in the return).

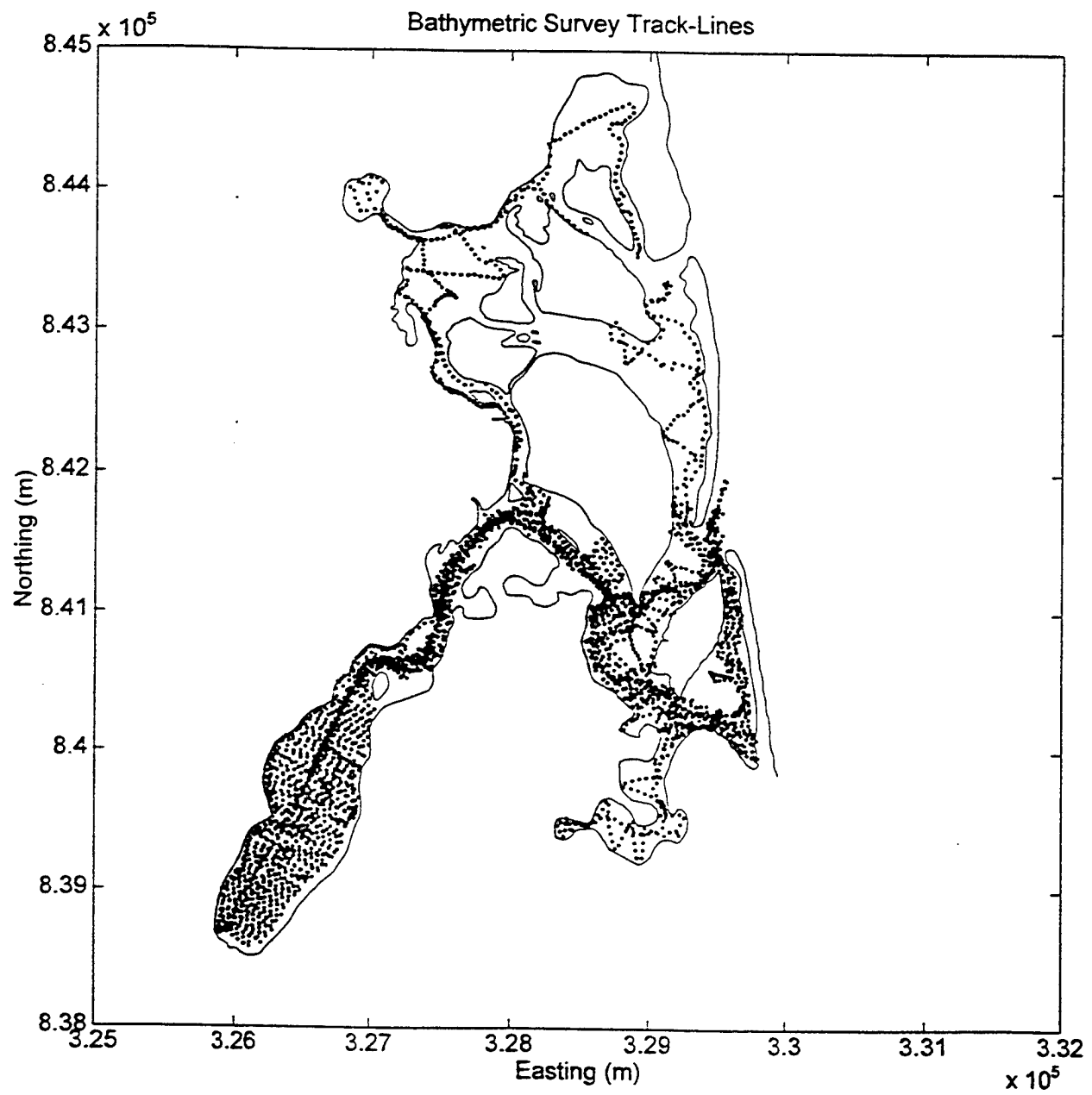


Figure 4: Location of track lines for bathymetric surveying.

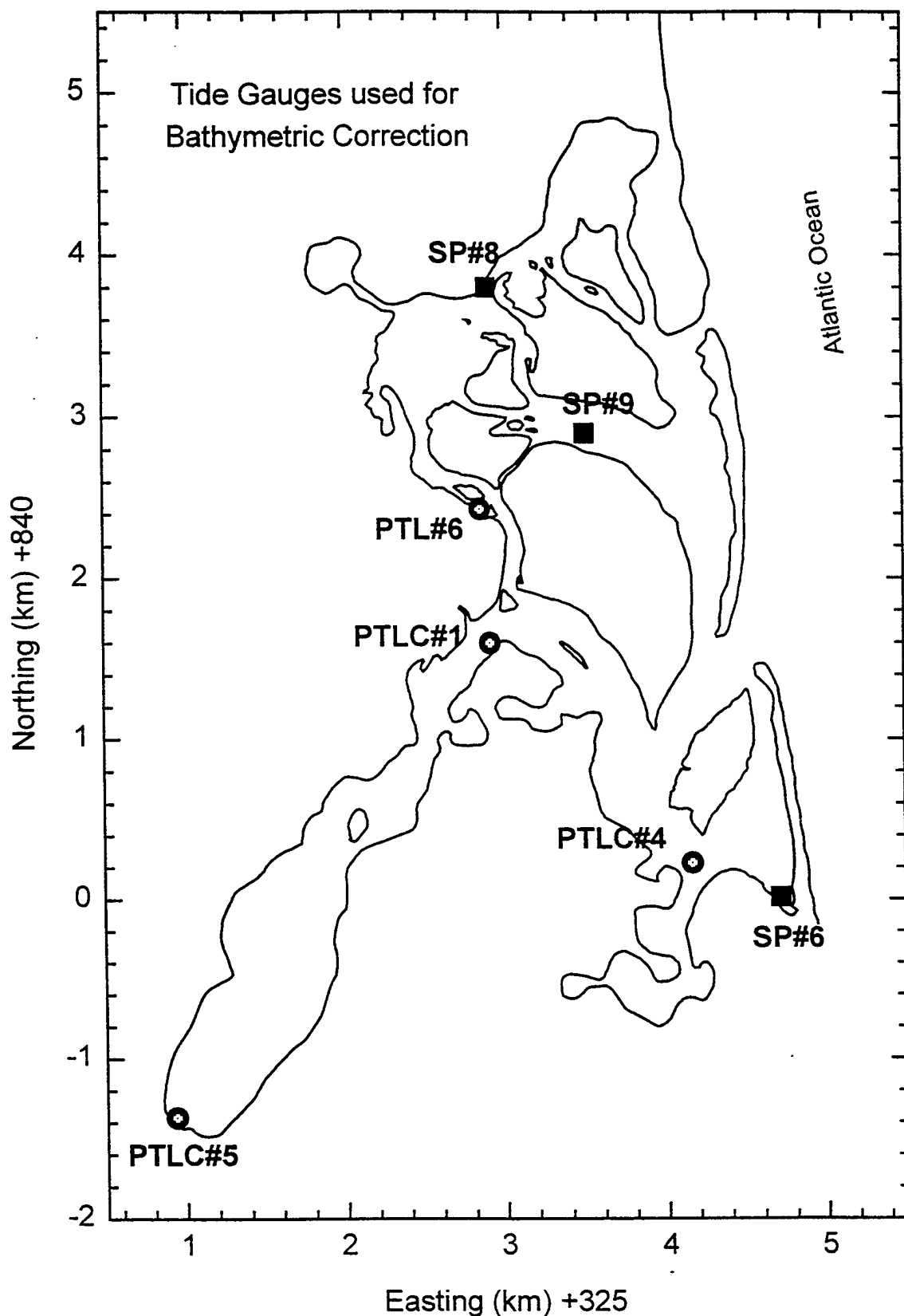


Figure 5: Location of tide-gauge stations used for the tidal correction of the bathymetric data. Circles denote stations operational during the bathymetric survey whereas squares denote stations for which tidal elevation data were predicted based on measurements obtained by Aubrey and Speer (1985).

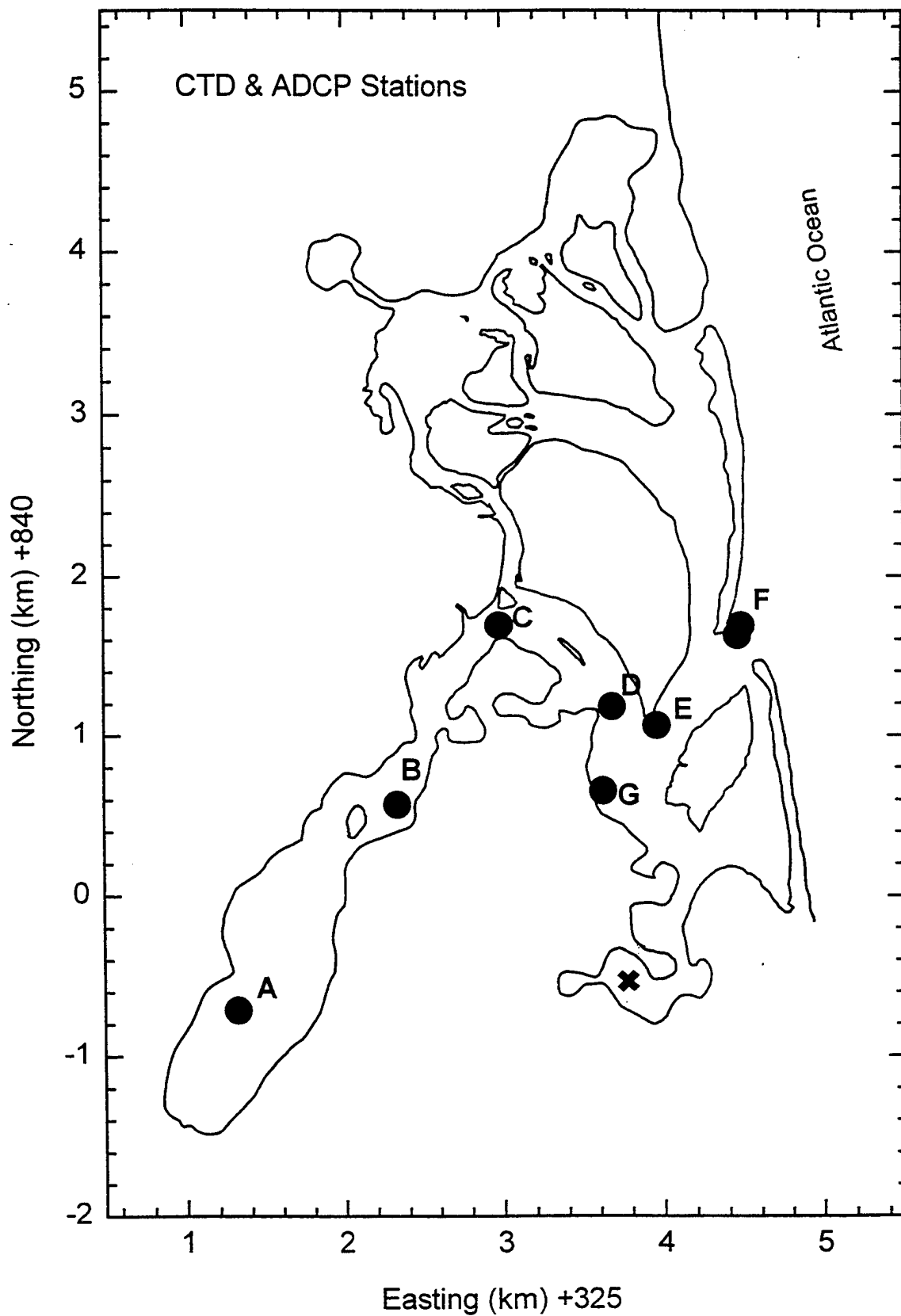


Figure 6: Location map of CTD casts and ADCP current measuring stations(A to F). (Note: cross indicates location of a single CTD cast collected in Mill Pond).

MEASUREMENT RESULTS

Bathymetry

The bathymetric data were corrected for tidal influence, prior to their inclusion to the circulation model and their use for creation of a bathymetric map. The bathymetry data were collected in raw format (recorded in ASCII) at maximum temporal resolution (about once every 1.7 sec.) using the hydrographic survey software package Hypack. Time, date, differential GPS, and raw depths relative to the boat were recorded in the original data file along with other important survey parameters. To correct these data to NGVD 1929 (NGVD), observations from the tide-gauge stations were corrected to NGVD then algebraically subtracted from the raw sounding data. This procedure gives elevations relative to NGVD. The PTL and PTLC data were corrected to average atmospheric pressure, which could yield a negligible potential error of about 5 cm (2 inches) of sea water. Other errors in the bathymetry data come from: 1) the accuracy of the fathometer (about 0.24 cm (0.1 inches) of sea water), 2) the accuracy of the PTL/PTLC vertical survey using standard land survey equipment (about 2.5 cm (1 inch)), and 3) vertical boat motion. The overall average accuracy of the bathymetry survey after totaling all error estimates was less than 15 cm (6 inches).

The bathymetry data were included with shoreline data in a file used to define the shape of the basins for the flushing model. The shape of the ebb tide delta was estimated. Data representing the 1996 shoreline was supplied by Dr. James Allen from the National Biological Survey (NBS).

The bathymetry of the Nauset system was adequately defined for modeling purposes but in the north basin area (Nauset Bay) bathymetry data are sparse. This was due to the shallow water in the north region restricting boat operations to specific channels at high tide. However, we have knowledge of the water depths over these large areas of flats from other observations.

Tidal Analysis & Prediction

The surface elevation data were collected by the PTL and PTLC instruments (Fig. 7). The data span a period of 50 days. Due to instrument settings, PTLC#4 did not record elevations below 20 cm whereas a similar problem was present in PTLC#5 for water elevations greater than 160 cm. The sea surface elevation data for the Salt Pond area (Fig. 8) were provided by the Town of Eastham, Conservation Department. These data have a gap covering a period of approximately 12 days. Also, positive and negative spikes are present at measurements obtained near low water. The deficiencies were remedied prior to data analysis, using both interpolation and extrapolation.

The above water surface elevation records were analyzed in order to derive the amplitude and phases of the tidal constituents. The results of this analysis were used: (i) to study the distortion of the tides inside the estuary and thus to understand the hydrodynamics of the system; and (ii) to reconstruct the water elevation due to the tides alone, which was subsequently used for the calibration of the numerical model. The latter approach eliminated problems with

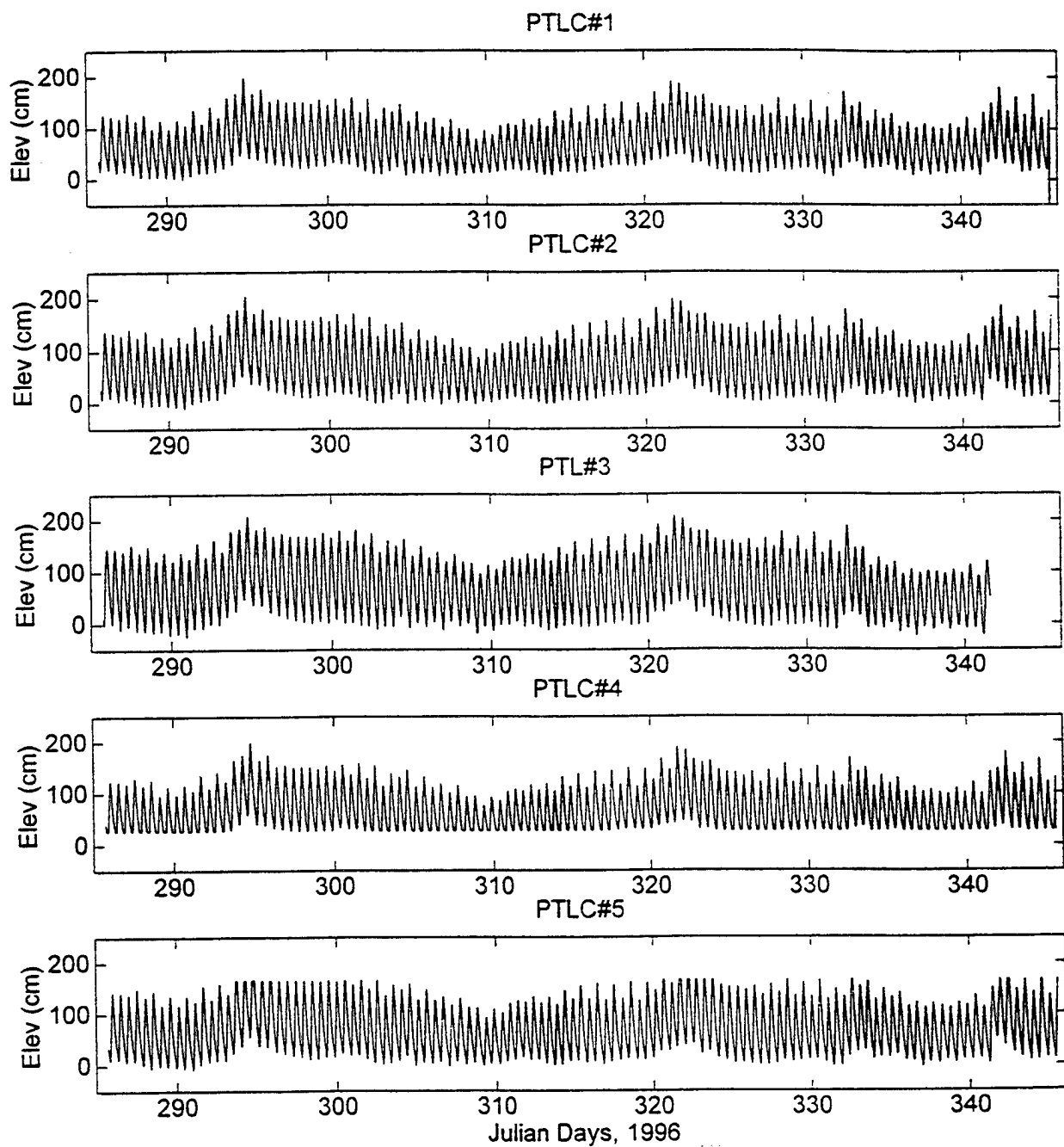


Figure 7: Time-series of sea surface elevation as collected during the October-December, 1996 deployment using the PTLC instruments. Elevation is referenced to NGVD of 1927.

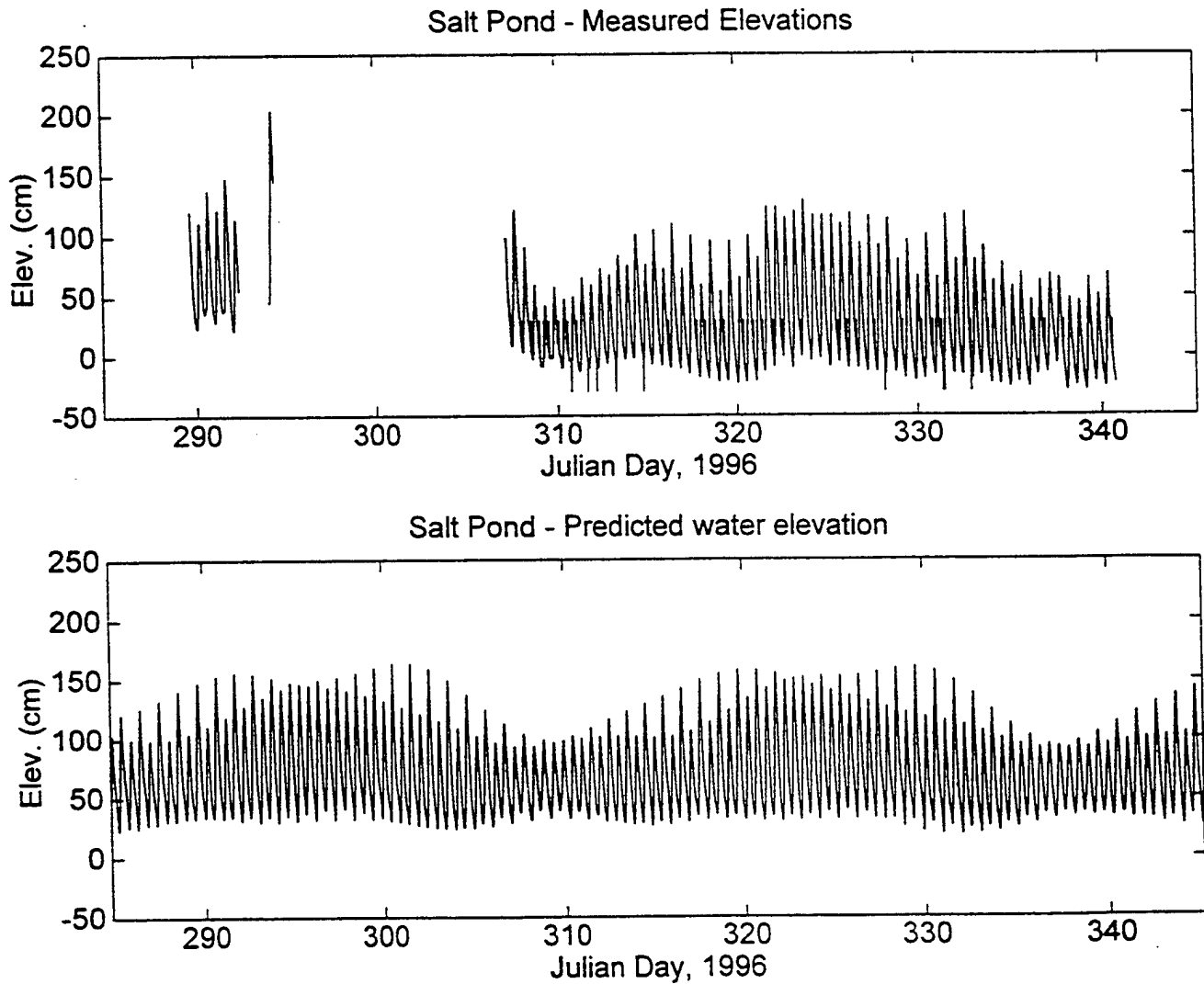


Figure 8: (a) Time-series of recorded sea surface elevation from Salt Pond tide gauge of the Town of Eastham, Department of Conservation. (b) Time-series of predicted sea surface elevation in Salt Pond using the result of the tidal analysis of the raw record (a).

missing and/or spiky data and it enabled us to calibrate the model without the occasional wind-induced surface elevation variations which might exist in the original records.

The analysis package developed by the Institute of Ocean Sciences (Canada) was used to carry out the tidal (harmonic) analysis. It consists of tidal height analysis and prediction programs (Foreman, 1977).

The tidal analysis program analyzes hourly tidal height data for a given period of time. Amplitudes and Greenwich phases are calculated via a least squares method coupled with nodal modulation only for those constituents that can be resolved over the length of the record. The standard data analysis considers 69 constituents. However, up to 77 additional shallow water constituents can be requested. Certain constituents which cannot be resolved from the data can be inferred directly using well-known astronomical theory (Foreman, 1977). Another advantage of the program is that it permits the analysis of tidal records even if data are missing. The tidal prediction component uses the previously derived amplitudes and Greenwich phases of the various tidal constituents to predict the sea surface elevation for a specified period and predetermined time interval.

Prior to tidal analysis, the data collected were decimated to hourly observations and the time base was corrected for Eastern Standard Time (EST). Then the data were reformatted in a format compatible for use with the tidal analysis package. The periods of data used for the analysis and the number of constituents for which amplitudes and phases were derived are listed in Table 3.

The tidal constituents derived from the analysis of the above records are listed in Appendix I. These constituents were used for the prediction of the water surface elevation for the period from 11 October, 1996 to 31 December, 1996. The prediction was carried out for each one of the stations listed in Table 3 and with a sample interval of 6 minutes. The predicted water elevations are shown in Figs. 8 and 9 for the Salt Pond and PTLC stations, respectively.

The same tidal prediction program was used to predict the offshore (ocean) sea water elevation that was used to drive the hydrodynamic model. The constituents used for this prediction, listed in Appendix I, were derived from combining the Aubrey and Speer (1985) data with information published by the National Ocean and Atmospheric Administration. The predicted oceanic tide is shown in the bottom panel of Fig. 9.

Table 3: Periods of hourly water elevation data used for the tidal analysis.

Station	Starting Date / Time (EST)	Ending Date / Time (EST)	Hours Analyzed	Constituents Derived
PTLC#1	11 th Oct '96 / 17:00	10 th Dec '96 / 11:00	1458	37
PTLC#2	11 th Oct '96 / 17:00	10 th Dec '96 / 11:00	1458	37
PTL#3	11 th Oct '96 / 17:00	06 th Dec '96 / 12:00	1363	37
PTLC#4	11 th Oct '96 / 17:00	10 th Dec '96 / 11:00	1458	37
PTLC#5	11 th Oct '96 / 17:00	10 th Dec '96 / 11:00	1458	37
Salt Pond	31 st Oct '96 / 24:00	03 rd Dec '96 / 24:00	816	37

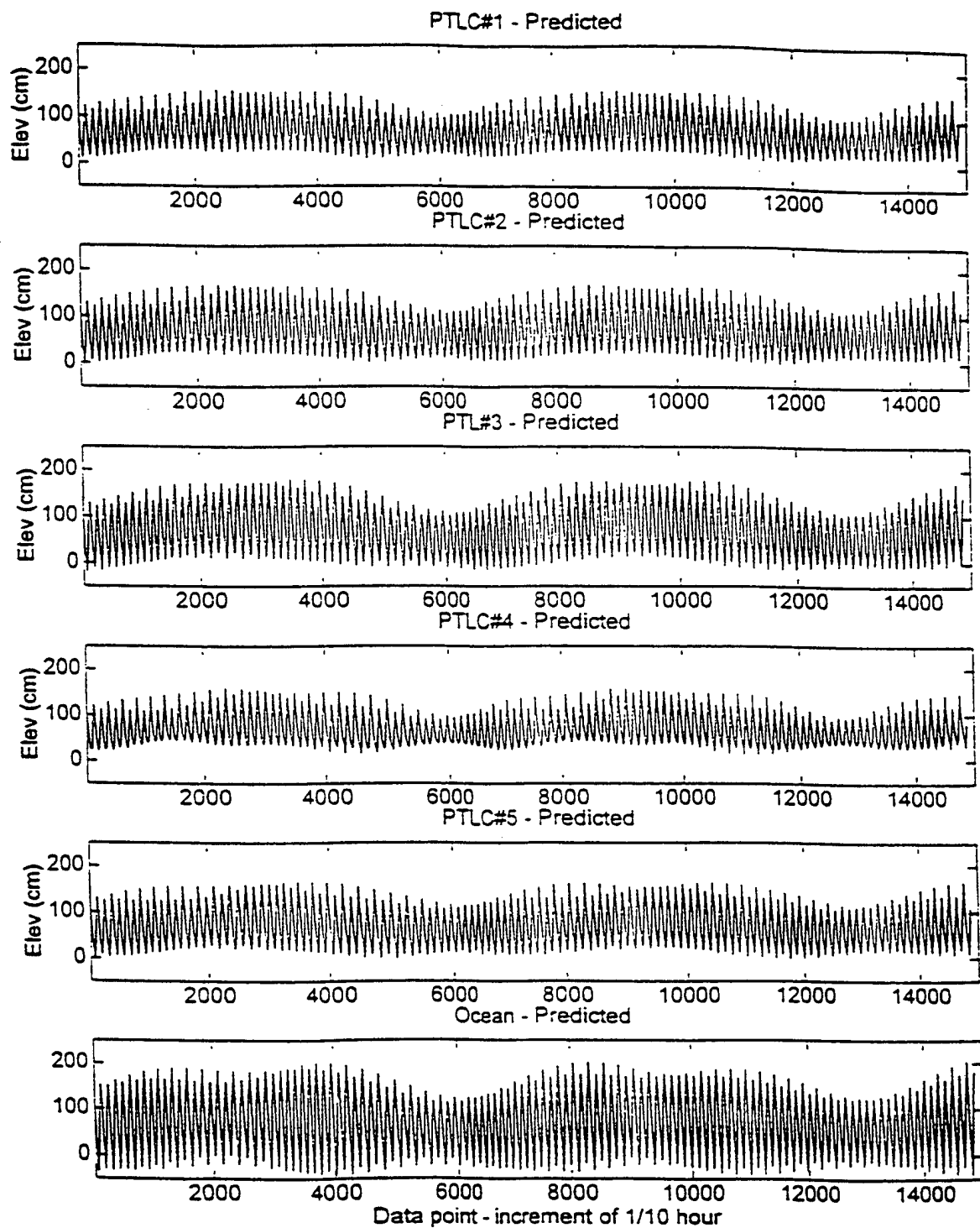


Figure 9: Time-series of predicted sea surface elevation at the PTLC deployment locations.

The harmonic analyses of the surface elevation records indicate that Nauset is a strongly non-linear as well as frictionally dominated inlet/estuarine system. The non-linear response to tidal forcing is reflected in growth of the high frequency M_2 overtones. The frictional nature of the estuary is demonstrated both by large phase changes in the tide and by amplitude decay of the total spectrum. The tidal distortion is shown in the diagrams (Fig. 10) as a function of distance along the main channel (solid line) and North Channel (dashed line), respectively. The ratio of the amplitudes, M_4/M_2 , increases with distance into the estuary (i.e., maximum ratio at Town Cove (0.21) and at Salt Pond (0.28)) reflecting both a frictional dissipation of M_2 and a growth of M_4 , the first harmonic of M_2 (Fig. 10). These effects are more pronounced in the north channel than in the main channel mainly due to the extensive shallow areas found in the north part of the estuary. Shallower areas are more strongly nonlinear, causing a stronger distortion of the tide. This results in a phase lag between the oceanic tides and the tides at Salt Pond and the baymouth constriction at Town Cove of 50° and 36° respectively for the M_2 constituent. This means that high water occurs at Salt Pond approximately 1.7 hours after high water in the ocean. In Town Cove high water occurs some 1.2 hours later than the ocean high water.

CTD & ADCP Results

CTD casts and current profiling were carried out for a full tidal cycle on 4 May, 1996. The stations were distributed along the main channel (Fig. 6). The objectives were to obtain: (i) information on stratification and water mixing both in the vertical and in the horizontal, and (ii) current measurements for the validation of the results of the numerical model.

The measurements were taken at 7 locations (Fig. 6). The number of CTD casts obtained at each location varied between 7 and 9. The vertical profiles of temperature and salinity for each station are included as Appendix IV. Examination of the profiles showed that Nauset is a well-mixed estuary. The most significant vertical water structure was found in Town Cove (Station A) where the bottom water is cooler (9°C) than the surface water (10.5 to 12°C). The salinity in Town Cove did not show any distinct structure, suggesting that the temperature differences are mainly due to atmospheric heating of the surface layer. A similar pattern was observed in the single CTD cast obtained in Mill Pond (see Appendix IV). For the rest of the stations, the water is well-mixed in the vertical. However, the collected CTD data reflect conditions representative of the period of data collected. Seasonal variation of these characteristics was not resolved in this experiment.

Depth-averaged values of temperature, salinity and water density were calculated for each cast and station. The results (Figs. 11, 12 and 13) are plotted together with the predicted ocean water elevation for the period of the CTD measurements. The depth-averaged temperature exhibits a periodicity with the tidal cycle: At all stations the temperature is higher at low water; it decreases during flood reaching a minimum at high water; and then it starts increasing again during the ebb tide. The salinity of the water exhibits a similar variation: it is slightly higher at high water than at low water. This pattern in salinity variation is similar at all stations with increasing amplitude nearer the head of the estuary (station B). Both temperature and salinity are different in Town Cove (Station A), showing that this part of the estuary is somehow

Tidal Distortion in Nauset Estuary

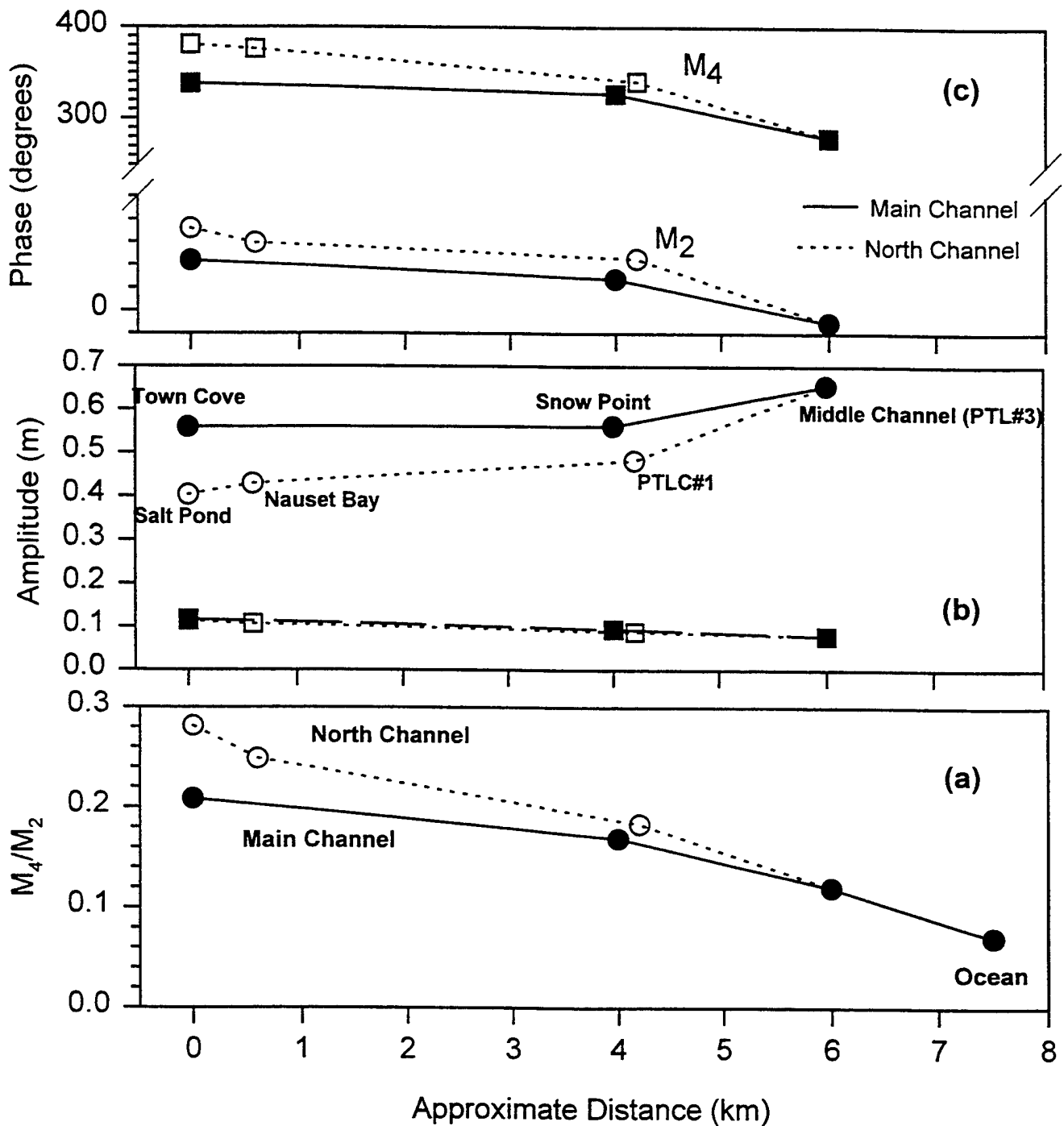


Figure 10: Tidal distortion indices as a function of distance into the estuary (abscissa) for the main (solid line, filled symbols) and North channels (dashed line, open symbols), respectively: (a) ratio of amplitude of the M_4 and the M_2 tidal constituents; (b) tidal amplitude variation for the M_4 (squares) and M_2 (circles) tidal constituents; and (c) phase variation in degrees.

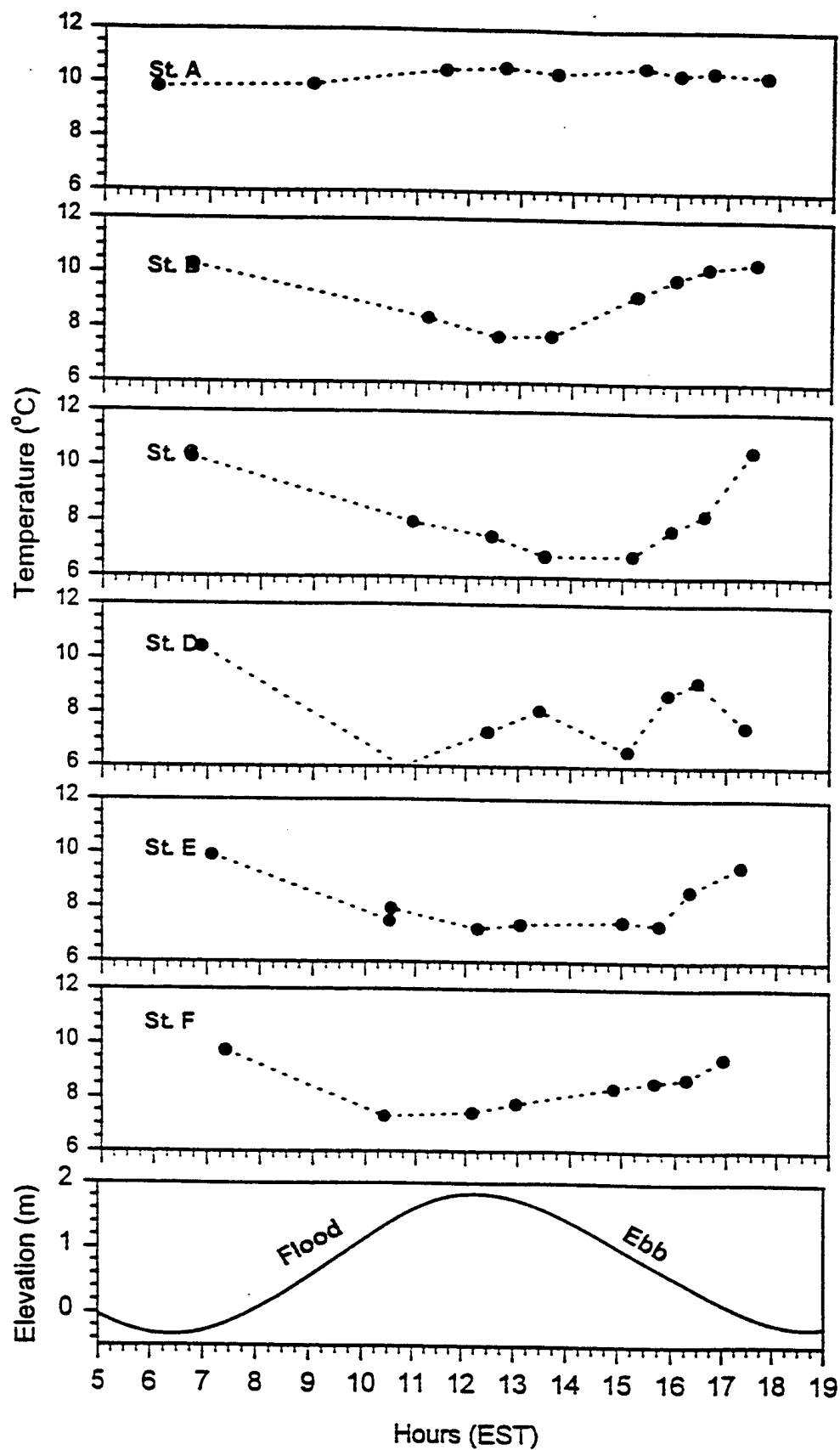


Figure 11: Tidal variation of depth-averaged water temperature calculated from the CTD measurements at stations A to F. Bottom panel: predicted oceanic sea surface elevation for the measurement period.

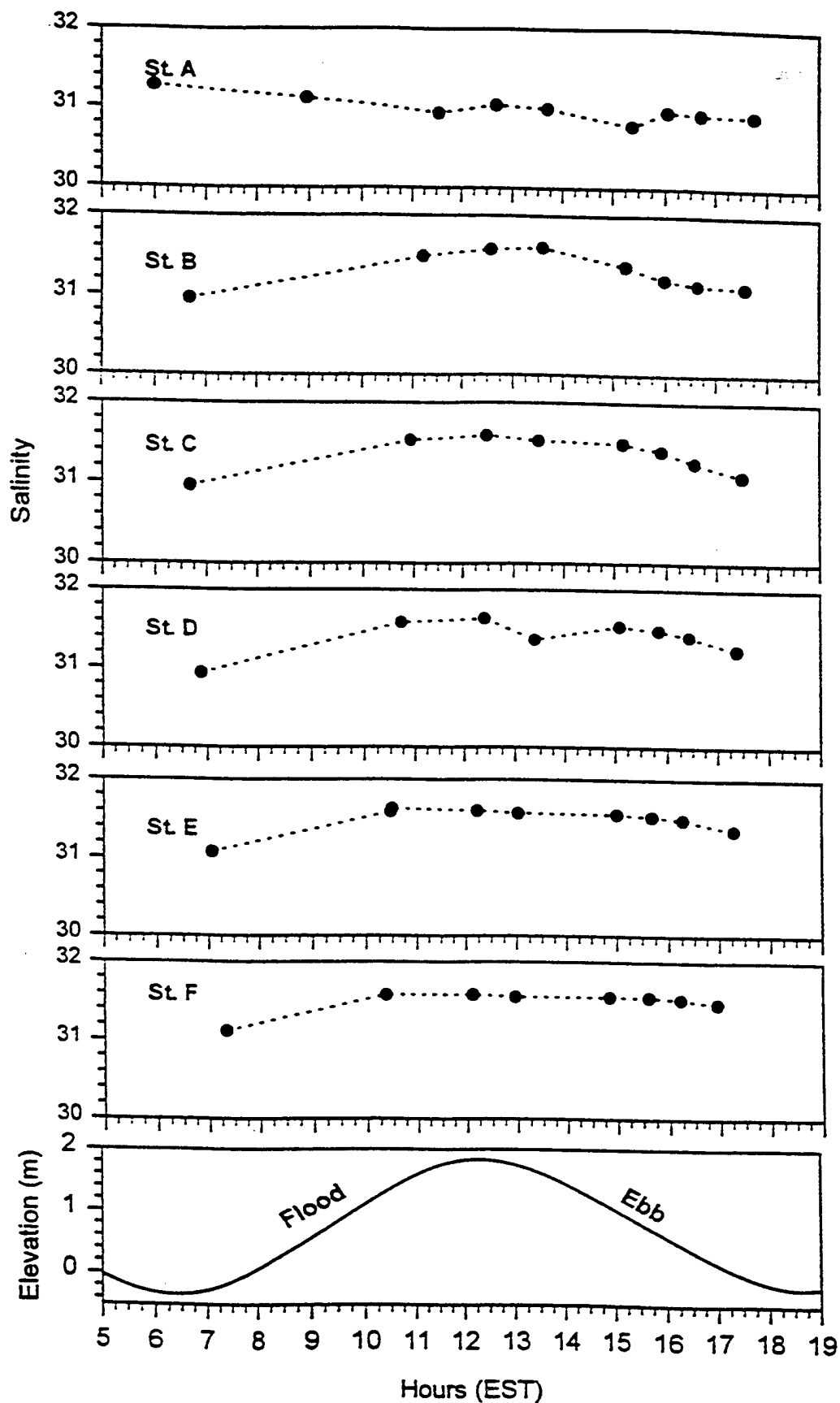


Figure 12: Tidal variation of depth-averaged water salinity calculated from the CTD measurements at stations A to F. Bottom panel: predicted oceanic sea surface elevation for the measurement period.

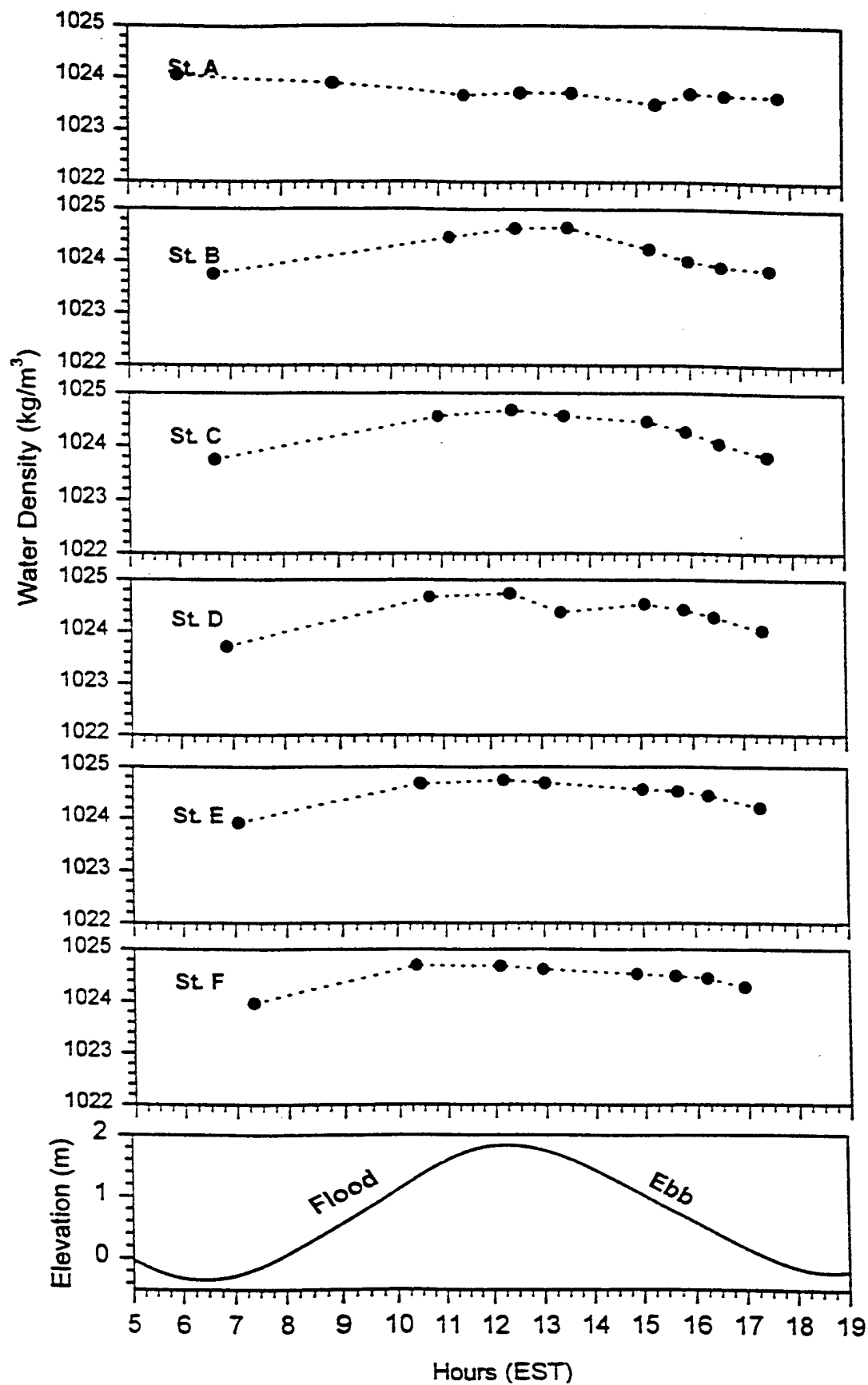


Figure 13: Tidal variation of depth-averaged water density calculated from the temperature (Fig. 11) and salinity (Fig. 12) measurements. Bottom panel: predicted oceanic sea surface elevation for the measurement period.

hydrodynamically distinct from the main channel of the system. The above observations of salinity and temperature can be seen also in the water density (Fig. 13). The maximum difference of depth-averaged water density occurs at low tide (fresh water influx dominance) and high water (tidal salt water intrusion). Its maximum value is approximately 0.8 Kg/m^3 and occurs at station B. The above described variations in temperature and salinity are small and overall the CTD measurements confirmed that Nauset is generally a vertically well-mixed system.

The ADCP measurements were reduced to depth-averaged current speeds (Fig. 14). The relative current speeds increase during the ebb and flood stage of the tide as expected. The absolute current magnitude is minimum at Station A (Town Cove) and increases toward the inlet (Station F). The limited circulation in Town Cove reflects the greater water depth and sill-controlled tidal flow for this sub-embayment.

HYDRODYNAMIC MODELING

Model Identification

In order to characterize the flushing characteristics of the Nauset system, a finite element hydrodynamic model was applied. The main objectives of the modeling were to identify and quantify accurately the water circulation inside the estuary and the exchange of estuarine water with fresh, open sea water. Initially, the three-dimensional model (RMA-10), operating in a two-dimensional, depth-averaged mode, was applied. The advantage of RMA-10 is that in addition to the hydrodynamics, it is able to predict distributions of temperature and salinity. However, application of this specific model was abandoned due to instabilities created by the extensive areas of inter-tidal marshes present in the north part of the system. In its place, we applied the related RMA-2V model, also developed by Resource Management Associates (King, 1996, 1990). It is capable of simulating either time-dependent or steady-state systems and is well suited to analysis of shallow lagoon or river systems. In its present form, the model allows the combined use of two-dimensional and one-dimensional elements. This capability permits economical simulation of bays with tributary rivers, or complex delta areas. Also, it has better stability under wetting and drying situations, as in these salt marshes, by simulating the drying elements as flow through porous media (King, 1996). In contrast with the RMA-10, it does not model the temperature and salinity distributions, but as the CTD measuring program revealed, most of the estuary is well-mixed thus no specific need was presented for modeling those two parameters. However, during late spring when the maximum fresh water input is expected or at late summer when the maximum temperatures occur, the mixing conditions may differ in deeper ponds (Salt and Mill ponds, Town Cove).

Model Theory

In its original form, RMA-2V was developed by William Norton and Ian King under a development contract with the U.S. Army Corps of Engineers (Norton et al., 1973). Further development included the introduction of one-dimensional elements, state-of-the-art pre- and post-processing data presentation programs, and the use of elements with curved borders. The

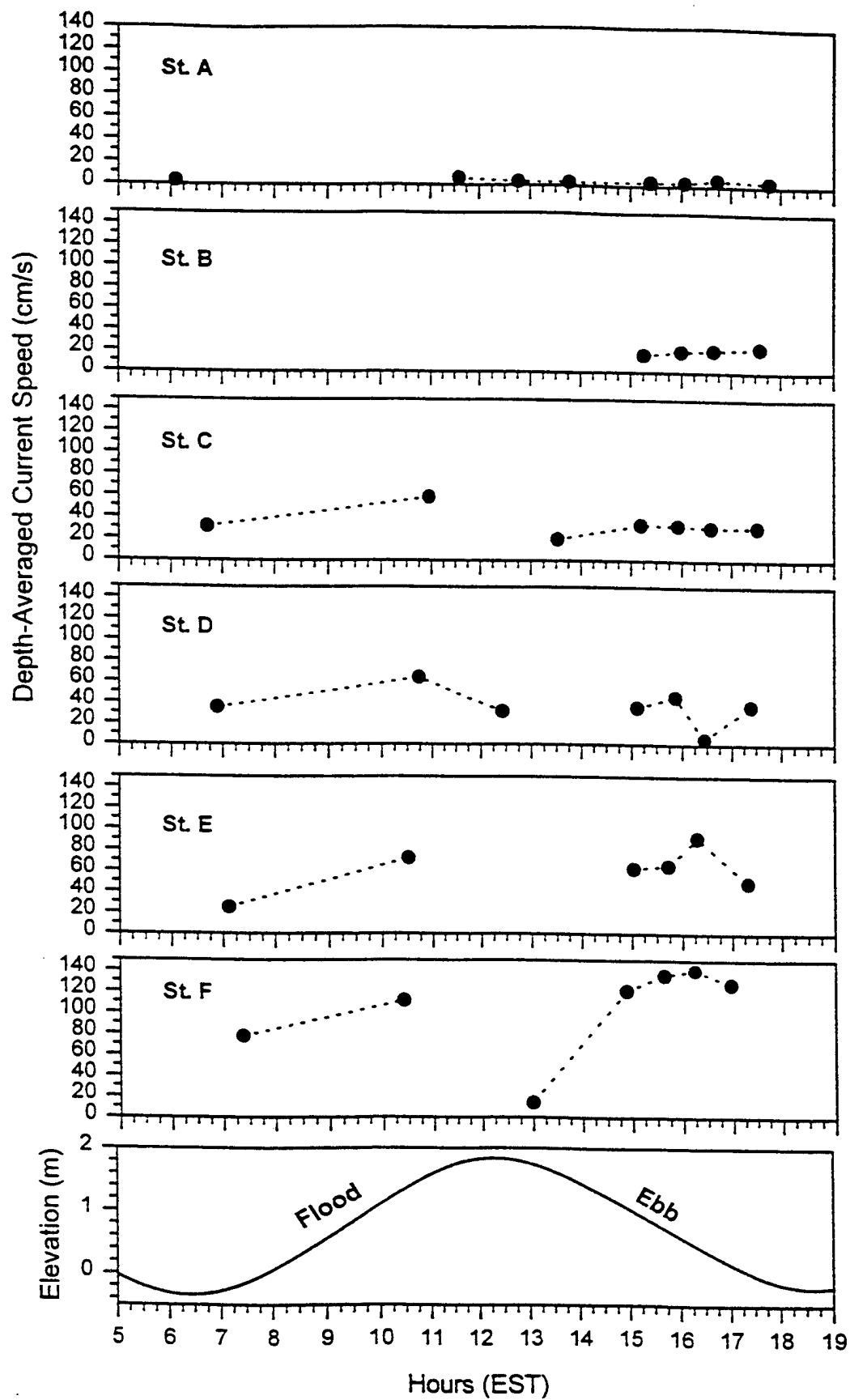


Figure 14: Depth-averaged current speed calculated from ADCP measurements at stations A to F. The predicted ocean sea surface elevation for the measurement period is also shown at the bottom as a reference.

most recent update to the model was completed in 1996 (King, 1996), which included the wet and dry node routines and their simulation as porous media.

RMA-2V is a finite element model designed for the simulation of one- and two-dimensional depth-averaged hydrodynamic systems. The dependent variables are velocity and water depth, and the equations solved are the depth-averaged Stokes equations. Reynolds assumptions are incorporated as eddy equations. The model incorporates friction losses (approximated either by a Chezy or Manning formulation), Coriolis effects, and surface wind stresses. All the coefficients associated with these terms are allowed to vary from element to element.

The generalized governing equations are: (i) momentum equations, along the x and y directions, and (ii) the continuity equation (see Appendix II).

Model Setup

To employ the RMA-2V model properly, generally three steps are required: (i) creation of a finite element grid which adequately represents the bathymetry, (ii) development of boundary conditions, and (iii) determination of friction, turbulence, and wind stress coefficients (i.e., calibration).

Finite element grid development

The grid generation process was undertaken using the data pre-processing program, RMAGEN, developed by Resource Management Associates. The digital shoreline and bathymetry data were imported into this program and the finite element grid was generated to represent the estuary. Two grids were created simulating: (i) the present geometry/bathymetry of the estuary with the presence of only one inlet (Case 1) and (ii) the case (Case 2) where a second inlet was assumed to exist north of the present inlet. This latter case simulates the Nauset system as it was during the period 1992 - 1996 (Roman et al., 1996). Since the north inlet was closed in late May, 1996, the first case simulates present conditions. The bathymetry used for both runs was identical with the exception of an inlet channel (approximately 2m deep) and a tidal delta that were created for the second case. The single inlet case grid contained 4331 nodes which formed 1320 elements, whereas the dual inlet grid contained 4483 nodes that formed 1381 elements (Figs. 15 and 16, respectively). The entire system utilized two-dimensional elements. The water depths at each nodal position were interpolated from the collected bathymetric data. For the shallow areas where no bathymetric survey was carried out (Fig. 4), depths were filled in from existing maps and from information obtained from staff of the National Park and the Towns of Orleans and Eastham who have extensive navigational knowledge of the field site.

Figs. 15 and 16 illustrate the varying grids employed in this study. Areas of relatively high velocity flow and where flow directions were expected to change over a short distance had closely spaced nodes. The inlet entrance and the area at the bend of the main channel (south of the central salt marsh island) are examples of this type of region (node spacing approximately

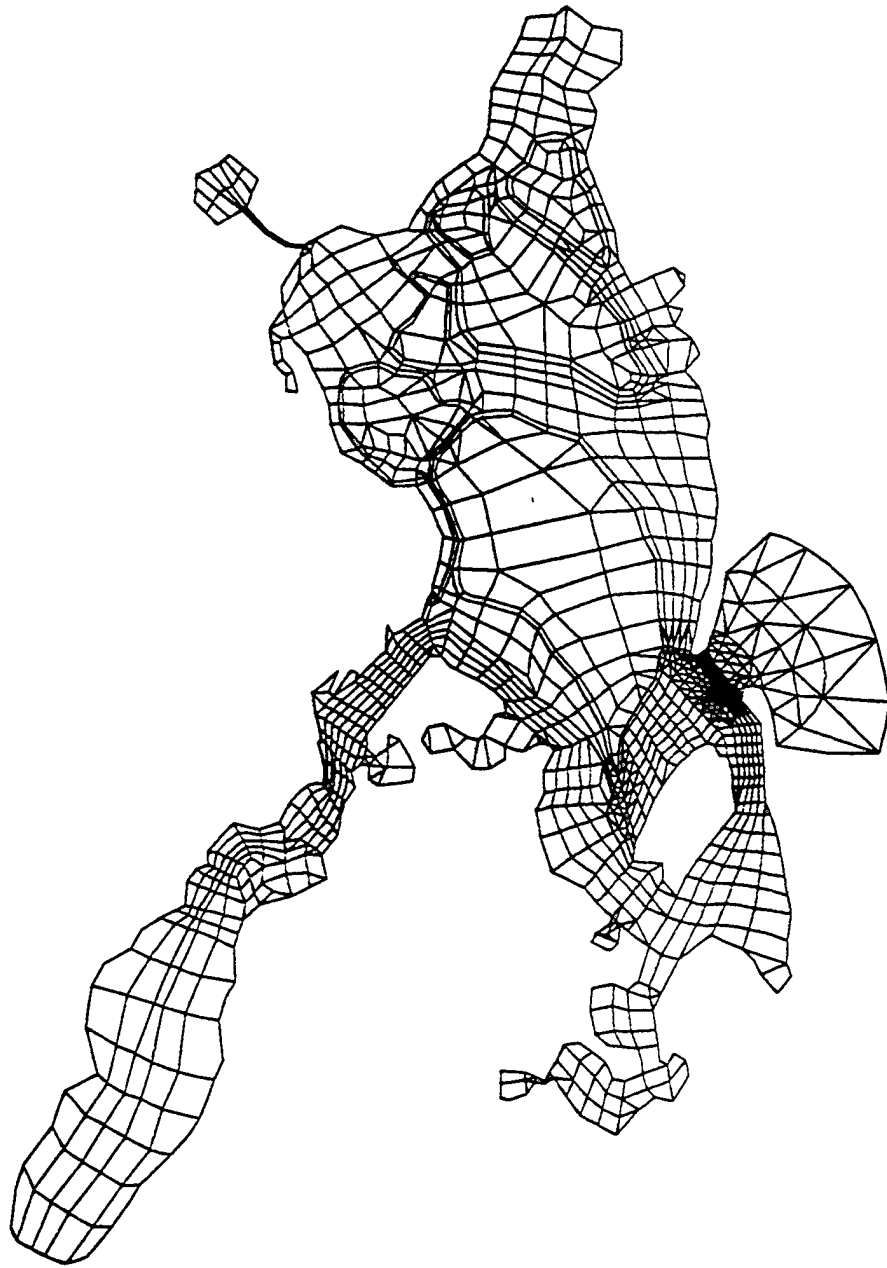


Figure 15: Finite element grid for the case of a single inlet. It consists of 4331 nodes and 1320 elements.

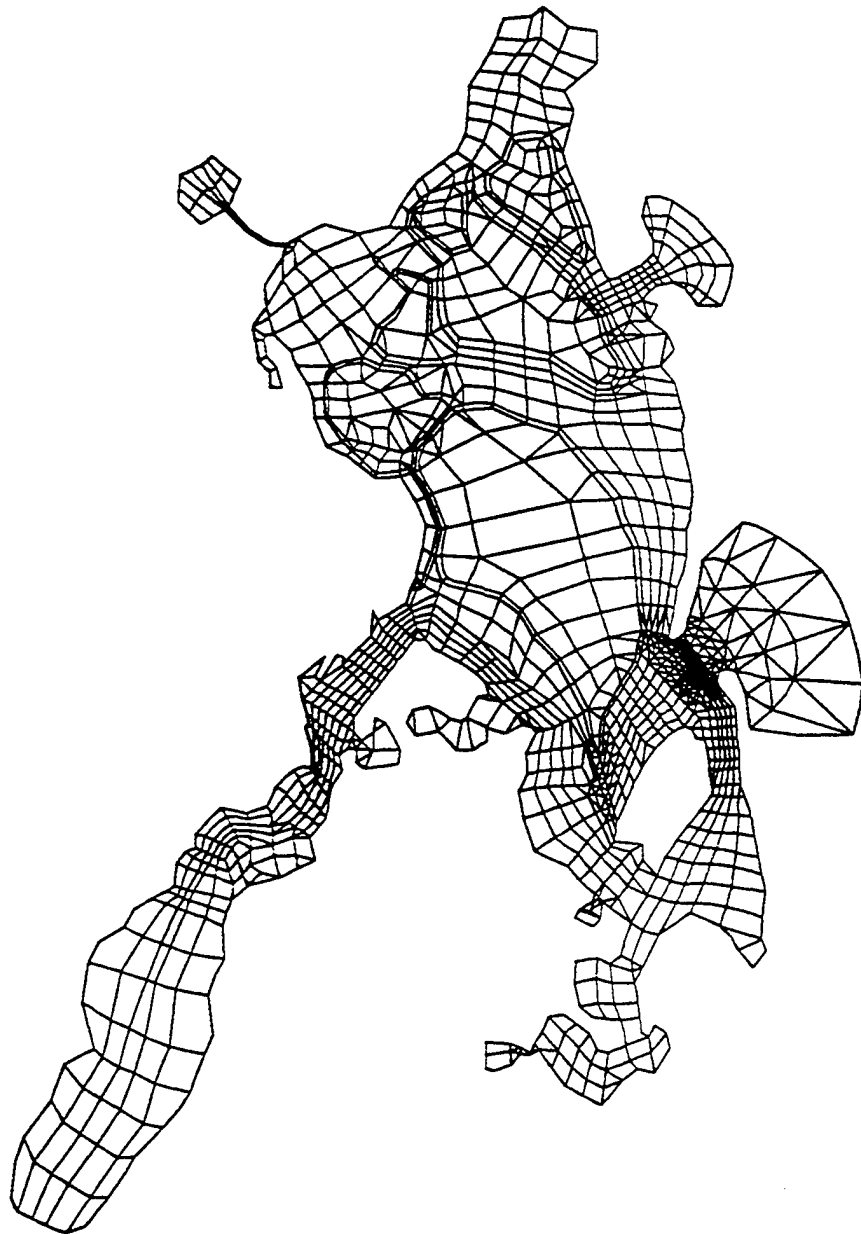


Figure 16: RMA-2V Finite element grid for the case of 2 inlets. It consists of 4483 nodes and 1381 elements.

40 m). Regions of the Nauset system which have slowly varying flow properties have widely spaced nodes (i.e., Town Cove, salt marsh areas). Detailed bathymetric and velocity information in these regions is not required.

Boundary Conditions

Three types of boundary conditions can be used with the RMA-2V model: (i) "slip", (ii) freshwater inflow; and (iii) tidal elevation boundaries.

All of the elements which had land borders were required to have "slip" boundary conditions. At these locations, the direction of flow was constrained to be along the shoreline. The model generated all internal boundary conditions from the governing conservation equations.

The freshwater inflow into the system is mainly in the form of groundwater seepage and takes place primarily in the Town Cove area. The groundwater discharge has not been included in the present modeling since no quantitative information exists and its contribution to hydrodynamic flushing action is considered to be small. Hence, the present estimates are considered to be conservative.

Since no new offshore surface elevation data were recorded, the offshore tidal boundary was created using existing information on the amplitude and phase of the offshore tidal constituents (see relevant section). Sea surface elevation at the ocean site for a period of 15 days (covering the period 12th October to 27th October 1996) and with a time step of 0.1 hours (6 minutes) was used as the driving force (boundary condition) for the model. For the single inlet case, the boundary condition was applied at the main inlet only, whereas for the dual inlet case, the same boundary condition (oceanic sea surface elevation) was applied simultaneously at both inlets. Since the offshore boundary data were of pure tidal origin (i.e., no wind effects), the predicted sea surface elevations from the gauge data collected inside the estuary were used to calibrate the model. Thus the hydrodynamic model runs and calibrations were carried out for pure tidal forcing.

The boundary condition (oceanic tide, see Fig. 9) exhibits a daily variation in the amplitude of the tide. Although the variation between the amplitudes of the two daily high tides is typically less than 20 percent, accurate determination of flushing rates must account for fluctuations of this nature. Similarly, neap-spring variations must be included in estimates of residence time.

Model Calibration Procedures and Results

Values for eddy viscosity and friction were required for this application of the RMA-2V model. However, since the wind field was ignored, no coefficients related to wind stress were involved in the analysis. The calibration procedure consisted of matching the phases and elevations predicted by the model with those measured by the six tide-gauge stations (Fig. 3). Trial runs (>50) of the hydrodynamic model were performed to determine appropriate values for the various coefficients. In addition, coefficient values were chosen that matched the physical

representation of the estuary. Past tidal hydrodynamic studies supplied the proper range for these coefficients (e.g., Speer and Aubrey, 1985; Friedrichs and Aubrey, 1989).

Initial model runs utilized "typical" values for the Manning's friction coefficient between 0.02 and 0.04. These values correspond to Manning's coefficients determined experimentally in smooth earth-lined channels with no winding channels with pools and shoals (Henderson, 1966). The Nauset estuary was basically divided into three major morphological units: (i) channels; (ii) flat sandy areas and (iii) salt marshes. Friction within the model affects tidal damping in areas of relatively high water velocities whereas areas of low velocity contribute little to tidal damping. The model was run for various values of friction coefficients, after which the sea surface elevations predicted by the model were compared to those corresponding to the measurements. The selected friction coefficients varied between 0.02 and 0.075. The best fit between model and data (Figs. 17 and 18) was achieved for the selection of values described below.

The flat sandy areas were assigned a friction coefficient of 0.02; the channels were assigned a friction coefficient of 0.04. The higher friction coefficient accounts for the form drag generated by the creation of ripples and sand waves on the bottom of the channels. Exceptions to this were the channels in the Nauset Harbor area which were assigned a value of 0.03. The intertidal salt marsh areas were assigned a high (0.065 to 0.075) friction coefficient, representative of their greater dissipation potential (e.g., Burke and Stolzenbach, 1990).

The turbulent exchange coefficients within the model are an approximate representation of energy losses due to turbulent effects at the space scale of the numerical modeling elements. According to King (1990a), these values are proportional to element dimensions and flow velocities. The suggested value for this coefficient is approximately 0.1 times the element dimension. This value was used for the entire area except the inlet entrances, where the multiplier of 0.2 was used to account for the high turbulence found there.

The numerical model was run using a 200 MHz, Pentium® Pro computer. The computational time for a 15-day simulation was approximately 30 hours.

The current speed predicted by the model for the locations of the ADCP measurement stations was compared to the data collected (Fig. 19). Measured current speeds are site-specific and can exhibit high variability within short distances, while model predictions are both depth- and spatially averaged. The scale of the spatial averaging is a function of the element size of the grid which was variable throughout the system. Therefore, simple inter-comparison of measured current speeds, at a single location, with simulated data are usually less successful than with surface elevation data. Despite the above limitations, the model, in this particular application, predicts correctly the phases of the current speed (Fig. 19). The reduction of the magnitude of the current away from the inlet, captured by the data, is also predicted by the model. In some case (stations C and D), even the magnitude of the current predicted by the model agrees with the measured values. In Town Cove, the model predicted lower current speeds than the measurements indicated. This is attributed to the large size of the elements in this area and thus to large spatial averaging. The good agreement between model-predicted current speeds and

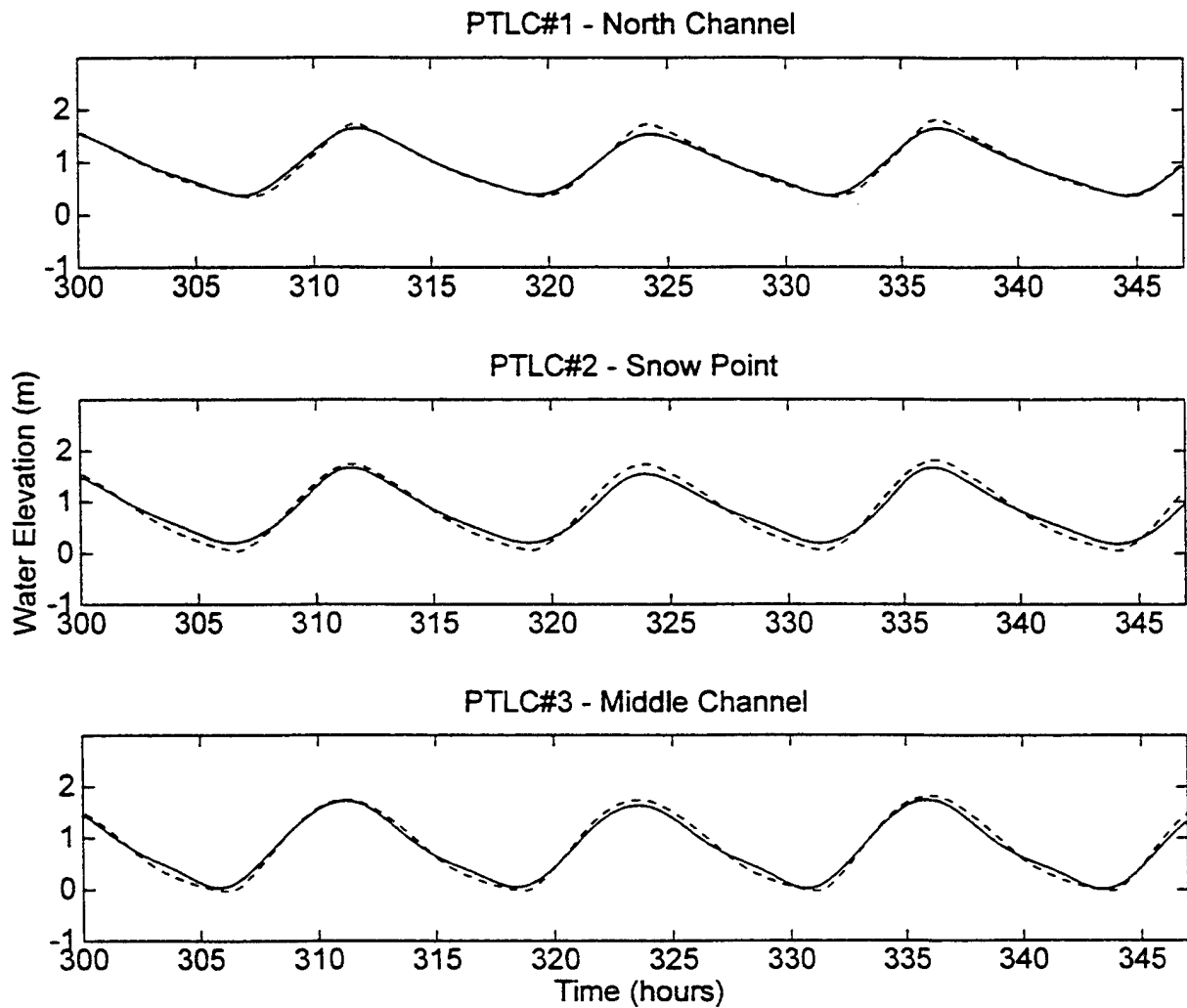


Figure 17: Model Calibration. Sea surface elevations: measured (solid line) versus predicted by the hydrodynamic model (dashed line).

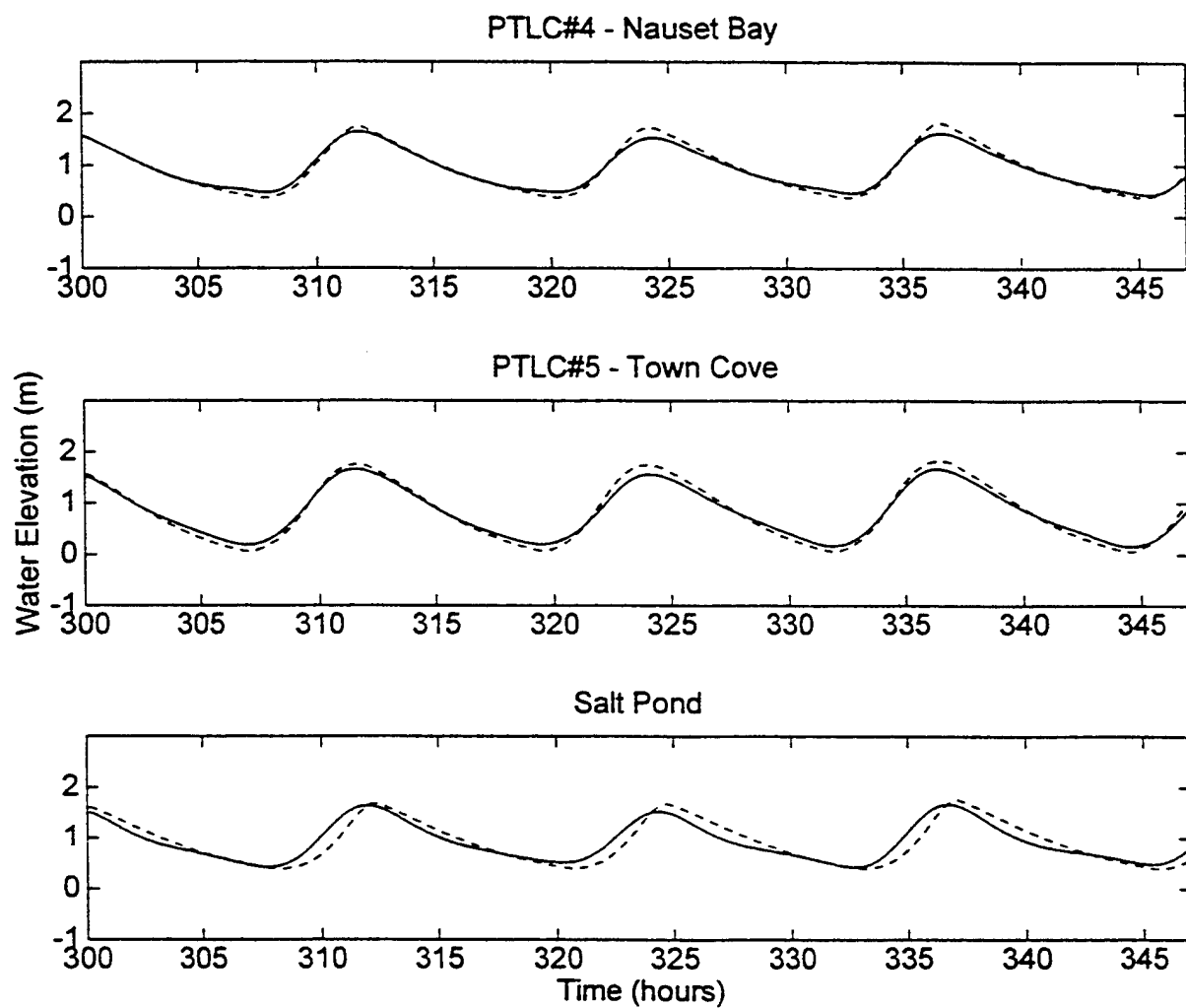


Figure 18: Model Calibration: Sea surface elevations: measured (solid line) versus predicted by the hydrodynamic model (dashed line).

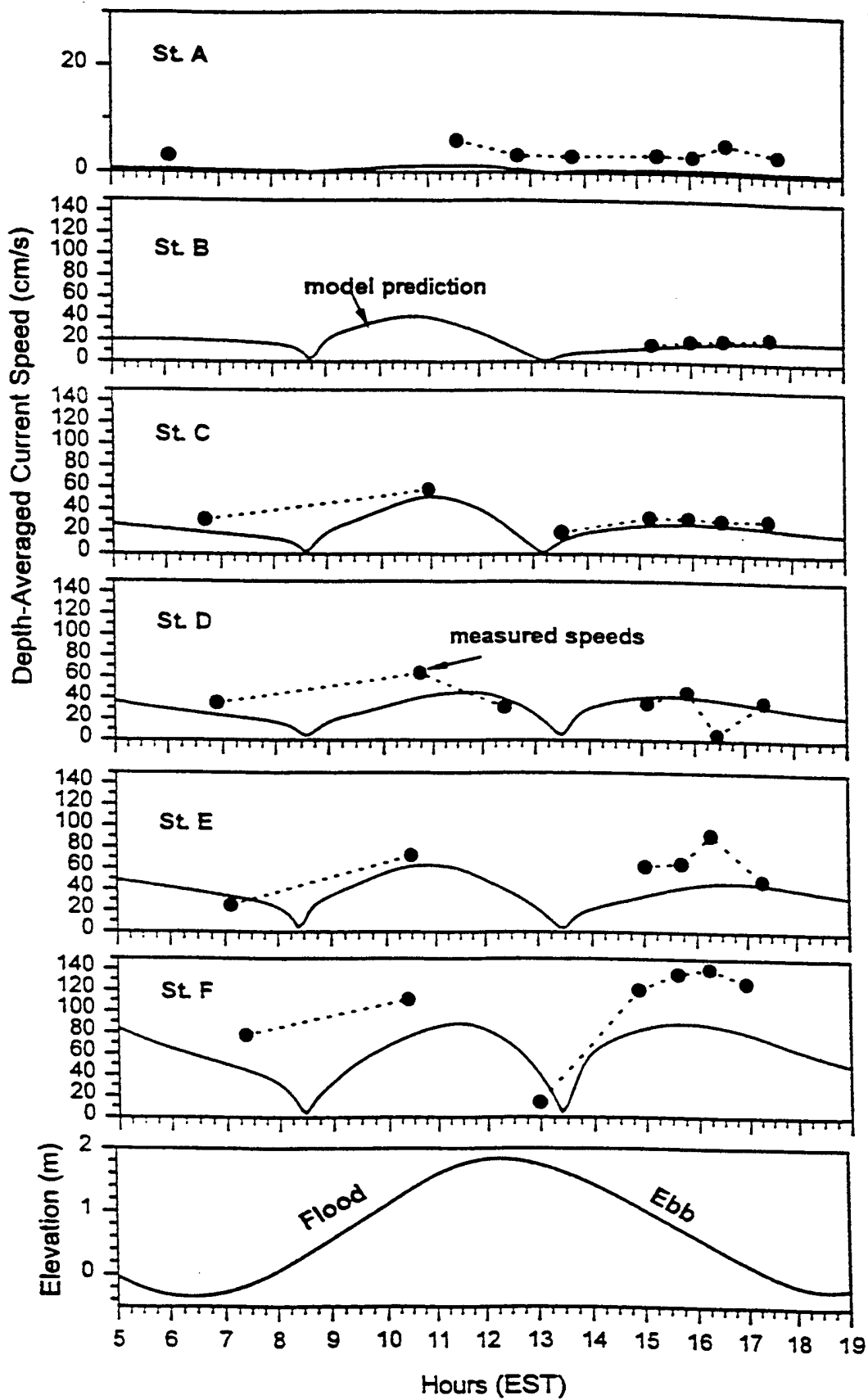


Figure 19: Intercomparison of depth-averaged current speeds: measured (solid circles) versus predicted by the model (solid lines). The forcing tide is also shown for reference.

measurements offers another independent degree of confidence on the accuracy of this numerical simulation.

An example of the model velocity output is shown in Fig. 20. A series of vector diagrams of flow velocity, for the two cases of single and dual inlets, respectively, and for different stages of the tide, is shown in Appendix III. In the appendix, the vectors are the result of averaging/interpolating the irregularly-spaced original output of the model into a regular, uniformly-spaced grid.

Model Results and Residence Times

The applied scientific goal of this study is to predict the residence times for different portions of Nauset embayment under different inlet/barrier states. We use the results from the field observations and the numerical analysis to estimate residence times. To gain further insight into the residence times and to provide more input for management, we used the hydrodynamics in various ways to estimate residence times based on different assumptions. This approach reveals the sensitivity of the Nauset embayment under different scenarios and provides a tool for appropriate management of the ecosystem.

Hydrodynamics and Water Circulation

The calibrated hydrodynamic model may be used to predict water elevations and depth-averaged water velocities throughout the estuarine system. In addition, flushing rates of the various sub-embayments can be calculated as an index of relative water quality. The marsh system was divided into sub-embayments (basins), and the flow rate (Q , m^3/s) across their boundaries and the inlet(s) was calculated by the model for each time step (6 min). In total, six basins were defined (Fig. 21, Table 4). Prior to calculating the residence times, the modelled hydrodynamics of the system are examined both for the present configuration (single inlet) and for the case of dual inlets.

Table 4: Definition of sub-embayments used for calculation of flow rates across their boundaries and residence time (see Fig. 21).

Basin	No. of adjacent boundaries
Town Cove (1)	1
Mill Pond (2)	1
Nauset Harbor (3)	2
Salt Pond (4)	1
North Basin (5)	1
Middle Channel (6)	1

The Nauset estuary is a complex system consisting of a main channel (Middle Channel) which carries the main volume of water; it connects Town Cove with the open ocean. The north part of the system is fairly shallow with extensive intertidal areas. There, the average tidal fluctuation is larger than the average local mean depth. During a typical tidal cycle, the volume of water exchanged between the ocean and the system is approximately equal to the area of the



Figure 20: Example of the current velocity results, during the flood stage of the tide, obtained by application of the model. One vector is shown for each node of the finite element grid; the length of the vector represents the magnitude of current velocity (in m/s). Appendix III contains more examples of model simulations.

Nauset Estuary

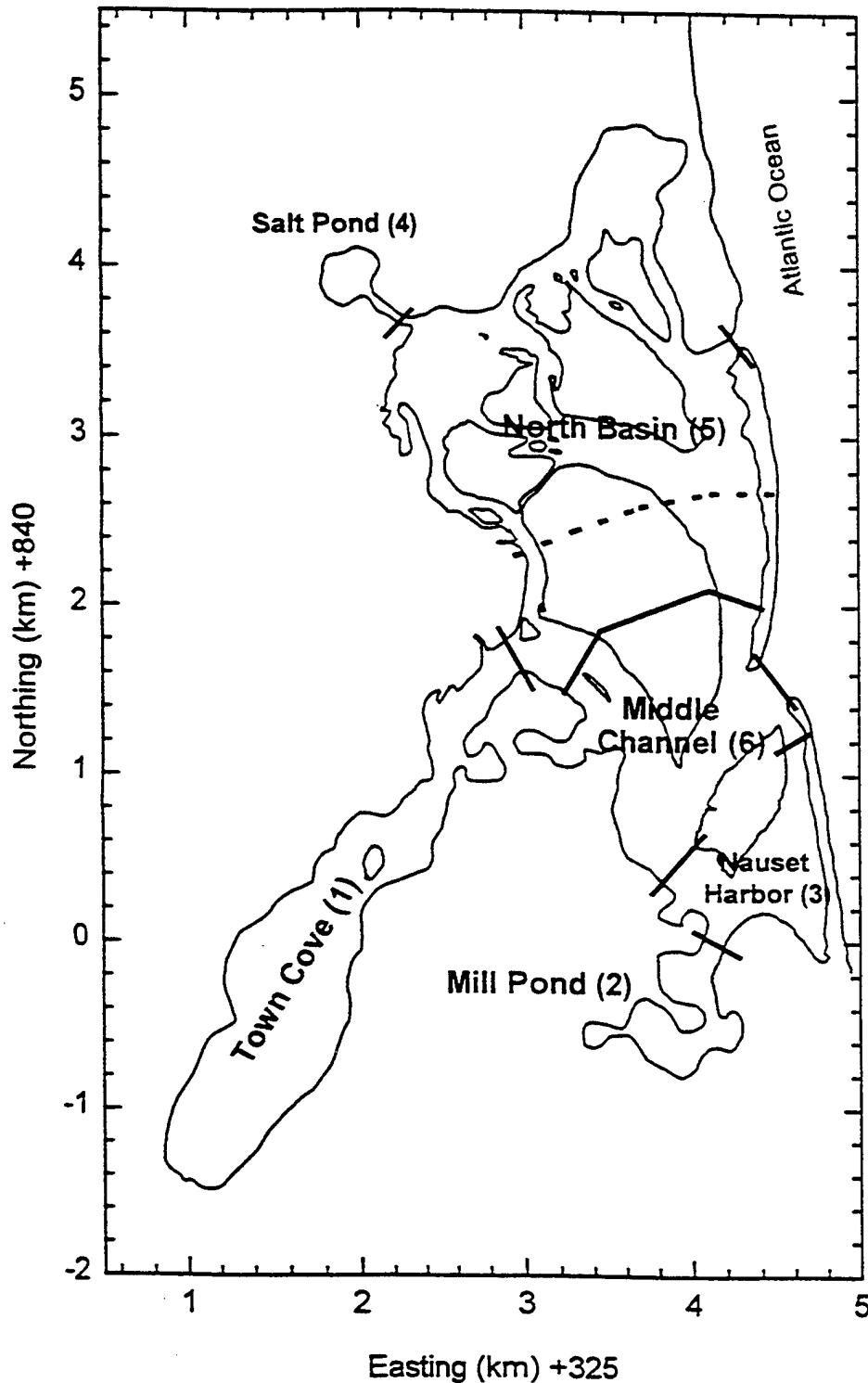


Figure 21: Map showing the sub-embayments into which the Nauset estuary was divided. The solid lines represent the boundaries between adjacent basins where flow rates were calculated for each time step during the numerical simulation. (Note: A 2nd line (dotted line) was defined for separating the North from the Middle Channel basins; this is examined as option 2).

system times the tidal range. This approximation does not account for tidal damping (decreasing tide range with distance from the inlet) for the volume of estuarine water which returns through Nauset inlet from offshore during a typical tidal cycle (recycled water). The offshore currents and dispersion are the mechanisms that control the amount of recycled estuarine water which returns into the system during flood tide. For our purposes, we assumed that the water entering the embayment from the ocean contained no recycled estuarine water discharged during the previous tidal cycle.

The RMA-2V model computed tidal damping and flow rates throughout the system (see calibration procedure). For the case of two inlets, the tidal damping and flow rates were changed significantly from the single inlet case. In particular, tidal damping was reduced for all stations (see Fig. 22). The reduction was greater at the stations located at the north part of the system (i.e., PTLC#1 in the North Channel near the second inlet, PTLC#4 in Nauset Bay and in the station in Salt Pond; see Figs. 22a and b). The reduction in frictional damping was much less in the stations located at Town Cove (PTLC#5), Snow Point (PTLC#2) and Middle Channel (PTLC#3). The second inlet serves mainly the northern part of the system, whereas the southern part continues to be served by the main (south) inlet. In the case where Nauset has only one inlet, as was the case prior to the southern breach in December 1992, the system is expected to behave in a fashion similar to the single inlet scenario presented in this study. Compared to the dual inlet scenario, the single inlet scenario will create greater phase lags and increased amplitude decay in the southern segment of the embayment, leading to longer residence times. This situation arises because of the greater separation of the single inlet from Town Cove (for instance) compared to the dual inlet scenario.

A better understanding of the impact of the second inlet on the general circulation of the system can be achieved by comparing the flow rates between the different sub-embayments. This comparison (Figs. 23a and b) shows flow rates across the sub-embayment boundaries as a function of time, for the cases of a single inlet (solid line) and dual inlets (dashed line), respectively. The existence of a second inlet results in reduction of the flow through the main inlet. However, the exchange of water between Nauset Harbor and Middle Channel, and between Town Cove and Middle Channel, does not change significantly. The major changes occur across the boundaries located on the northern part of the estuary. The flow across the boundary which separates the northern part of the estuary from the remaining part (dotted line in Fig. 21) is insignificant after the opening of the second inlet, suggesting that this line can be used to approximate the partition of the system into two major sub-embayments that are served by each of the two inlets respectively.

Finally, a schematic diagram of the water circulation in the Nauset estuary during the flood and ebb stage of the estuary is shown as Fig. 24, for both cases (single and dual inlets). The area served by the second (northern) inlet can be seen clearly.

Residence Times

Based on the results of the model, predictions of residence times for the embayment system were possible for both cases. These predictions were carried out using both the mean low water (Aubrey Consulting, Inc., 1996) and mean tide volume (Zimmerman, 1988) of the

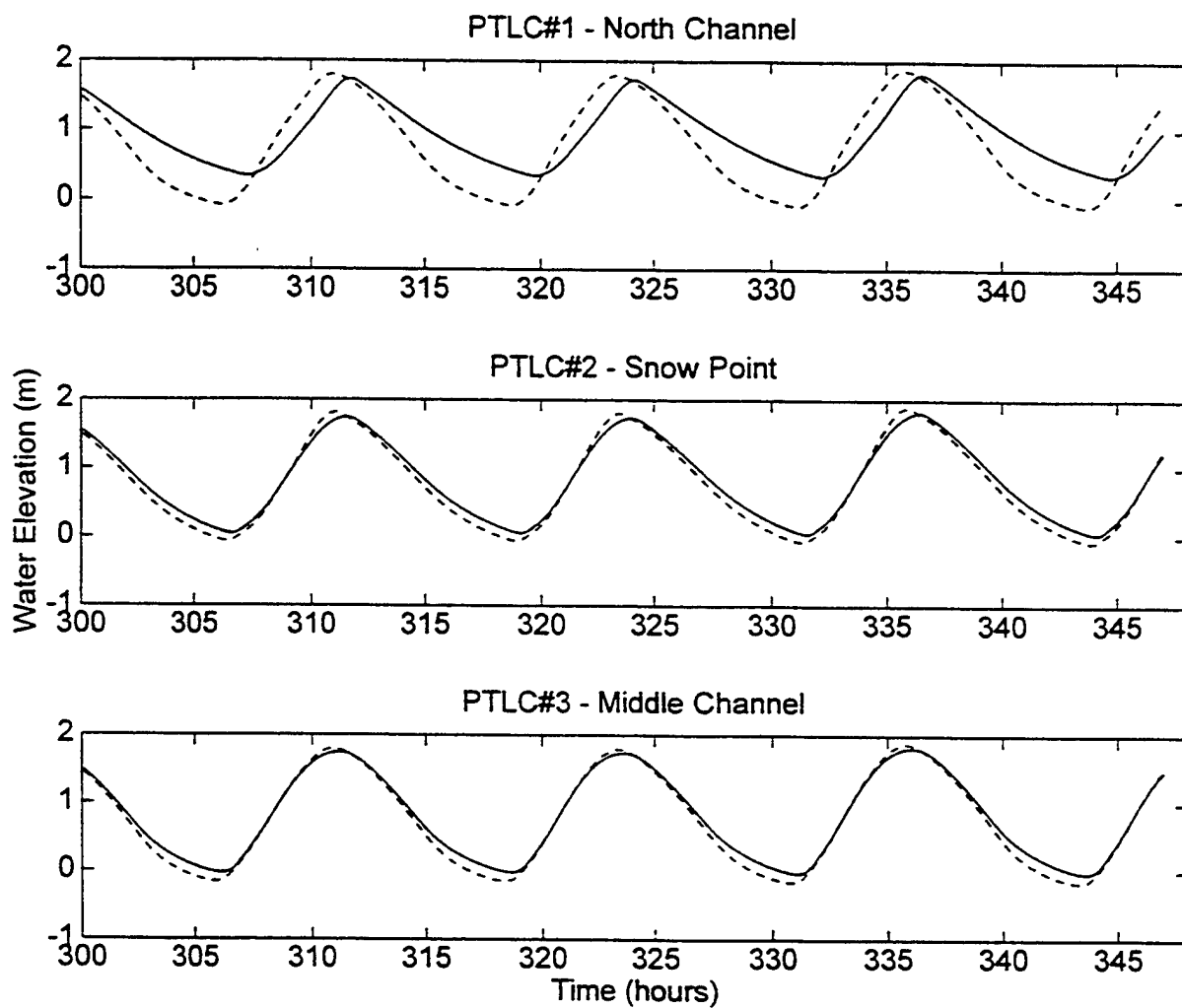


Figure 22a: Water elevation at the tide-gauge stations, predicted by the model for the cases of single (solid line) and dual inlets (dotted line), respectively.

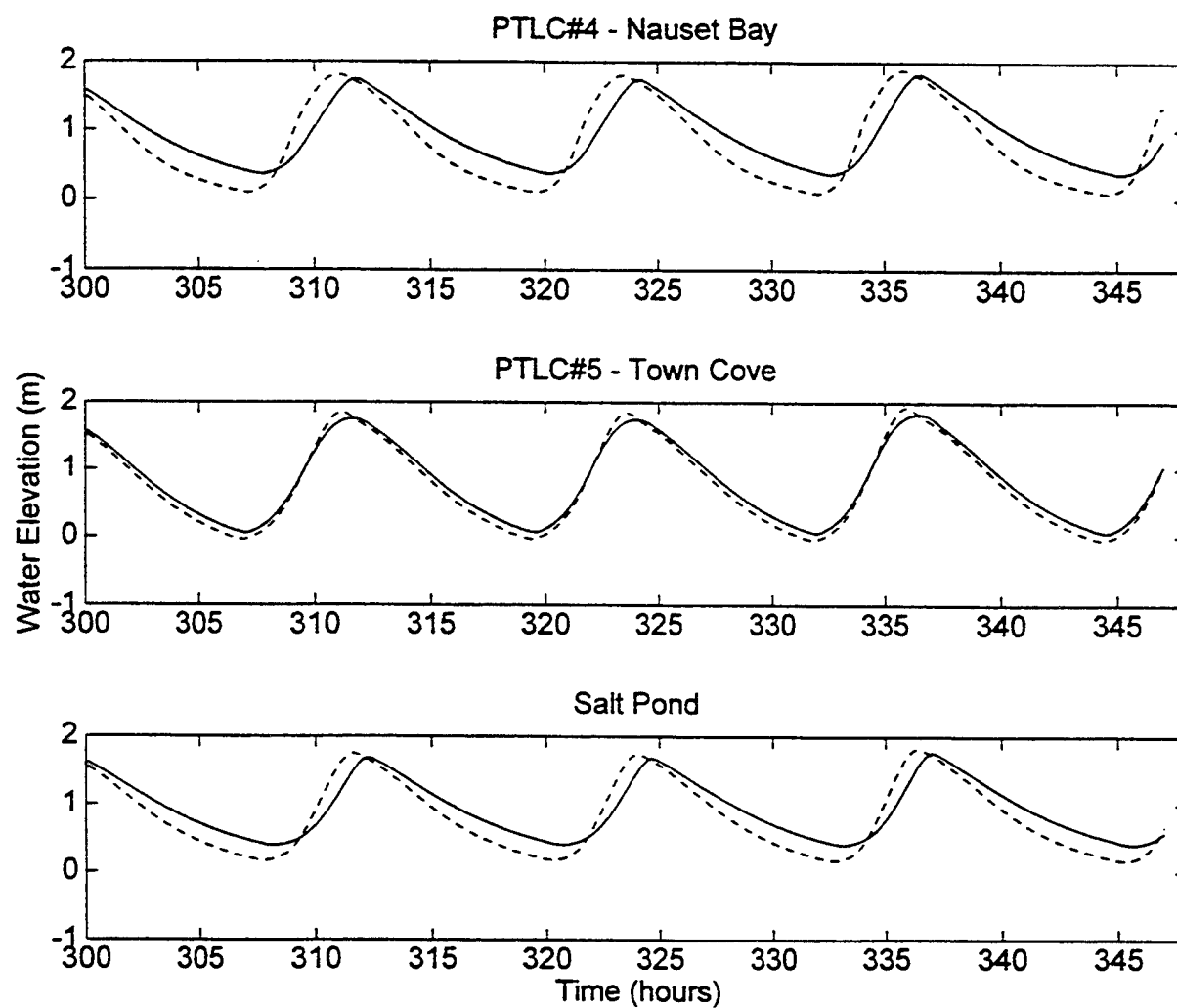


Figure 22b: Water elevation at the tide-gauge stations, predicted by the model for the cases of single (solid line) and dual inlets (dotted line), respectively.

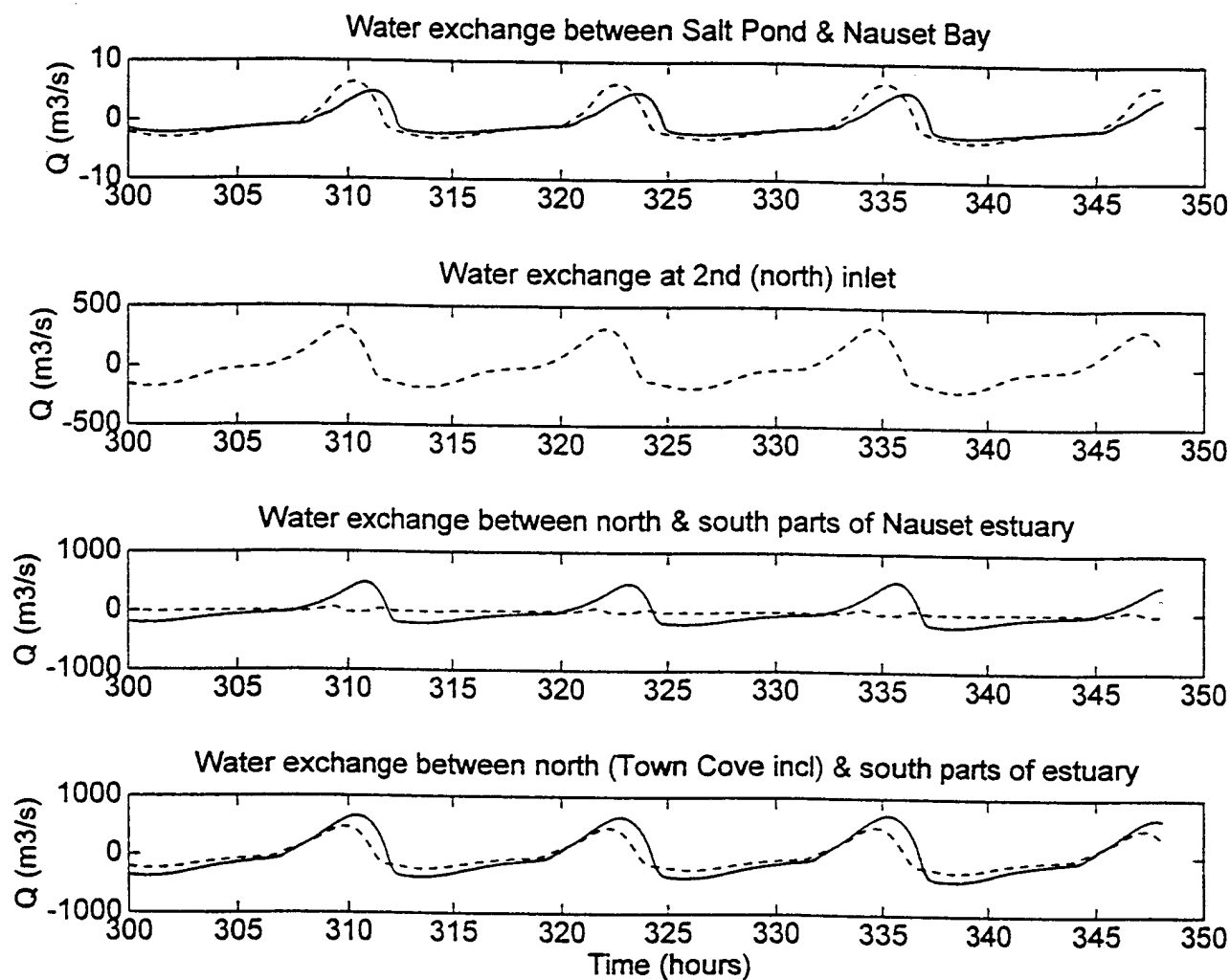


Figure 23a: Time-series of flow rates across the sub-embayment boundaries for the case of single (solid line) and dual inlets (dotted line), respectively.

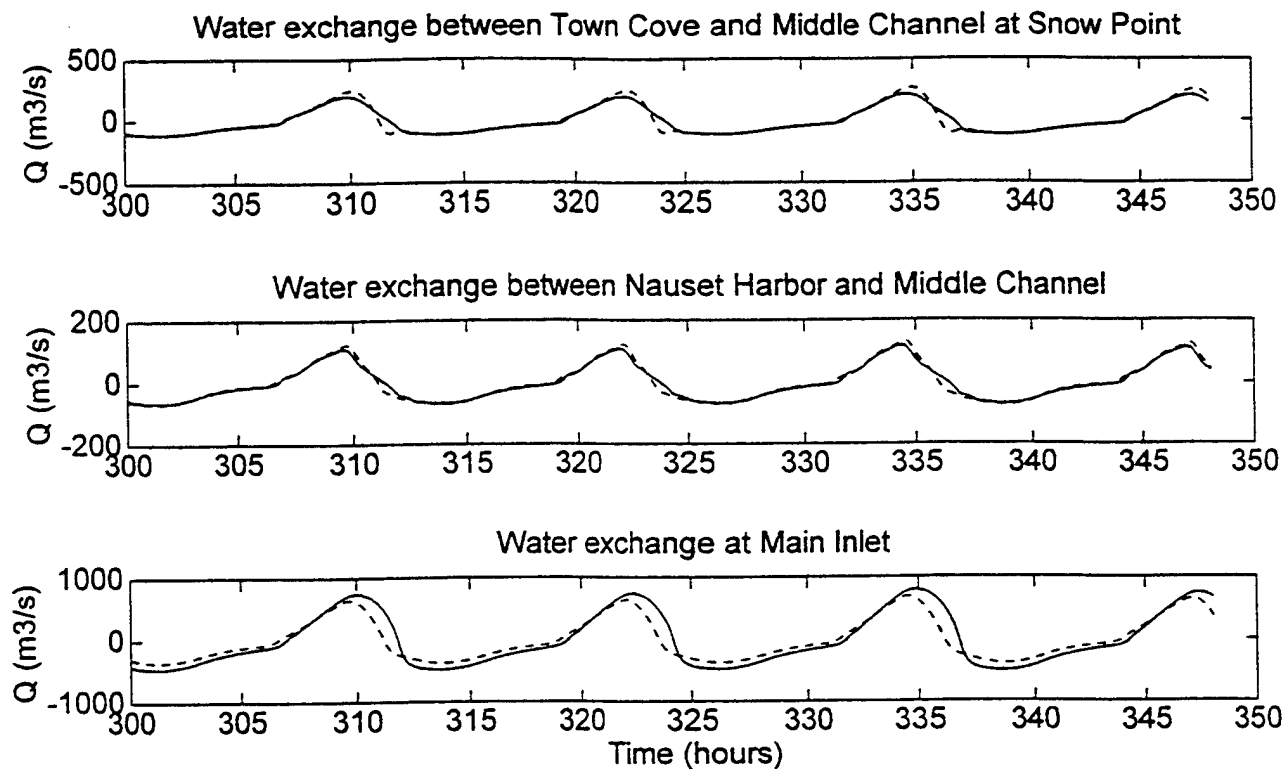


Figure 23b: Time-series of flow rates across the sub-embayment boundaries for the case of single (solid line) and dual inlets (dotted line), respectively.

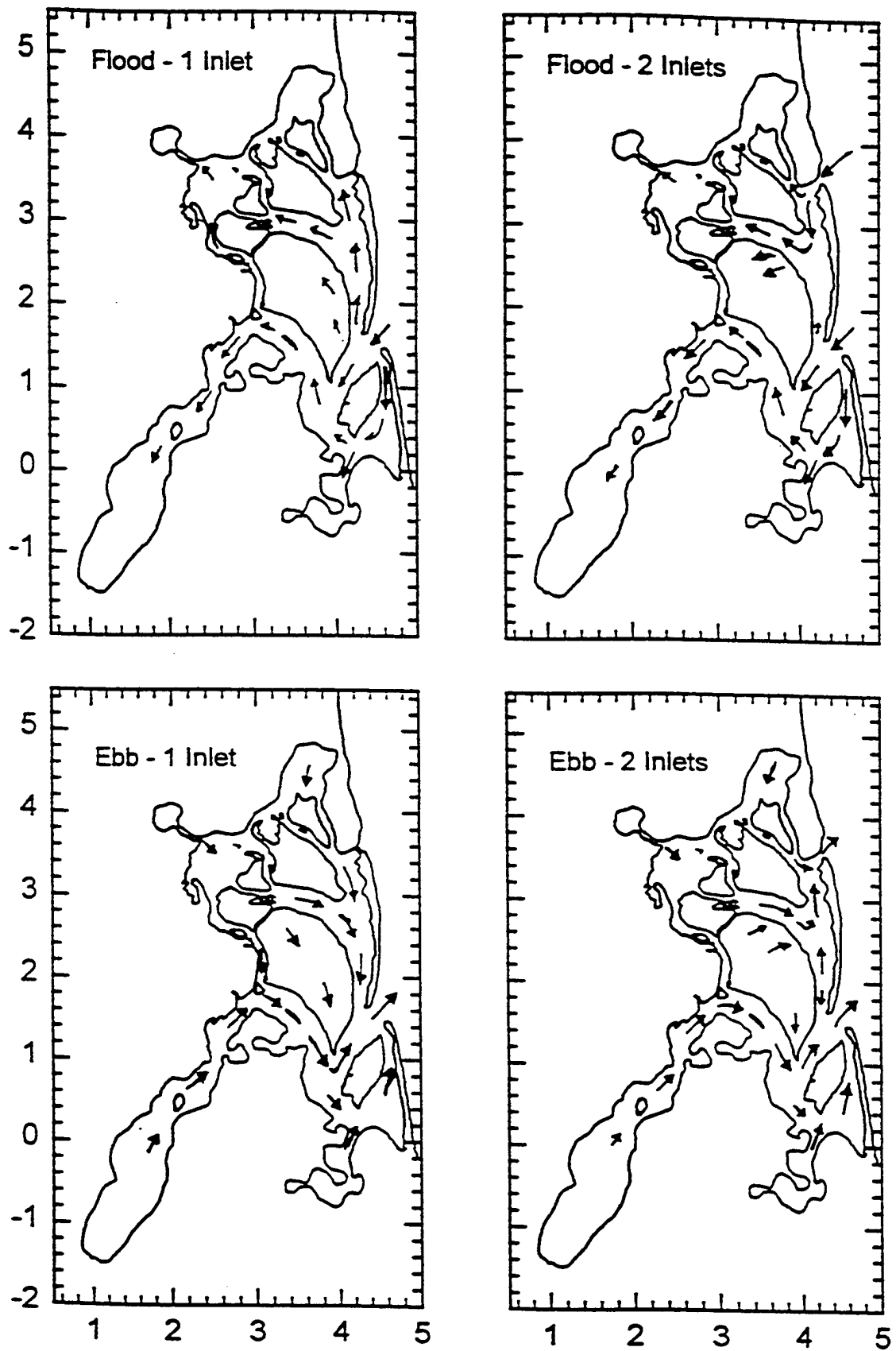


Figure 24: Schematic diagram of water circulation in Nauset estuary during the flood and ebb stages of the tide for the case of single and dual inlets respectively

system and flow at the boundaries shown in Fig. 21. The tidal volumes of each sub-embayment for high, low and mean water were calculated from the instantaneous water volumes of each element as calculated by the numerical model. These volumes are listed in Table 5.

Table 5: Volume of water in the various sub-embayments of the Nauset Marsh System at Mean High (V_{MHW}), Mean Low (V_{MLW}) and Mean Water Level (V_{MWL}), respectively.

Basin	$V_{MHW} (m^3)$	$V_{MLW} (m^3)$	$V_{MWL} (m^3)$
Town Cove (1)	5.02×10^6	2.60×10^6	3.44×10^6
Mill Pond (2)	3.60×10^5	1.38×10^5	2.00×10^5
Nauset Harbor (3)	1.01×10^6	2.12×10^5	4.80×10^5
Salt Pond (4)	3.30×10^5	2.26×10^5	2.65×10^5
North Basin (5)	5.54×10^6	1.15×10^6	2.11×10^6
Middle Channel (6)	2.54×10^6	6.04×10^5	1.13×10^6
Whole System	2.06×10^7	4.91×10^6	7.62×10^6

The volumes presented here are averaged over a neap-spring tidal cycle (15 days).

Residence times were calculated for both cases (single and dual inlets) and using both the local basin volume and the total volume of the whole estuary. The results of the calculations are listed in Tables 6 and 7.

Table 6: Case: 1 Inlet. "Local" Flushing times (in hours) of the sub-embayments defined in Fig. 21.

	$V_i = V_{MLW}$			$V_i = V_{MWL}$		
	Neap Tide	Spring Tide	Average	Neap Tide	Spring Tide	Average
Middle Channel.	1	1	1	2	2	2
Town Cove	21	16	19	30	23	26
Mill Pond	8	5	6	12	9	10
Nauset Harbor	3	3	3	9	6	7
Salt Pond	87	65	74	103	77	88
North Basin	3	2	2	6	4	5

Flushing times listed are for the smallest Neap, largest Spring and tidal elevation averaged over a 15-day period.

Table 7: Case: 1 Inlet. Residence times (in hours) for the whole Nauset Marsh System and for the sub-embayments as defined in Fig. 21.

	$V_o = V_{MLW}$			$V_o = V_{MWL}$		
	Neap Tide	Spring Tide	Average	Neap Tide	Spring Tide	Average
Whole System	9	7	8	17	12	14
Town Cove	37	28	32	68	52	59
Mill Pond	245	177	206	450	326	378
Nauset Harbor	72	54	62	132	98	113
Salt Pond	1737	1303	1482	3190	2392	2720
North Basin	11	8	9	21	15	17

Flushing times listed are for the smallest neap, largest spring and tidal elevation averaged over a 15-day period. Values shown were calculated using equation (4) with the volume of water (V_o) estimated at mean low water (MLW) and mean water level (MWL), respectively.

Based on the average “local” residence times, most of the sub-embayments of the system are able to recycle their water volume within a few hours (Table 6). Restricted basins such as Mill Pond, Town Cove and Salt Pond require much larger times to locally renew their water volume (10, 26 and 88 hours respectively).

Due to the relatively large tidal range (1.5m) in relation to mean depth (1.25m), the average residence time for the entire embayment system is relatively short and most of the water contained in the Nauset system is exchanged almost every tidal cycle (residence time 14 hours). The residence time for Town Cove is approximately 2.5 days. Salt Pond and Mill Pond are the two areas of the system with the longest residence times (approximately, 113 and 16 days, respectively). Nauset Harbor has a flushing time of approximately 5 days.

The high residence time predicted for Mill and Salt Ponds may be misleading. Small sub-embayments which are relatively far from the main inlet to the system exhibit high residence times due to the nature of the residence time definition. However, an average water parcel within either of the Ponds will require only a fraction of the computed residence time to migrate into the main channel and then to the open ocean. Since the major purpose for calculating residence times is to establish relative water quality parameters within an estuarine system, care should be exercised when applying the extreme high values. Nevertheless, the calculated values shown in Table 7 combined with the “local” residence values listed in Table 6 can be used to identify Salt Pond, Mill Pond and Town Cove as the most sensitive areas of the system.

Calculation of residence times also was undertaken for the case of dual inlets. The results are shown in Tables 8 and 9 for the “local” and “total” times, respectively.

Table 8: Case: 2 Inlets. "Local" residence times (in hours) of the sub-embayments defined in Fig. 21.

	$V_i=V_{MLW}$			$V_i=V_{MWL}$		
	Neap Tide	Spring Tide	Average	Neap Tide	Spring Tide	Average
Middle Channel.	1	1	1	3	2	2
Town Cove	19	14	16	21	19	22
Mill Pond	7	5	6	10	8	9
Nauset Harbor	3	2	3	7	5	6
Salt Pond	66	52	66	77	61	68
North Basin	<1	<1	<1	5	3	4

Residence times listed are for the smallest neap, largest spring and tidal elevation averaged over a 15-day period. Values shown were calculated using equation (3) with the volume of water (V_i) estimated at mean low water (MLW) and mean water level (MWL), respectively.

Table 9: Case: 2 Inlets. Residence times (in hours) for the whole Nauset Marsh System and for the sub-embayments as defined in Fig. 21.

	$V_o=V_{MLW}$			$V_o=V_{MWL}$		
	Neap Tide	Spring Tide	Average	Neap Tide	Spring Tide	Average
Whole System	8	6	7	13	10	11
Town Cove	36	27	31	56	42	48
Mill Pond	245	177	207	400	311	354
Nauset Harbor	72	54	61	112	83	95
Salt Pond	1436	1132	1262	2227	1754	1956
North Basin	1	1	1	17	13	14

Residence times listed are for the smallest neap, largest spring and tidal elevation averaged over a 15-day period. Values shown were calculated using equation (4) with the volume of water (V_o) estimated at Mean Low Water (MLW) and Mean Water Level (MWL), respectively.

The existence of the second inlet induces a new circulation pattern, which reduces the residence time of the whole system by 18%. The individual sub-embayments have their residence times reduced from 6% (Mill Pond) up to 28% (Salt Pond).

Since the new circulation pattern showed that the whole system is hydrodynamically separated into two parts having relatively independent hydrodynamics (i.e., northern and southern parts served by the northern and southern inlets, respectively), then it is reasonable to assume that water particles from the one part do not mix with water particles from the other part (assuming that diffusion processes at high water have minimal effect in the transfer of pollutants). In such a case, the residence times shown in Table 9 can be re-calculated using equation (4) but replacing the total volume of the whole embayment with the volume of each part of the estuary ($V_{MLW} = 1.37 \times 10^6$ and $3.54 \times 10^6 \text{ m}^3$; $V_{MWL} = 2.37 \times 10^6$ and $5.25 \times 10^6 \text{ m}^3$, for

the northern and southern parts of the system, respectively), depending on the location of the sub-embayment under consideration. The new residence times are listed in Table 10.

The separation of the Nauset system into two independent systems under the dual inlet scenario reduces the residence times by approximately 30% and 70% for sub-embayments in the southern and northern sub-systems, respectively, contributing to overall better flushing characteristics.

Table 10: Case: 2 Inlets. Residence times (in hours) for the Nauset Marsh System assuming the existence of two inlets. The numerical simulation showed that the basin is separated into two parts (northern and southern) with independent hydrodynamic behavior. Flushing times were calculated using equation (4) with the volume of water V_o being defined as the volume of the northern segment for Salt Pond and North Basin, whereas for the remaining sub-embayments the volume of water of the southern segment was used. Residence times listed are for the smallest neap, largest spring and tidal elevation averaged over a 15-day period.

	$V_o = V_{MLW}$			$V_o = V_{MWL}$		
	Neap Tide	Spring Tide	Average	Neap Tide	Spring Tide	Average
Whole North Part	6	5	5	9	7	8
Whole South Part	2	2	2	4	4	4
Town Cove	26	20	22	38	29	33
Mill Pond	176	128	148	276	214	244
Nauset Harbor	52	39	44	77	57	66
Salt Pond	402	319	353	692	545	608
North Basin	<1	<1	<1	5	4	4

CONCLUSIONS AND RECOMMENDATIONS

The WHOI study provides estimates of residence times that are useful for estimating the effects of build-out in the watershed of the system on water quality. The study examined the dependence of residence time on a number of factors:

- use of mean low water volume versus mean water volume
- assumption of neap, spring, or mean tidal range
- assumption of one versus two inlets
- assumption of use of "local" sub-embayment cleansing versus cleansing of the entire embayment (recycled water argument).

Significant differences in residence times arise from the use of the various assumptions. The most conservative residence time is one that is based on mean water volume, neap tidal

range, single inlet, and use of cleansing of the entire embayment by exchange of water with the "cleaner" ocean (Table 9). The predicted times should be viewed as relative only.

The longest residence times are found in Mill and Salt ponds, as anticipated. Residence times here are 10 to 100 times longer than those of other portions of the embayment. Town Cove has a relatively slow turnover rate (short residence time), not as rapid as the main channels serving the entire embayment. The residence times of Mill and Salt ponds and Town Cove are only roughly approximated by the present modeling. Vertical temperature stratification and greater water depths suggest that mixing under some conditions may be three-dimensional not two-dimensional as the present model assumed. Biological and biogeochemical processes may lead to accumulation of nutrients in the sediments of these deeper water bodies. Such nutrient accumulation may lead to poorer water quality when these nutrients are released to the water column (benthic flux), and stratification may lead to anoxia or hypoxia in deeper bottom waters. A more sophisticated modeling effort is required to predict these dynamics. Algal blooms in Town Cove are a reflection of these more complex dynamics.

The Nauset embayment experiences rapid and significant morphological changes on a rapid basis. New inlets, rapid migration of inlets, barrier roll-over, barrier attachment, and various other conditions occur on a time scale of less than a decade. Implications for these changes on the water quality within various embayments are profound. Hence, the following recommendations are made:

- 1) A department (preferably also an individual) within the Town(s) should be charged with oversight of the residence time and water quality issues. A preferred alternative would be a standing technical committee addressing multi-agency concerns.
- 2) One or more individuals from that department or committee should receive training on the numerical model module provided to the Town of Orleans under this contract. Use of this module would be for demonstration purposes, as well as education and training to understand how the Nauset system "behaves", under various barrier island/inlet configurations using the bathymetric data presented in this report.
- 3) Every five years, or as a significant morphological change in the inlet barrier beach system occurs, the model should be rerun with new bathymetry and morphology to estimate the sensitivity of the water quality to these changes. National Park Service could provide updates via their Investigation and Monitoring Program on Shoreline Dynamics.
- 4) Routine water quality measurements and tidal measurements should be taken within Town Cove, as an early indication of rapid changes in flushing and/or water quality within the embayment. Other more sensitive areas such as Salt Pond and Mill Pond should also be monitored to build baseline inventory data. Multi-agency support may be required to address the federal to local concerns. Specific contributors would include:

- i) National Park Service
 - ii) Town of Orleans
 - iii) Town of Eastham
- 5) The frequency and magnitude of stochastic events, such as non-tidally induced forcings (i.e., wind, storm surges) might change the simulated responses. Although these forces were not included in the model, their effect is believed to be of short duration and does not affect the long-term behavior of the system, except by altering the number of the inlets and thus the morphology of the basin.
- 6) A low-trophic level ecosystem model should be developed for Town Cove, to clarify specific conditions under which water quality will be worse than predicted by this depth-averaged model. Such models are becoming more commonplace for management purposes. Bloom occurrence and effects of build-out on their frequency could be assessed by such models.

ACKNOWLEDGMENTS

This project was contracted to the Woods Hole Oceanographic Institution directly by the Town of Orleans who identified the need for the flushing study of Town Cove. The authors wish to thank the Town of Orleans for its support during this project, including the Town Planner (Paul Halkiotis) and the Conservation Officer (Sandra McFarlane).

We would like to acknowledge the support of the National Park Service through which Dr. James Allen (of the USGS/BRD) identified the need for a full estuarine circulation model under both single and dual inlet systems. He provided partial funding as part of the NPS-funded study of Storm Breaches in northeast U.S. Also the Town of Eastham (Mr. Henry Lind) and the Cape Cod Commission contributed to and participated in this study.

Support for one of the authors, George Voulgaris, was provided by the Andrew W. Mellon Foundation to the Woods Hole Oceanographic Institution (D.G. Aubrey, Principal Investigator).

REFERENCES

- Aubrey, D.G., 1986. Hydrodynamic controls on sediment transport in well-mixed bays and estuaries. In: J. van de Kreeke (ed.), *Physics of Shallow Estuaries and Bays*, Springer-Verlag, p. 245-258.
- Aubrey, D.G. and C.T. Friedrichs, 1987. Ebb tidal delta bypassing. U.S. Army Waterways Experiment Station, Coastal Engineering Research Center, 80 pp.
- Aubrey, D.G. and C.T. Friedrichs, 1988. Seasonal climatology of tidal non-linearities in a shallow estuary. In: Aubrey, D.G. and Weishar, L. (eds.), *Hydrodynamics and Sediment Dynamics of Tidal Inlets*, Coastal and Estuarine Studies, Springer-Verlag, v. 29, p. 103-124.
- Aubrey, D.G. and P.E. Speer, 1983. Sediment transport in a tidal inlet. Woods Hole Oceanographic Institution Technical Report, WHOI-83-20, 110 pp.
- Aubrey, D.G. and P.E. Speer, 1984. Physical modeling. In: J.M. Teal, The Coastal Impact of Ground Water Discharge: An Assessment of Anthropogenic Nitrogen Loading in Town Cove, Orleans, MA. Final Report to Town of Orleans, MA, 170 pp.
- Aubrey, D.G. and P.E. Speer, 1984. Updrift migration of tidal inlets. *J. Geol.*, v. 92, p. 531-545.
- Aubrey, D.G. and P.E. Speer, 1985. A study of non-linear tidal propagation in shallow inlet/estuarine systems. Part I: Observations. *Estuarine, Coastal and Shelf Science*, v. 21, p. 185-205.
- Aubrey, D.G., D.C. Twichell and S.L. Pfirman, 1982. Holocene Sedimentation in the shallow nearshore zone off Nauset Inlet, Cape Cod, Massachusetts. *Marine Geology*, v. 47, p. 243-259.
- Aubrey Consulting, Inc., 1996. Field observations and hydrodynamic modeling of tidal flushing within the east bay/ Centerville river estuary: Existing conditions and effects of proposed dredging. Technical Report, 39 pp. plus Appendices.
- Foreman, M.G.G., 1977. Manual for Tidal Heights Analysis and Prediction. Pacific Marine Science Report 77-10, Institute of Ocean Sciences, Patricia Bay, Sidney, B.C., 97 pp.
- Friedrichs, C.T. and D.G. Aubrey, 1988. Non-linear tidal distortion in shallow well-mixed estuaries: A synthesis. *Estuarine, Coastal and Shelf Science*, v. 27, p. 521-545.
- Friedrichs, C.T. and D.G. Aubrey, 1989. Numerical modeling of Nauset Inlet/Marsh. In: C.T. Roman and K.W. Able (eds.), *An Ecological Analysis of Nauset Marsh*, Center for Coastal and Environmental Studies, Rutgers - The State University of New Jersey, New Brunswick, NJ, Appendix D, p. A179-A222.
- Fry, V.A. and D.G. Aubrey, 1990. Tidal velocity asymmetries and bedload transport in shallow embayments. *Estuarine, Coastal and Shelf Science*, vol. 30, p. 453-473.
- Geyer, W.R., 1997. Influence of wind on dynamics and flushing of shallow estuaries. *Estuarine, Coastal and Shelf Science*, v. 44, p. 713-722.
- Giese, G.S. and D.G. Aubrey, 1987. Bluff erosion on Outer Cape Cod. In: Kraus, N.C. (ed.), *Coastal Sediments '87*, ASCE, New York, NY, p. 1871-1876.
- Henderson, F.M., 1966. Open Channel Flow. Macmillan Publishing Company, New York, p. 96-101.
- Hess, F.R. and D.G. Aubrey, 1985. Use of radio-controlled miniature aircraft for drifter and dye current studies in a tidal inlet. *Limnology and Oceanography*, v. 30, p. 426-431.

- King, I.P., 1988. Combined Modeling of One and Two Dimensional Flow Systems. Submitted to Hydraulic Division, ASCE.
- King, I.P., 1990. Program Documentation - RMA-2V- A Two-Dimensional Finite Element Model for Flow in Estuaries and Streams. Resource Management Associates, Lafayette, CA.
- King, I.P., 1996. Update Documentation - RMA-2V - A Two Dimensional Finite Element Model for Flow in Estuaries and Streams. Resource Management Associates, Lafayette, CA.
- Kramer, K.J.M., U.H. Brockman and R.M. Warwick, 1994. Tidal Estuaries: Manual of Sampling and Analytical Procedures. Balkema, Rotterdam, 304 pp.
- Miller, M.C. and D.G. Aubrey, 1985. Beach changes on Eastern Cape Cod, Massachusetts, from Newcomb Hollow to Nauset Inlet, 1970-1974. U.S.A.C.E. Coastal Engineering Research Center Vicksburg, MS, CERC-MP-85-10, 58 pp.
- Norton, W.R., I.P. King and G.T. Orlob, 1973. A Finite Element Model for Lower Granite Reservoir. Prepared for the Walla Walla District, U.S. Army Corps of Engineers, Walla Walla, WA.
- Roman, C.T., J. Peck, J.R. Allen, J.W. King and P.G. Appleby, 1996. Accretion of a New England Salt Marsh in Response to Inlet Migration, Storm and Sea-level Rise (Nauset Marsh, Cape Cod National Seashore). Technical Report NPS/NESO-RNR/NRTR/96-10, 34 pp. (*Estuarine, Coastal and Shelf Science*, in press).
- Speer, P.E. and D.G. Aubrey, 1985. A study of non-linear tidal propagation in shallow inlet/estuarine systems. Part II: Theory. *Estuarine, Coastal and Shelf Science*, v. 21, p. 207-224.
- Speer, P.E., D.G. Aubrey and C.T. Friedrichs, 1991. Non-linear hydrodynamics of shallow tidal inlet/bay systems. In: *Tidal Hydrodynamics*, B.B. Parker, (ed.), Wiley, New York, p. 321-340.
- Speer, P.E., D.G. Aubrey and E. Ruder, 1982. Beach changes at Nauset Inlet, Cape Cod, Massachusetts, 1670-1981. Woods Hole Oceanographic Institution Technical Report, WHOI-82-40, 92 pp.
- Uchupi, E., G.S. Giese and D.G. Aubrey. The *W. M. Davis Model* Of The Late Quaternary Construction Of Cape Cod, MA: A Reconsideration. *Geological Society of America* Special Paper 309, 69 pp.
- Zimmerman, J.T.F., 1988. Estuarine residence times. In: Kjerfve, B. J. (Editor), *Hydrodynamics of Estuaries*, Vol I. Estuarine Physics. CRC Press, Inc., p. 75-84.

APPENDIX I
RESULTS OF HARMONIC ANALYSES

KEY:

- AL, GL: Amplitude (in cm) and phase (in degrees) of tidal constituent as calculated by the least square method.
- A, G: Amplitude (in cm) and phase (in degrees) of tidal constituent, after modal modulation and astronomical argument adjustments.

STATION PTLC#1

NUMBER OF VALID DATA =1435
 STANDARD DEVIATION = 0.40
 MATRIX CONDITION = 0.82

AVERAGE VALUE= 1.35
 THEORETICAL RMS=0.12

ANALYSIS OF HOURLY TIDAL HEIGHTS FROM 17:00H 11/10/96 TO 11:00H 10/12/96
 NO.OBS.=1435 NO.PTS.ANAL.= 1435 MIDPT=14:00H 10/11/96 SEPARATION=1.00

NO	NAME	FREQUENCY	A	G	AL	GL
1	Z0	0.00000000	1.3499	000.00	1.3499	000.00
2	MM	0.00151215	0.1345	020.25	0.1345	109.74
3	MSF	0.00282193	0.0103	318.03	0.0103	325.88
4	ALP1	0.03439657	0.0060	190.64	0.0048	195.60
5	2Q1	0.03570635	0.0043	045.06	0.0034	328.79
6	Q1	0.03721850	0.0085	183.93	0.0068	197.36
7	O1	0.03873065	0.0701	187.74	0.0567	290.83
8	NO1	0.04026859	0.0004	339.11	0.0004	069.37
9	K1	0.04178075	0.0885	169.97	0.0781	358.95
10	J1	0.04329290	0.0240	165.94	0.0019	084.89
11	OO1	0.04483084	0.0057	328.70	0.0029	048.79
12	UPS1	0.04634299	0.0126	044.18	0.0063	220.45
13	EPS2	0.07617731	0.0332	147.59	0.0332	339.80
14	MU2	0.07768947	0.0334	164.92	0.0343	088.41
15	N2	0.07899925	0.0773	356.53	0.0803	199.21
16	M2	0.08051140	0.4826	022.76	0.5004	314.80
17	L2	0.08202355	0.0152	050.06	0.0158	242.60
18	S2	0.08333334	0.0428	048.77	0.0427	348.80
19	ETA2	0.08507364	0.0286	314.98	0.0169	244.84
20	MO3	0.11924210	0.0217	103.32	0.0182	138.45
21	M3	0.12076710	0.0056	171.68	0.0059	069.60
22	MK3	0.12229210	0.0289	109.41	0.0264	230.43
23	SK3	0.12511410	0.0048	096.52	0.0042	225.53
24	MN4	0.15951060	0.0231	313.41	0.0249	088.13
25	M4	0.16102280	0.0884	340.74	0.0951	204.83
26	SN4	0.16233260	0.0128	343.77	0.0132	126.48
27	MS4	0.16384470	0.0217	011.75	0.0225	243.82
28	S4	0.16666670	0.0022	075.91	0.0022	315.96
29	2MK5	0.20280360	0.0052	352.54	0.0049	045.60
30	2SK5	0.20844740	0.0001	317.50	0.0001	026.53
31	2MN6	0.24002200	0.0009	203.01	0.0010	269.78
32	M6	0.24153420	0.0013	080.08	0.0014	236.20
33	2MS6	0.24435610	0.0026	230.47	0.0028	034.57
34	2SM6	0.24717810	0.0014	342.76	0.0015	154.86
35	3MK7	0.28331490	0.0044	187.02	0.0044	172.13
36	M8	0.32204560	0.0085	053.05	0.0099	141.22
37	M10	0.40255700	0.0026	027.12	0.0031	047.32

STATION: PTL#2

NUMBER OF VALID DATA =1435 AVERAGE VALUE= 1.28
STANDARD DEVIATION = 0.46 THEORETICAL RMS = 0.13
MATRIX CONDITION = 0.82

ANALYSIS OF HOURLY TIDAL HEIGHTS FROM 17:00H 11/10/96 TO 11:00H 10/12/96
NO.OBS.=1435 NO.PTS.ANAL.=1435 MIDPT=14:00H 10/11/96 SEPARATION =1.00

NO	NAME	FREQUENCY	A	G	AL	GL
1	Z0	0.00000000	1.2881	000.00	1.2881	000.00
2	MM	0.00151215	0.1391	017.38	0.1391	106.87
3	MSF	0.00282193	0.0114	241.05	0.0114	248.90
4	ALP1	0.03439657	0.0099	186.96	0.0079	191.93
5	2Q1	0.03570635	0.0039	048.40	0.0031	332.14
6	Q1	0.03721850	0.0089	173.98	0.0071	187.41
7	O1	0.03873065	0.0675	177.83	0.0545	280.92
8	NO1	0.04026859	0.0025	001.77	0.0025	091.94
9	K1	0.04178075	0.0947	162.48	0.0836	351.46
10	J1	0.04329290	0.0037	125.28	0.0030	044.21
11	OO1	0.04483084	0.0058	313.62	0.0030	033.70
12	UPS1	0.04634299	0.0142	034.59	0.0071	210.86
13	EPS2	0.07617731	0.0296	133.70	0.0296	325.92
14	MU2	0.07768947	0.0355	152.50	0.0365	075.99
15	N2	0.07899925	0.0867	343.91	0.0901	186.59
16	M2	0.08051140	0.5619	013.80	0.5827	305.84
17	L2	0.08202355	0.0225	057.75	0.0233	250.29
18	S2	0.08333334	0.0540	039.45	0.0539	339.48
19	ETA2	0.08507364	0.0242	305.04	0.0143	234.88
20	MO3	0.11924210	0.0248	089.02	0.0208	124.16
21	M3	0.12076710	0.0066	161.34	0.0069	059.26
22	MK3	0.12229210	0.0318	093.48	0.0291	214.50
23	SK3	0.12511410	0.0059	096.27	0.0052	225.28
24	MN4	0.15951060	0.0298	297.57	0.0321	072.29
25	M4	0.16102280	0.0949	327.12	0.1021	191.20
26	SN4	0.16233260	0.0109	331.31	0.0113	114.02
27	MS4	0.16384470	0.0258	356.54	0.0267	228.61
28	S4	0.16666670	0.0017	054.12	0.0017	294.17
29	2MK5	0.20280360	0.0022	009.40	0.0021	062.46
30	2SK5	0.20844740	0.0006	046.14	0.0005	115.17
31	2MN6	0.24002200	0.0025	279.35	0.0028	346.11
32	M6	0.24153420	0.0096	008.80	0.0107	164.93
33	2MS6	0.24435610	0.0022	012.87	0.0023	176.98
34	2SM6	0.24717810	0.0001	111.31	0.0001	283.41
35	3MK7	0.28331490	0.0043	097.15	0.0043	082.25
36	M8	0.32204560	0.0091	338.94	0.0105	067.10
37	M10	0.40255700	0.0017	284.81	0.0020	305.01

STATION: PTL#3

NUMBER OF VALID DATA =1339 AVERAGE VALUE= 2.19
STANDARD DEVIATION = 0.53 THEORETICAL RMS = 0.12
MATRIX CONDITION = 0.85

ANALYSIS OF HOURLY TIDAL HEIGHTS FROM 17:00H 11/10/96 TO 12:00H 6/12/96
NO.OBS.=1340 NO.PTS.ANAL.=1340 MIDPT=14:00H 8/11/96 SEPARATION=1.00

NO	NAME	FREQUENCY	A	G	AL	GL
1	Z0	0.00000000	2.1874	360.00	2.1874	360.00
2	MM	0.00151215	0.2046	022.72	0.2046	138.34
3	MSF	0.00282193	0.0163	061.73	0.0163	118.34
4	ALP1	0.03439657	0.0106	149.24	0.0084	028.62
5	2Q1	0.03570635	0.0020	046.56	0.0016	227.33
6	Q1	0.03721850	0.0126	152.44	0.0101	089.03
7	O1	0.03873065	0.0719	162.89	0.0581	215.27
8	NO1	0.04026859	0.0048	018.49	0.0047	084.44
9	K1	0.04178075	0.1012	149.66	0.0893	340.59
10	J1	0.04329290	0.0023	177.87	0.0019	124.87
11	OO1	0.04483084	0.0057	306.34	0.0030	080.98
12	UPS1	0.04634299	0.0158	013.80	0.0079	270.78
13	EPS2	0.07617731	0.0179	129.71	0.0179	198.28
14	MU2	0.07768947	0.0391	139.37	0.0401	325.33
15	N2	0.07899925	0.0971	324.54	0.1009	092.33
16	M2	0.08051140	0.6554	354.73	0.6797	238.00
17	L2	0.08202355	0.0242	040.84	0.0251	210.74
18	S2	0.08333334	0.0798	011.52	0.0797	311.54
19	ETA2	0.08507364	0.0115	295.19	0.0068	255.04
20	MO3	0.11924210	0.0242	051.67	0.0203	347.33
21	M3	0.12076710	0.0057	121.05	0.0060	305.82
22	MK3	0.12229210	0.0304	045.94	0.0278	120.15
23	SK3	0.12511410	0.0088	068.97	0.0077	199.93
24	MN4	0.15951060	0.0296	257.30	0.0319	268.35
25	M4	0.16102280	0.0784	279.75	0.0844	046.30
26	SN4	0.16233260	0.0097	281.37	0.0100	349.18
27	MS4	0.16384470	0.0296	300.31	0.0306	123.61
28	S4	0.16666670	0.0032	324.48	0.0032	204.53
29	2MK5	0.20280360	0.0094	218.60	0.0089	176.08
30	2SK5	0.20844740	0.0012	009.56	0.0011	080.55
31	2MN6	0.24002200	0.0063	061.10	0.0070	315.43
32	M6	0.24153420	0.0188	072.29	0.0210	082.11
33	2MS6	0.24435610	0.0076	094.42	0.0081	161.00
34	2SM6	0.24717810	0.0014	147.30	0.0015	270.63
35	3MK7	0.28331490	0.0043	062.17	0.0043	262.92
36	M8	0.32204560	0.0044	302.91	0.0051	196.00
37	M10	0.40255700	0.0018	114.74	0.0021	251.11

STATION: PTL#4

NUMBER OF VALID DATA =1232
STANDARD DEVIATION = 0.37
MATRIX CONDITION = 0.21

AVERAGE VALUE= 0.99
THEORETICAL RMS = 0.12

ANALYSIS OF HOURLY TIDAL HEIGHTS FROM 17:00H 11/10/96 TO 11H 10/12/96
NO.OBS.=1435 NO.PTS.ANAL.=1435 MIDPT=14:00H 10/11/96 SEPARATION=1.00

NO	NAME	FREQUENCY	A	G	AL	GL
1	Z0	0.00000000	0.7200	000.00		
2	MM	0.00151215	0.1270	015.16	0.1270	104.65
3	MSF	0.00282193	0.0125	214.07	0.0125	221.92
4	ALP1	0.03439657	0.0079	198.96	0.0063	203.94
5	2Q1	0.03570635	0.0064	014.14	0.0051	297.88
6	Q1	0.03721850	0.0046	148.62	0.0037	162.05
7	O1	0.03873065	0.0713	192.61	0.0577	295.70
8	NO1	0.04026859	0.0018	160.45	0.0018	250.63
9	K1	0.04178075	0.0825	171.63	0.0728	000.61
10	J1	0.04329290	0.0044	215.68	0.0036	134.61
11	OO1	0.04483084	0.0037	303.41	0.0019	023.48
12	UPS1	0.04634299	0.0117	047.59	0.0086	223.86
13	EPS2	0.07617731	0.0424	164.42	0.0423	356.64
14	MU2	0.07768947	0.0306	142.14	0.0315	065.63
15	N2	0.07899925	0.0839	359.16	0.0872	201.84
16	M2	0.08051140	0.4289	029.59	0.4447	321.61
17	L2	0.08202355	0.0039	329.17	0.0041	161.71
18	S2	0.08333334	0.0438	059.43	0.0437	359.45
19	ETA2	0.08507364	0.0593	322.39	0.0351	252.24
20	MO3	0.11924210	0.0238	120.56	0.0199	155.70
21	M3	0.12076710	0.0062	179.38	0.0066	077.30
22	MK3	0.12229210	0.0299	137.46	0.0274	258.48
23	SK3	0.12511410	0.0035	081.81	0.0031	210.82
24	MN4	0.15951060	0.0287	324.56	0.0309	099.28
25	M4	0.16102280	0.1066	016.22	0.1147	240.30
26	SN4	0.16233260	0.0090	037.51	0.0094	180.22
27	MS4	0.16384470	0.0266	038.50	0.0276	270.57
28	S4	0.16666670	0.0038	194.57	0.0037	074.62
29	2MK5	0.20280360	0.0120	086.68	0.0014	139.74
30	2SK5	0.20844740	0.0024	307.33	0.0021	016.36
31	2MN6	0.24002200	0.0049	273.86	0.0055	340.62
32	M6	0.24153420	0.0304	347.62	0.0339	143.74
33	2MS6	0.24435610	0.0084	338.07	0.0090	142.17
34	2SM6	0.24717810	0.0020	071.06	0.0020	243.16
35	3MK7	0.28331490	0.0046	011.12	0.0045	356.23
36	M8	0.32204560	0.0058	297.93	0.0067	026.10
37	M10	0.40255700	0.0046	147.26	0.0055	167.47

STATION: PTL#5

NUMBER OF VALID DATA =1401 AVERAGE VALUE= 3.86
 STANDARD DEVIATION = 0.45 THEORETICAL RMS = 0.13
 MATRIX CONDITION = 0.72

ANALYSIS OF HOURLY TIDAL HEIGHTS FROM 17:00H 11/10/96 to 11H 10/12/96
 NO.OBS.=1435 NO.PTS.ANAL.=1435 MIDPT=14:00H 10/11/96 SEPARATION=1.00

NO	NAME	FREQUENCY	A	G	AL	GL
1	Z0	0.00000000	3.8853	000.00	3.8853	000.00
2	MM	0.00151215	0.1252	019.82	0.1252	109.31
3	MSF	0.00282193	0.0188	270.60	0.0188	278.45
4	ALP1	0.03439657	0.0145	194.67	0.0115	199.65
5	2Q1	0.03570635	0.0024	054.38	0.0019	338.12
6	Q1	0.03721850	0.0094	174.61	0.0075	188.05
7	O1	0.03873065	0.0635	179.40	0.0514	282.50
8	NO1	0.04026859	0.0030	015.30	0.0029	105.46
9	K1	0.04178075	0.0930	167.22	0.0821	356.20
10	J1	0.04329290	0.0070	120.80	0.0056	039.73
11	OO1	0.04483084	0.0060	304.84	0.0031	024.91
12	UPS1	0.04634299	0.0156	031.91	0.0078	208.17
13	EPS2	0.07617731	0.0275	111.58	0.0275	303.80
14	MU2	0.07768947	0.0291	150.49	0.0299	073.98
15	N2	0.07899925	0.0798	346.41	0.0829	189.09
16	M2	0.08051140	0.5594	021.87	0.5801	313.91
17	L2	0.08202355	0.0265	060.67	0.0275	253.21
18	S2	0.08333334	0.0555	044.75	0.0554	344.78
19	ETA2	0.08507364	0.0190	332.99	0.0112	262.83
20	MO3	0.11924210	0.0290	096.13	0.0243	131.26
21	M3	0.12076710	0.0082	165.64	0.0087	063.56
22	MK3	0.12229210	0.0375	099.24	0.0344	220.26
23	SK3	0.12511410	0.0054	100.97	0.0047	229.97
24	MN4	0.15951060	0.0302	299.22	0.0325	073.94
25	M4	0.16102280	0.1165	338.11	0.1253	202.19
26	SN4	0.16233260	0.0193	353.30	0.0200	136.01
27	MS4	0.16384470	0.0376	010.55	0.0389	242.62
28	S4	0.16666670	0.0046	132.39	0.0045	012.44
29	2MK5	0.20280360	0.0133	017.09	0.0126	070.15
30	2SK5	0.20844740	0.0027	182.00	0.0023	251.03
31	2MN6	0.24002200	0.0076	226.82	0.0085	293.59
32	M6	0.24153420	0.0125	293.21	0.0139	089.33
33	2MS6	0.24435610	0.0111	326.00	0.0119	130.11
34	2SM6	0.24717810	0.0009	071.43	0.0009	243.52
35	3MK7	0.28331490	0.0040	351.75	0.0039	336.85
36	M8	0.32204560	0.0042	345.26	0.0048	073.42
37	M10	0.40255700	0.0023	296.48	0.0028	316.69

STATION: SALT POND

NUMBER OF VALID DATA = 801 AVERAGE VALUE= 0.27
 STANDARD DEVIATION = 0.35 THEORETICAL RMS = 0.13
 MATRIX CONDITION = 0.45

ANALYSIS OF HOURLY TIDAL HEIGHTS FROM 08:00H 02/11/96 to 16H 5/12/96
 NO.OBS.=801 NO.PTS.ANAL.=801 MIDPT=00:00H 19/11/96 SEPARATION=1.00

NO	NAME	FREQUENCY	A	G	AL	GL
1	Z0	0.00000000	0.2850	360.00	0.2850	360.00
2	MM	0.00151215	0.1040	026.76	0.1040	006.30
3	MSF	0.00282193	0.0219	261.60	0.0219	064.23
4	ALP1	0.03439657	0.0057	096.93	0.0046	120.46
5	2Q1	0.03570635	0.0061	351.61	0.0048	198.67
6	Q1	0.03721850	0.0035	191.89	0.0028	018.67
7	O1	0.03873065	0.0684	201.71	0.0553	008.20
8	NO1	0.04026859	0.0039	127.38	0.0039	169.56
9	K1	0.04178075	0.1065	175.11	0.0940	205.88
10	J1	0.04329290	0.0015	100.55	0.0012	111.37
11	OO1	0.04483084	0.0201	357.98	0.0104	058.44
12	UPS1	0.04634299	0.0055	018.10	0.0028	064.67
13	EPS2	0.07617731	0.0322	186.46	0.0322	239.05
14	MU2	0.07768947	0.0489	204.62	0.0503	238.54
15	N2	0.07899925	0.0867	329.06	0.0901	186.93
16	M2	0.08051140	0.4033	035.89	0.4183	233.15
17	L2	0.08202355	0.0441	207.80	0.0455	195.58
18	S2	0.08333334	0.0603	064.79	0.0602	064.82
19	ETA2	0.08507364	0.0106	341.72	0.0063	205.32
20	MO3	0.11924210	0.0220	160.13	0.0184	163.89
21	M3	0.12076710	0.0066	220.42	0.0070	336.18
22	MK3	0.12229210	0.0417	148.17	0.0382	016.20
23	SK3	0.12511410	0.0039	179.68	0.0034	210.47
24	MN4	0.15951060	0.0433	320.06	0.0467	015.21
25	M4	0.16102280	0.1134	021.07	0.1219	055.61
26	SN4	0.16233260	0.0117	193.10	0.0121	051.00
27	MS4	0.16384470	0.0428	045.27	0.0443	242.57
28	S4	0.16666670	0.0077	039.93	0.0077	039.98
29	2MK5	0.20280360	0.0108	070.95	0.0102	136.25
30	2SK5	0.20844740	0.0039	232.29	0.0034	263.11
31	2MN6	0.24002200	0.0096	278.12	0.0107	170.53
32	M6	0.24153420	0.0173	001.53	0.0193	233.34
33	2MS6	0.24435610	0.0121	024.80	0.0130	059.36
34	2SM6	0.24717810	0.0018	358.31	0.0018	195.63
35	3MK7	0.28331490	0.0042	028.00	0.0041	290.58
36	M8	0.32204560	0.0024	008.50	0.0028	077.58
37	M10	0.40255700	0.0012	133.49	0.0014	039.84

STATION: **Oceanic**

CONSTITUENTS USED TO PREDICT OCEANIC FORCING

NO	NAME	FREQUENCY	A	G
1	Z0	0.00000000	0.7200	000.00
2	SA	0.00001141	0.0164	142.40
3	SSA	0.00022816	0.0103	095.90
4	MM	0.00151215	0.1461	146.00 ¹
5	MSF	0.00282193	0.0430	019.10
6	2Q1	0.03570635	0.0018	112.20
7	Q1	0.03721850	0.0131	109.50
8	O1	0.03873065	0.0746	127.10
9	K1	0.04178075	0.0945	141.90
10	J1	0.04329290	0.0061	145.10
11	OO1	0.04483084	0.0030	156.80
12	2N2	0.07748709	0.0262	298.70
13	MU2	0.07768947	0.0070	281.90
14	N2	0.07899925	0.1935	316.70
15	NU2	0.07920162	0.0427	325.80
16	M2	0.08051140	0.8735	346.50
17	LDA2	0.08182118	0.0134	021.20
18	L2	0.08202355	0.0375	035.40
19	T2	0.08321926	0.0125	351.90
20	S2	0.08333334	0.1384	018.40
21	K2	0.08356149	0.0396	020.20
22	MK3	0.12229210	0.0036	040.40
23	MN4	0.15951060	0.0064	130.80
24	M4	0.16102280	0.0475	226.20
25	MS4	0.16384470	0.0058	182.10
26	M6	0.24153420	0.0216	275.70
27	M8	0.32204560	0.0036	105.60

¹Average value from tidal elevation measurements within the estuary (all stations).

APPENDIX II

RMA-2V Governing Equations

APPENDIX II

The model utilizes isoperimetric quadrilaterals and triangles to represent the prototype system. Element boundaries may either be curved or straight. A Galerkin weighted residual approach is used to develop the finite element integral equations and Gaussian quadrature is employed to evaluate the final integral forms. The time dependence of the governing equations is incorporated by using a modified Crank Nicholson solution technique to solve the set of simultaneous equations. This technique is implicit and, therefore, unconditionally stable. The equations are non-linear and are solved by using the Newton-Raphson Method to develop a locally linear set of equations. Once solved, corrections to the initial estimate of velocity and water elevation are applied and the equations are re-solved until convergence criteria are met. The RMA-2V permits areas of the system to go dry during a tidal cycle. According to this method when the depth goes below a pre-specified value at a node, then the whole element to which that node belongs drops from the system and a new no slip boundary is created along the sides of the dry element.

In the RMA-2V model, the finite element method is applied to the following two dimensional depth averaged equations, repeated here for completeness from section 3

Momentum Equation X-Direction

$$\begin{aligned} \rho \left(h \frac{\partial u}{\partial t} + hu \frac{\partial u}{\partial x} + hv \frac{\partial u}{\partial y} + gh \left(\frac{\partial a}{\partial x} + \frac{\partial h}{\partial x} \right) + \frac{g}{C^2} u |V| + u q_s - \Omega v h \right) - h \frac{\partial}{\partial x} \left(\epsilon_{xx} \frac{\partial u}{\partial x} \right) \\ - h \frac{\partial}{\partial y} \left(\epsilon_{xy} \frac{\partial u}{\partial y} \right) - W_x = 0 \end{aligned} \quad A.1$$

Momentum Equation Y-Direction

$$\begin{aligned} \rho \left(h \frac{\partial v}{\partial t} + hu \frac{\partial v}{\partial x} + hv \frac{\partial v}{\partial y} + gh \left(\frac{\partial a}{\partial y} + \frac{\partial h}{\partial y} \right) + \frac{g}{C^2} v |V| + v q_s + \Omega u h \right) - h \frac{\partial}{\partial x} \left(\epsilon_{yx} \frac{\partial v}{\partial x} \right) \\ - h \frac{\partial}{\partial y} \left(\epsilon_{yy} \frac{\partial v}{\partial y} \right) - W_y = 0 \end{aligned} \quad A.2$$

Continuity Equation

$$\left(h \frac{\partial u}{\partial x} + \frac{\partial v}{\partial y} \right) + u \frac{\partial h}{\partial x} + v \frac{\partial h}{\partial y} + \frac{\partial h}{\partial t} = 0 \quad A.3$$

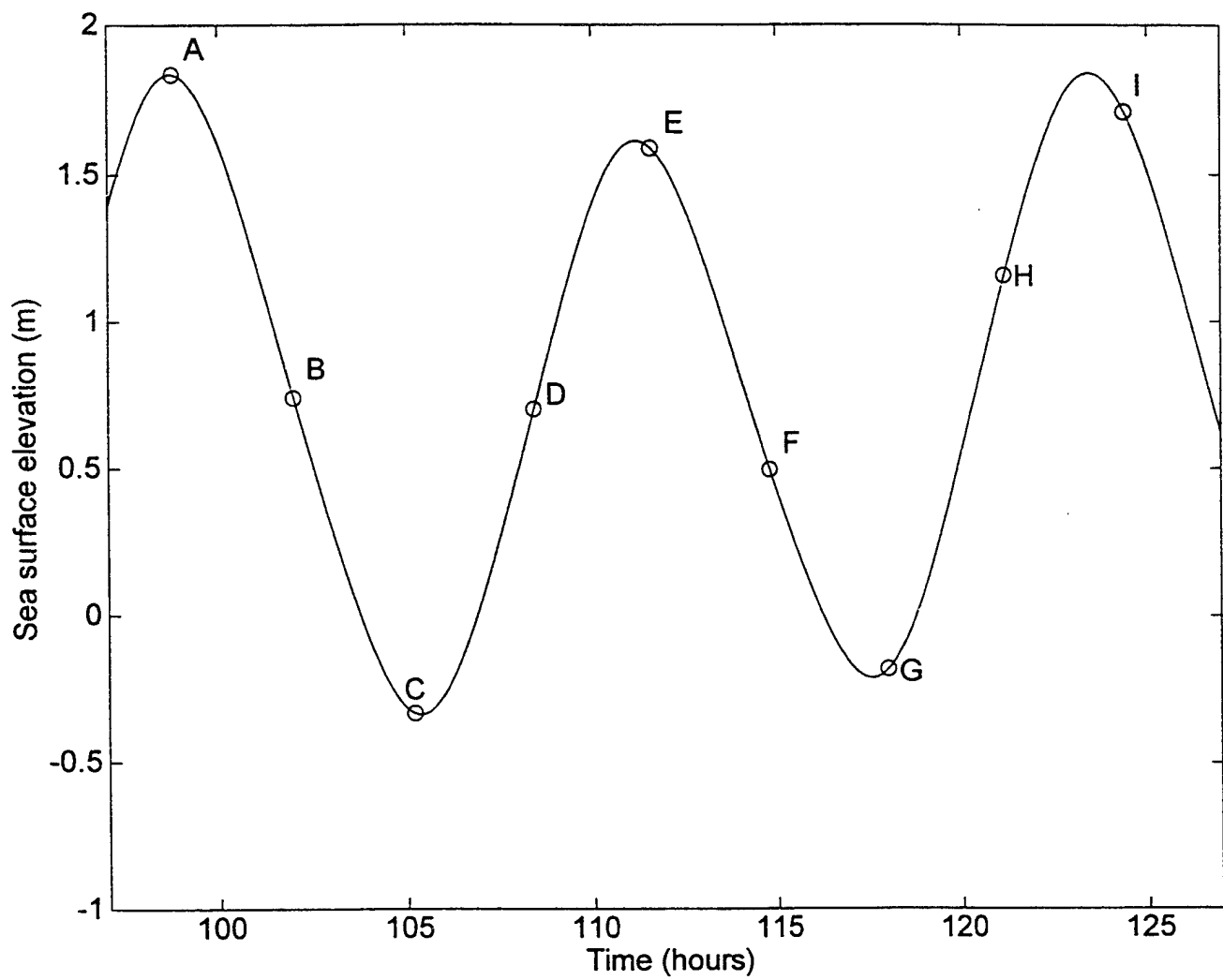
where

- x, y = horizontal cartesian coordinates
- t = time
- u, v = the horizontal velocity components in the x and y directions respectively
- h = depth
- a = bottom elevation

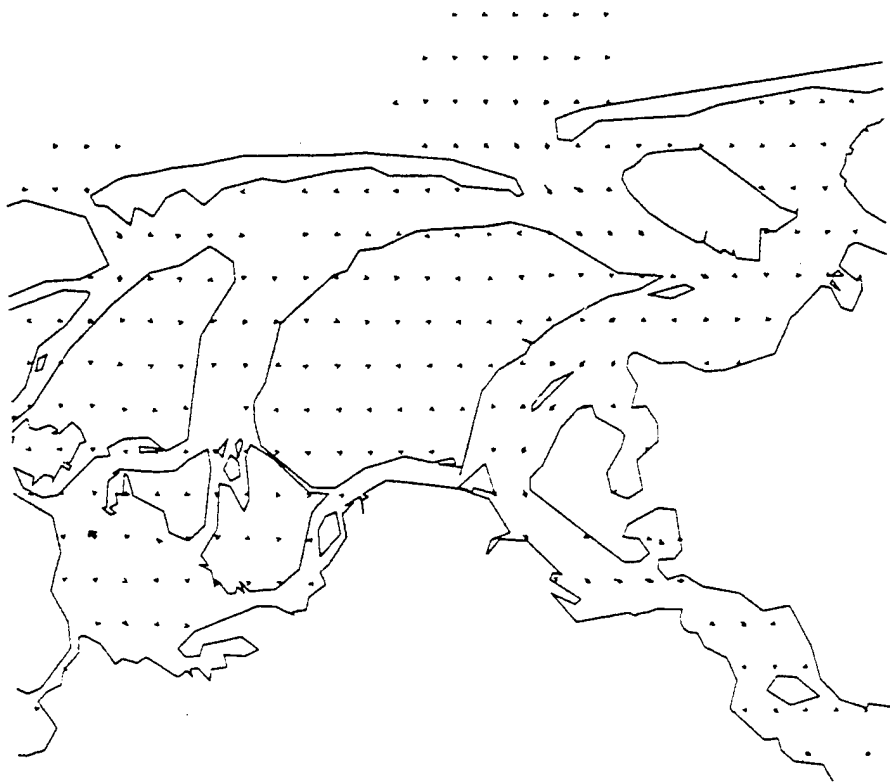
$\varepsilon_{xx}, \varepsilon_{xy}, \varepsilon_{yx}$ and ε_{yy}	=	the turbulent eddy coefficients.
C	=	Chezy bottom friction coefficient
V	=	Total water velocity
q_s	=	Tributary flow into the system
Ω_{vh} and Ω_{uh}	=	The Coriolis forcing in the x and y directions respectively.
W_x and W_y	=	forces due to wind stresses in the x and y directions respectively.

APPENDIX III

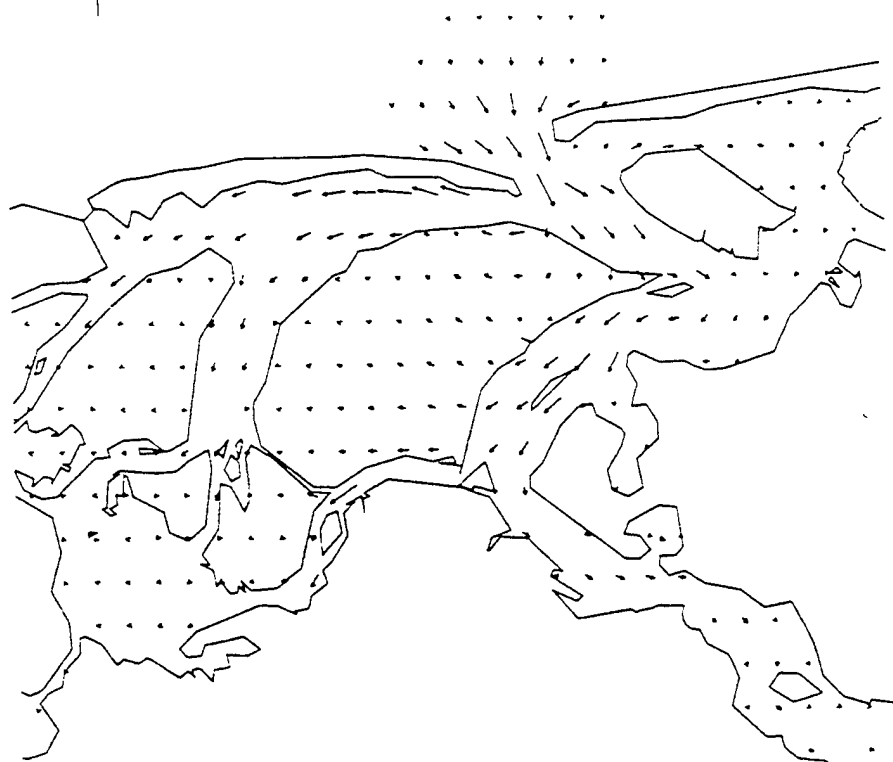
Vector diagram maps showing the water circulation in Nauset estuary for two cases (I) only one inlet (present situation); (ii) assuming the existence of two inlets. Figure III. 1 shows the stage of the tide each of the vector diagram maps (A to I) corresponds to.



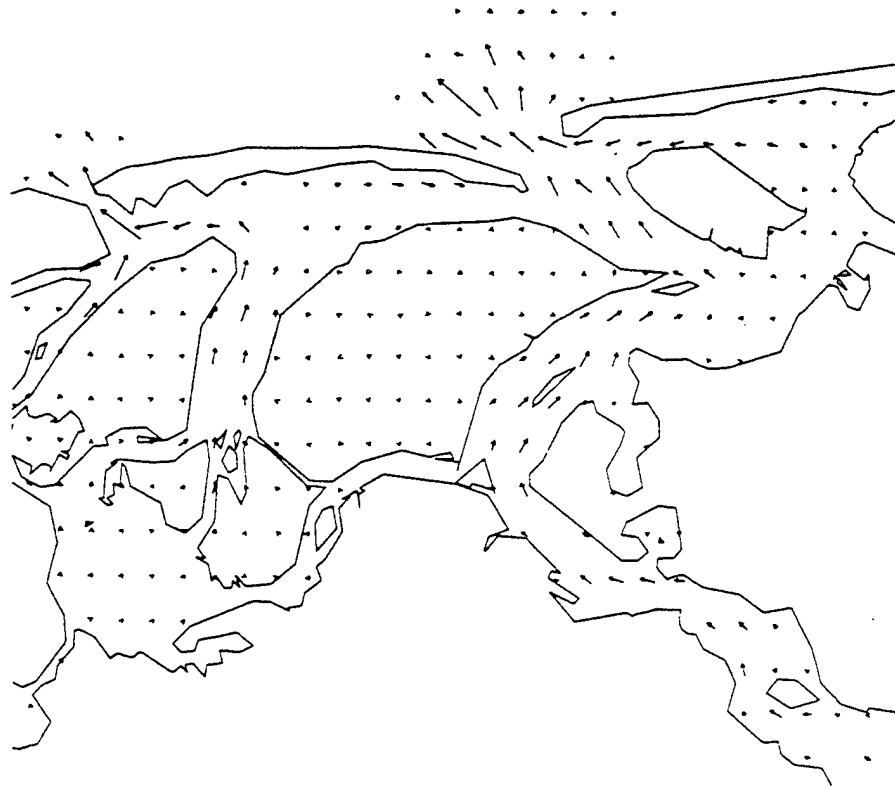
A



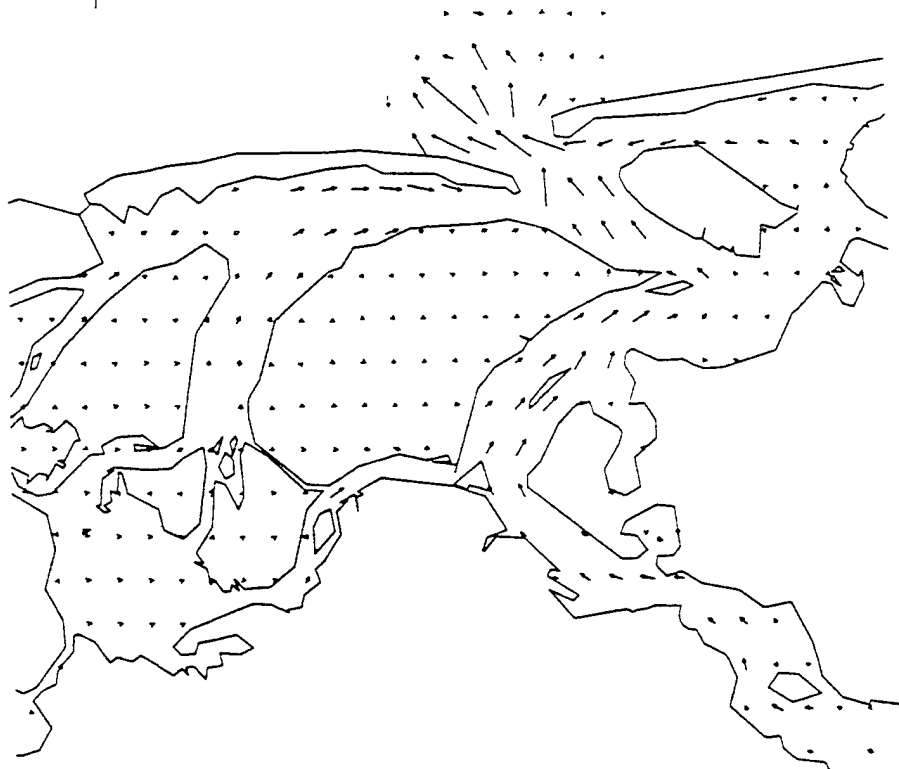
3.0
↑



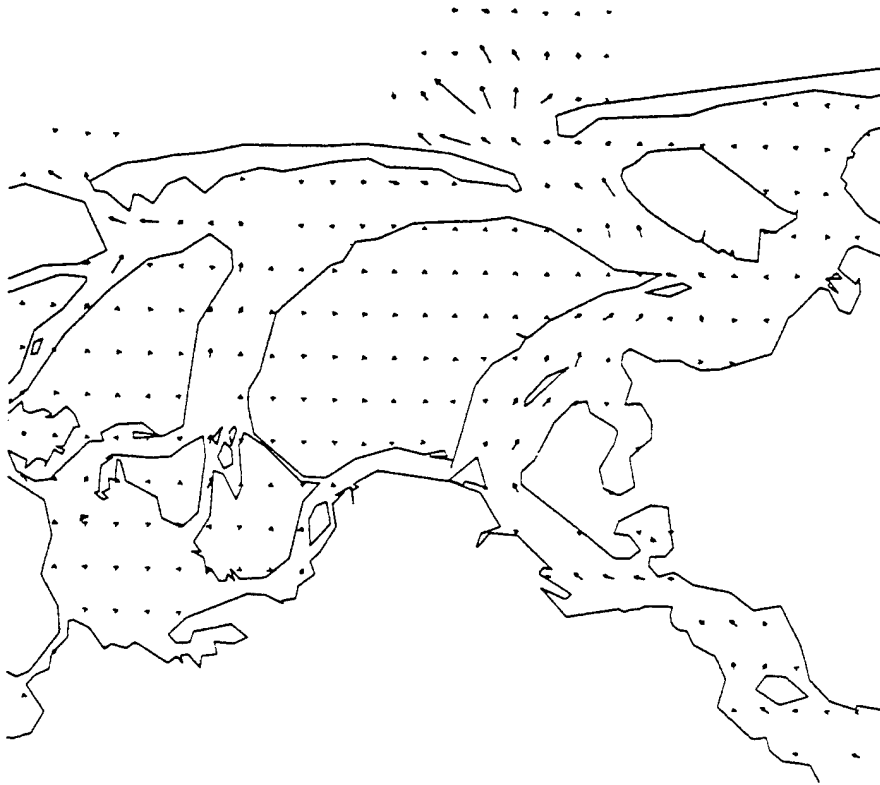
B



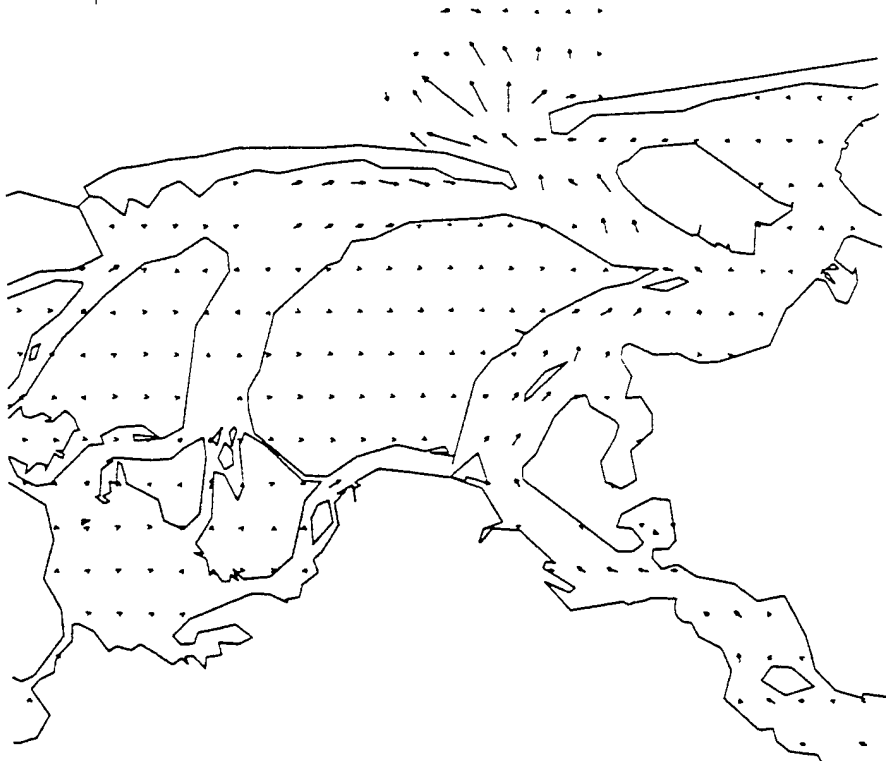
3.0



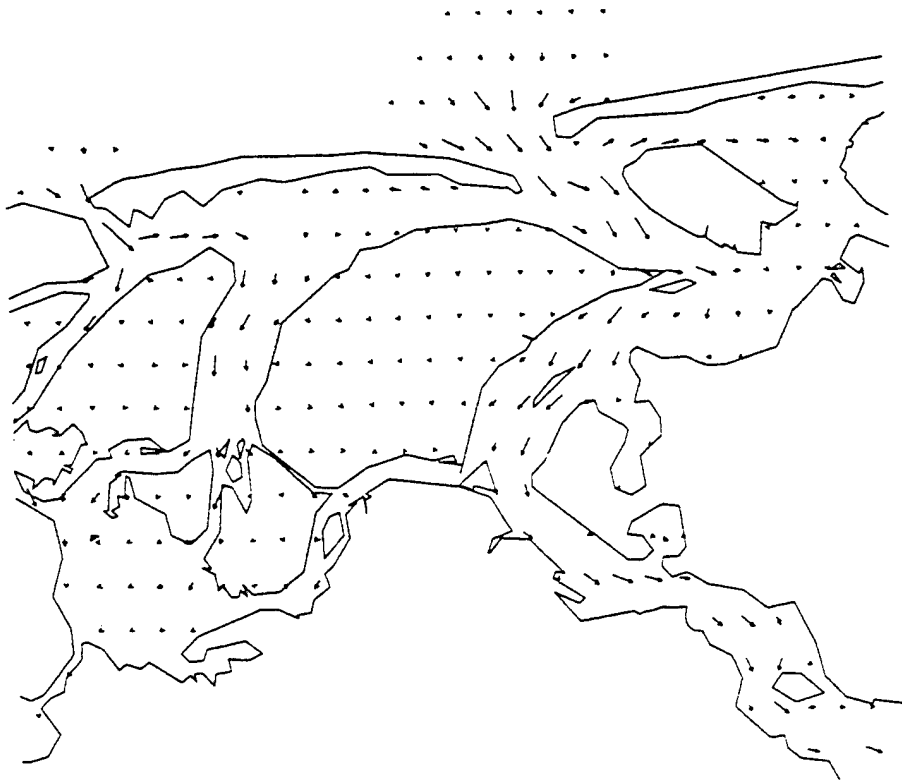
c



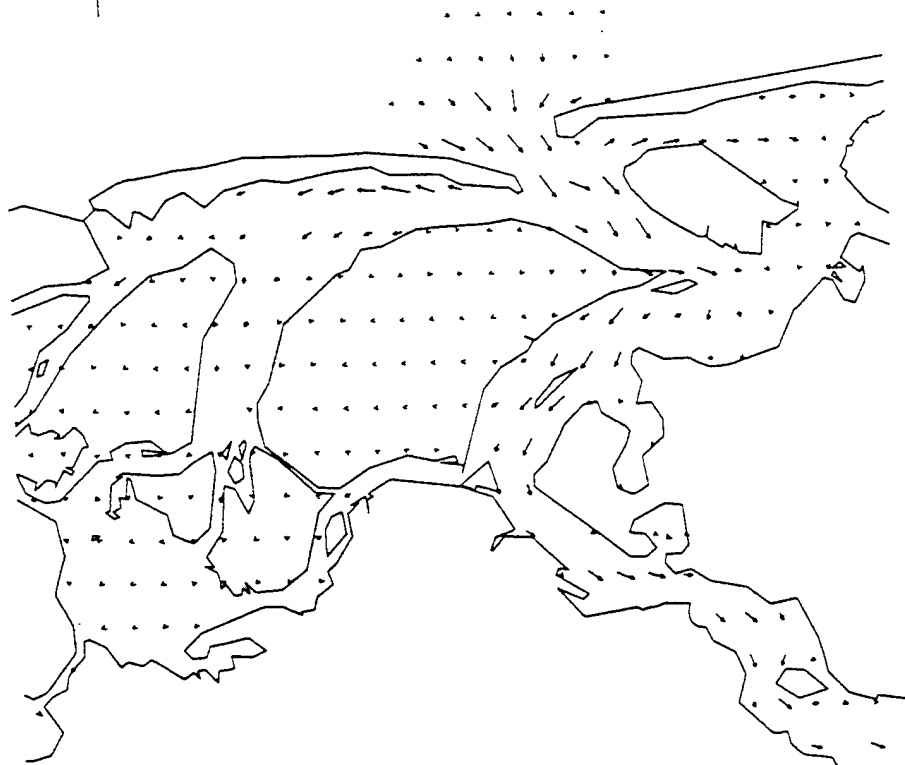
3.0
↑



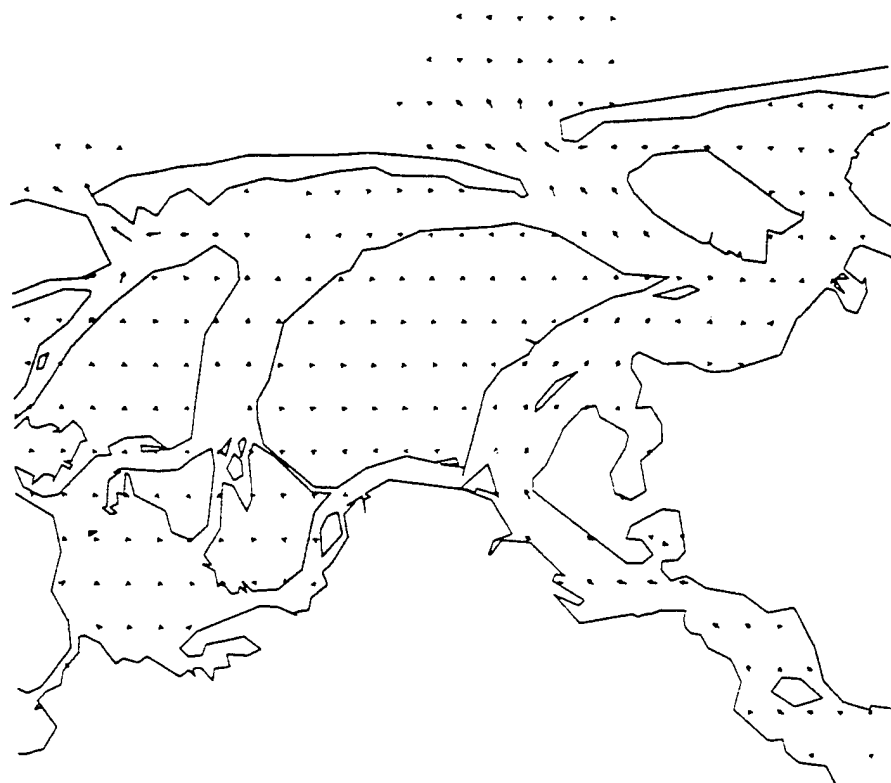
D



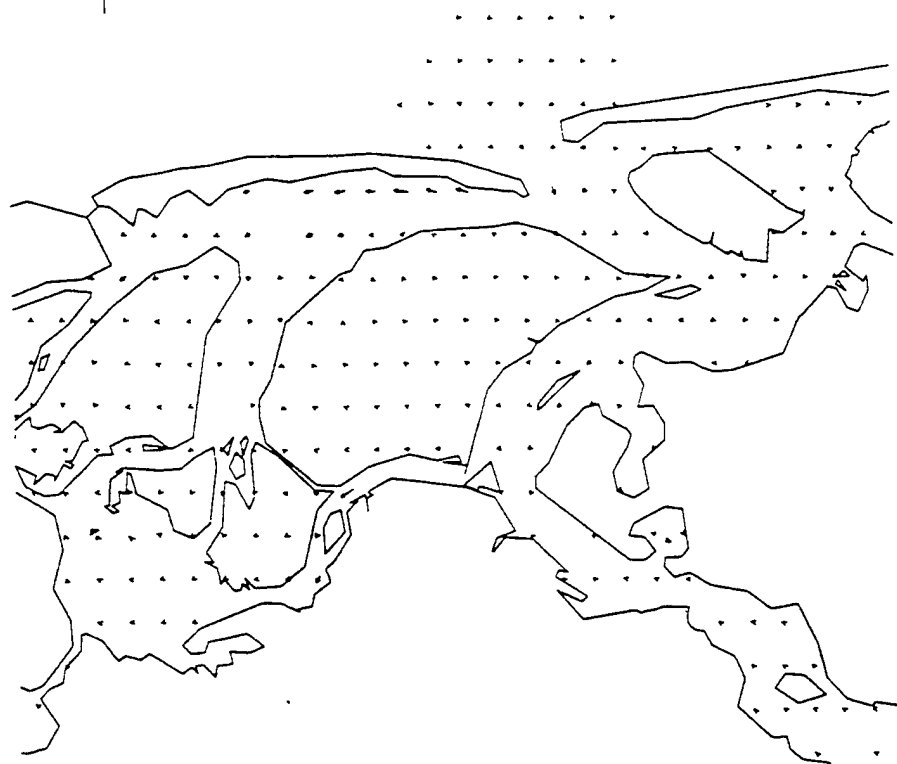
3.0
↑



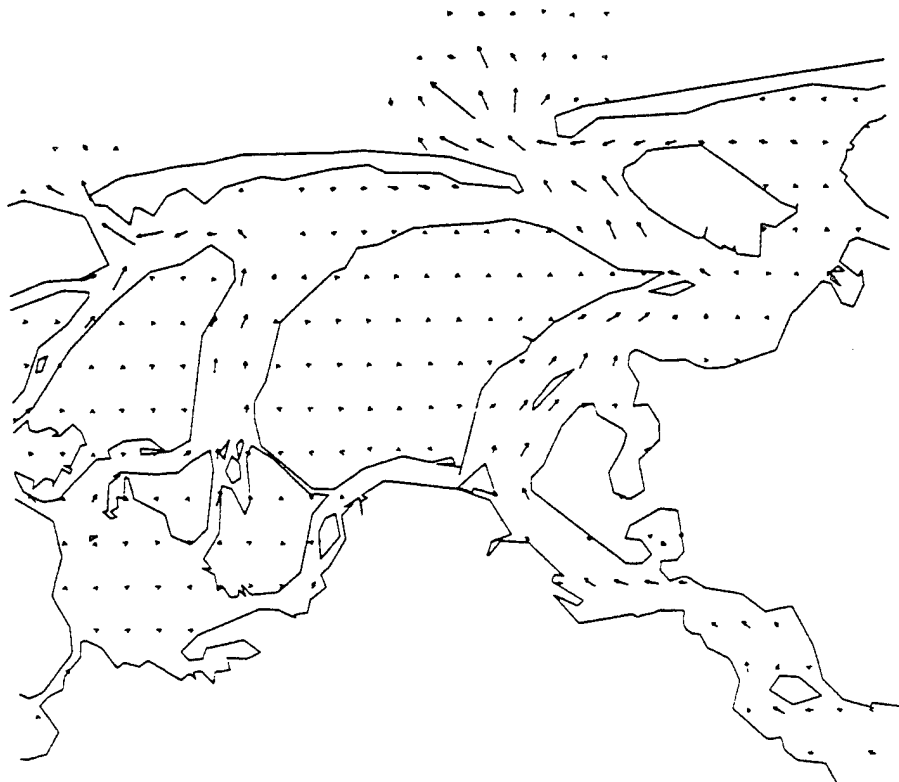
E



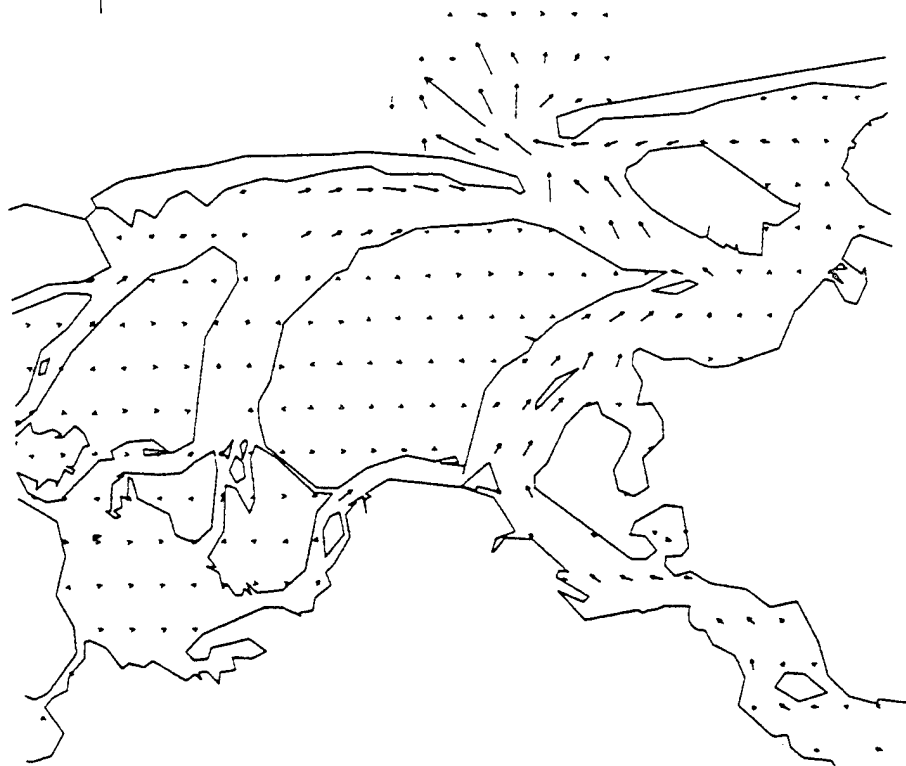
3.0
↑



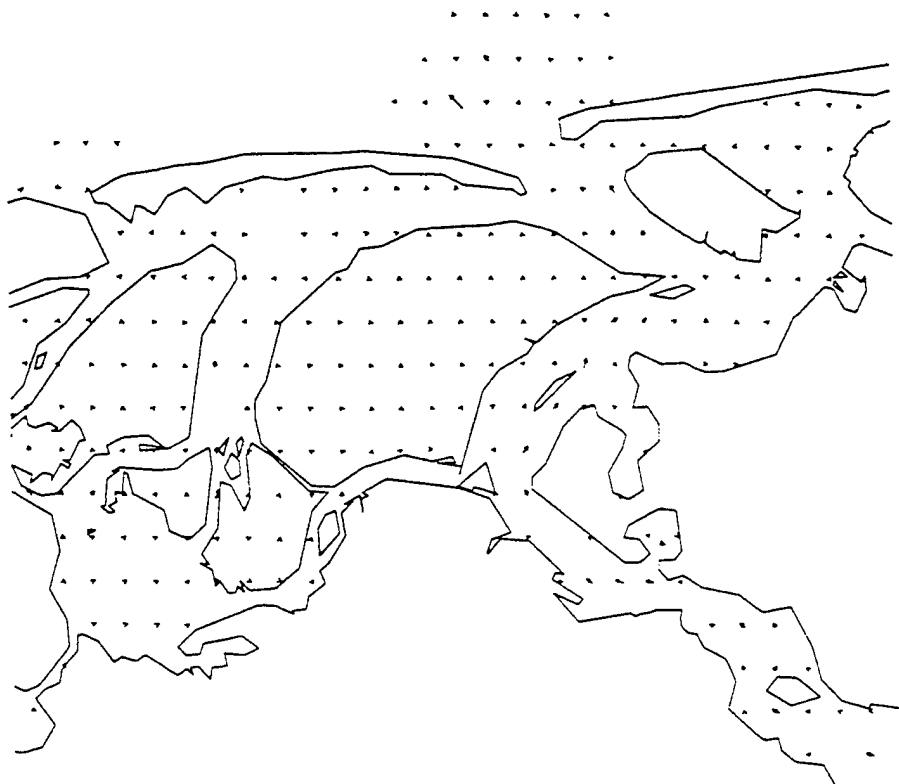
F



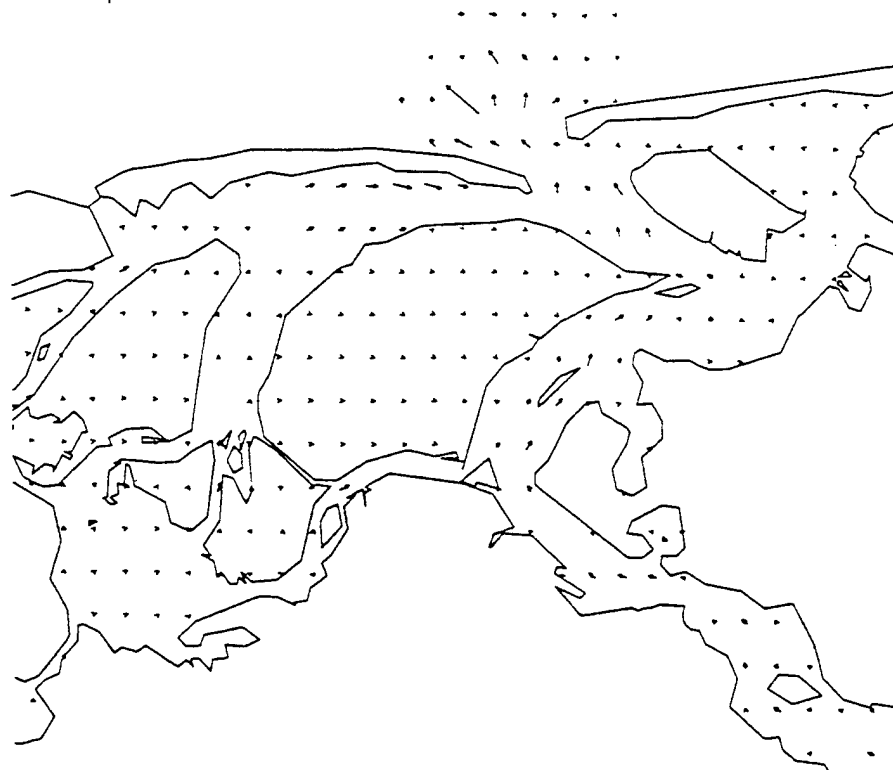
3.0
↑



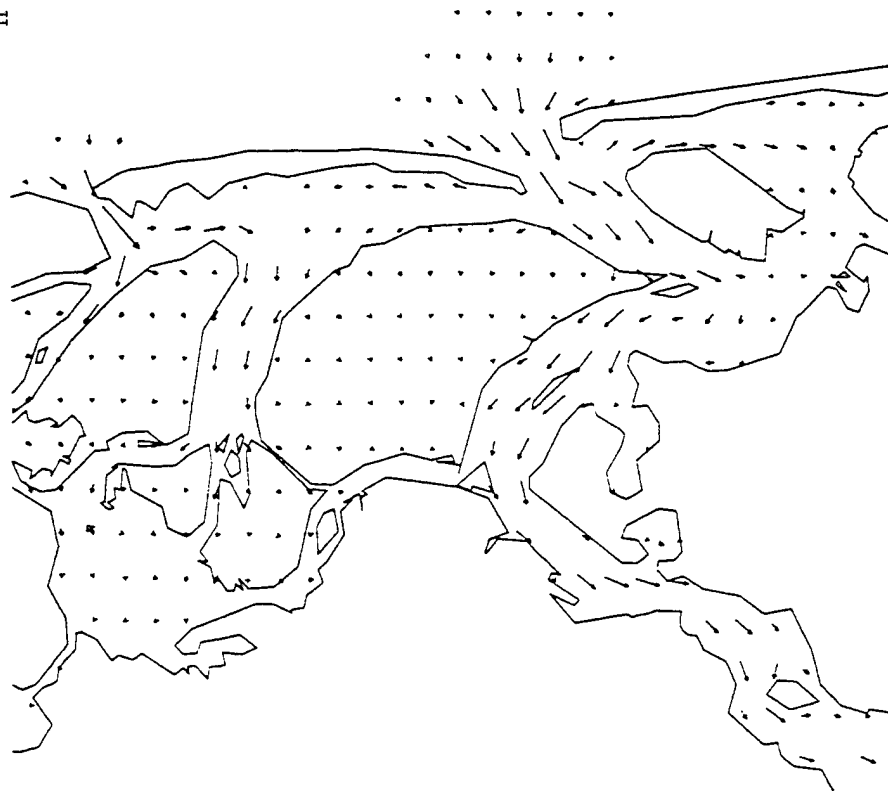
G



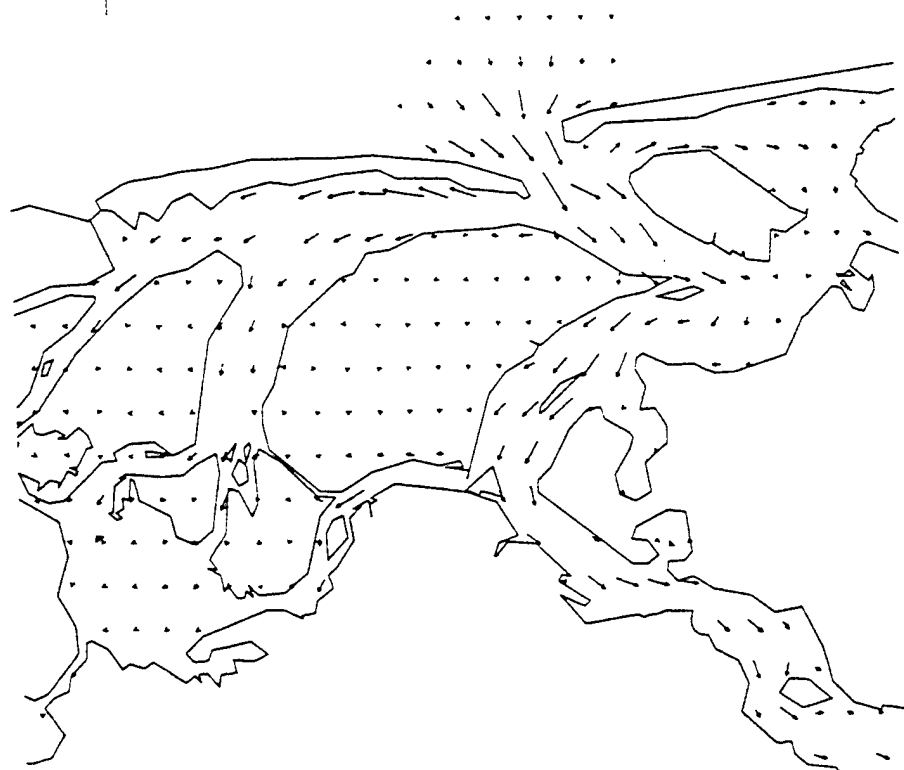
3.0
↑



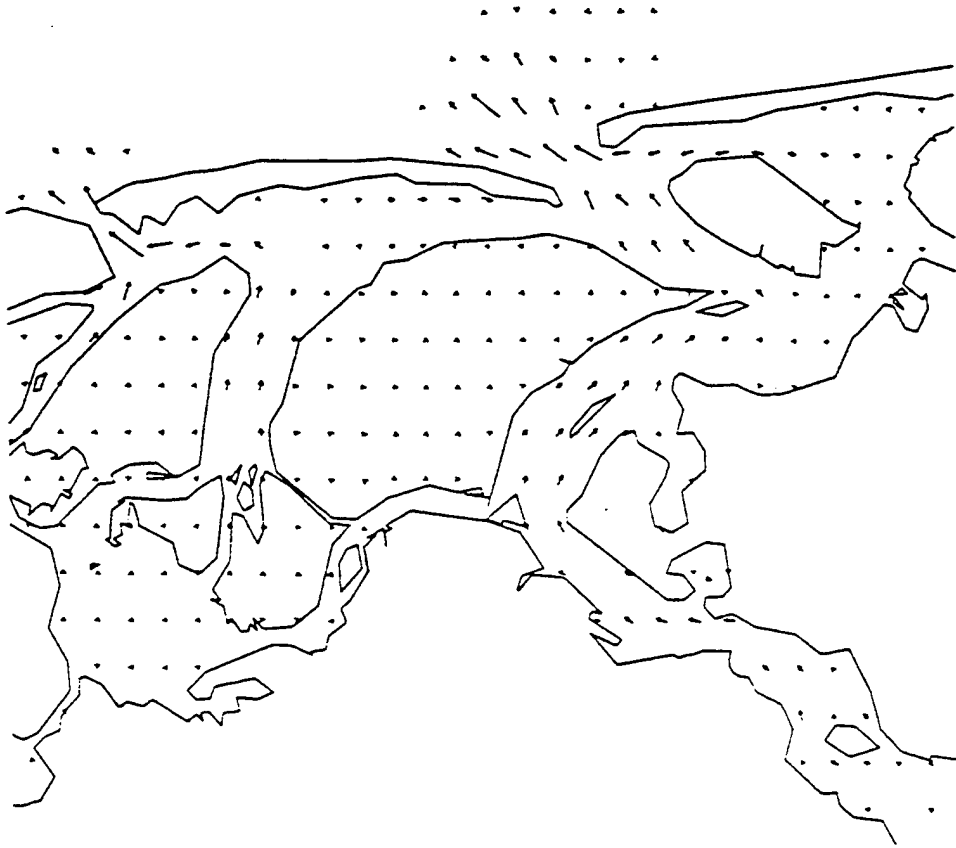
H



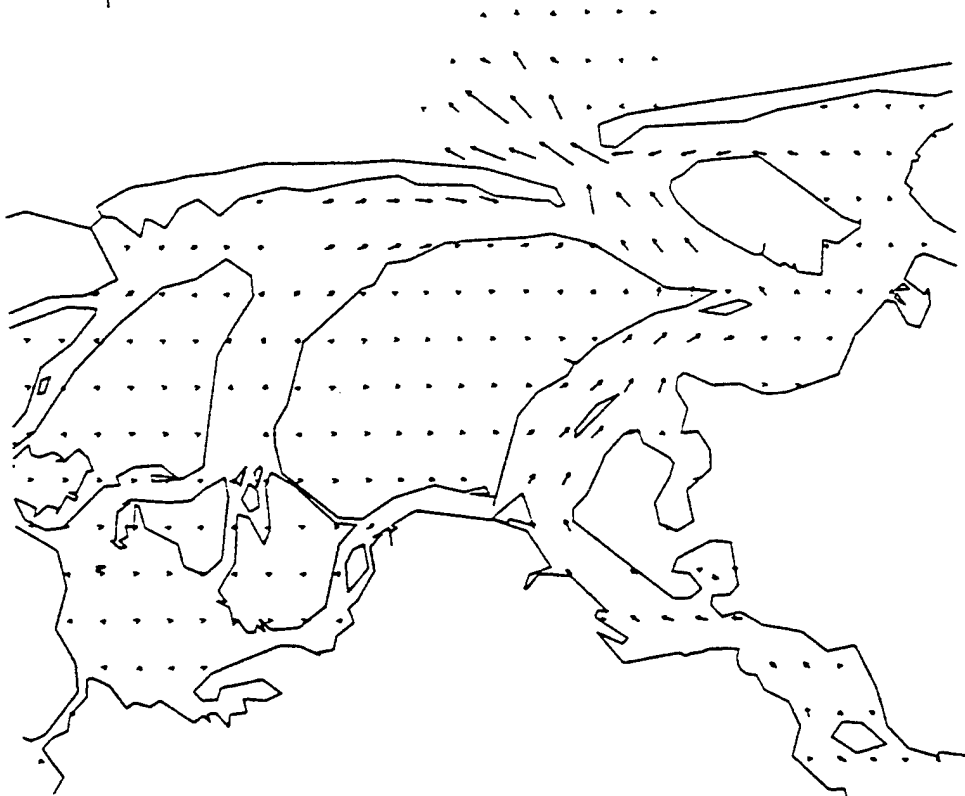
3.0
↑



I



3.0
↑



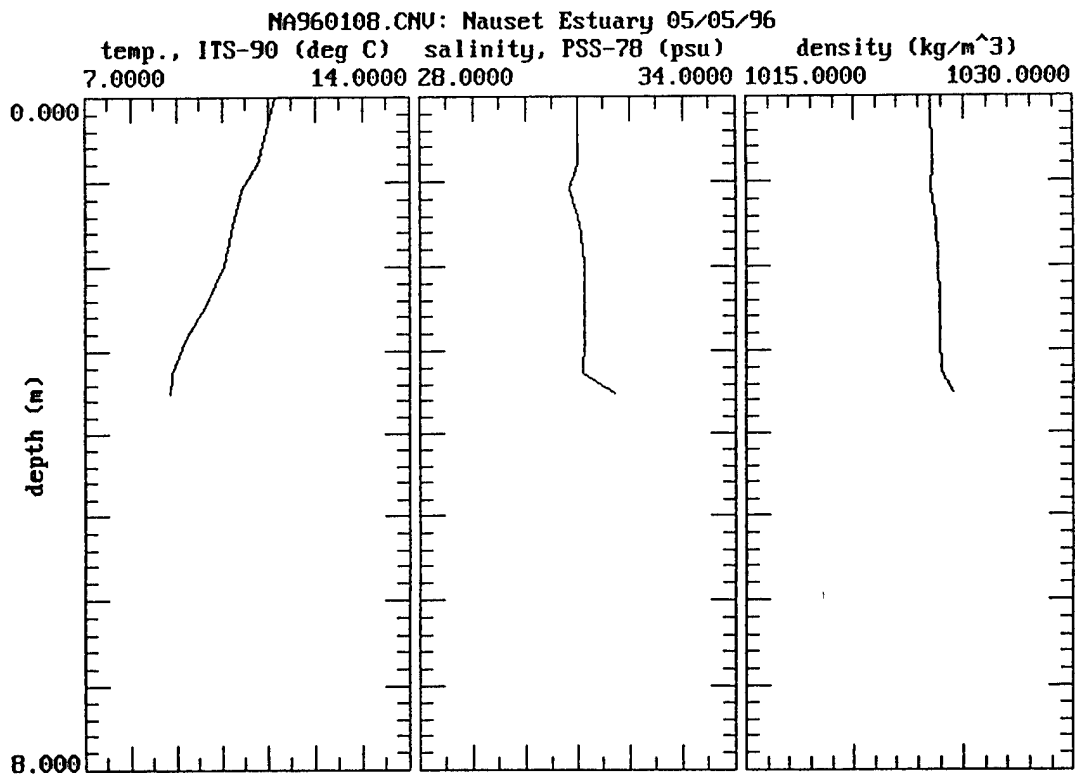
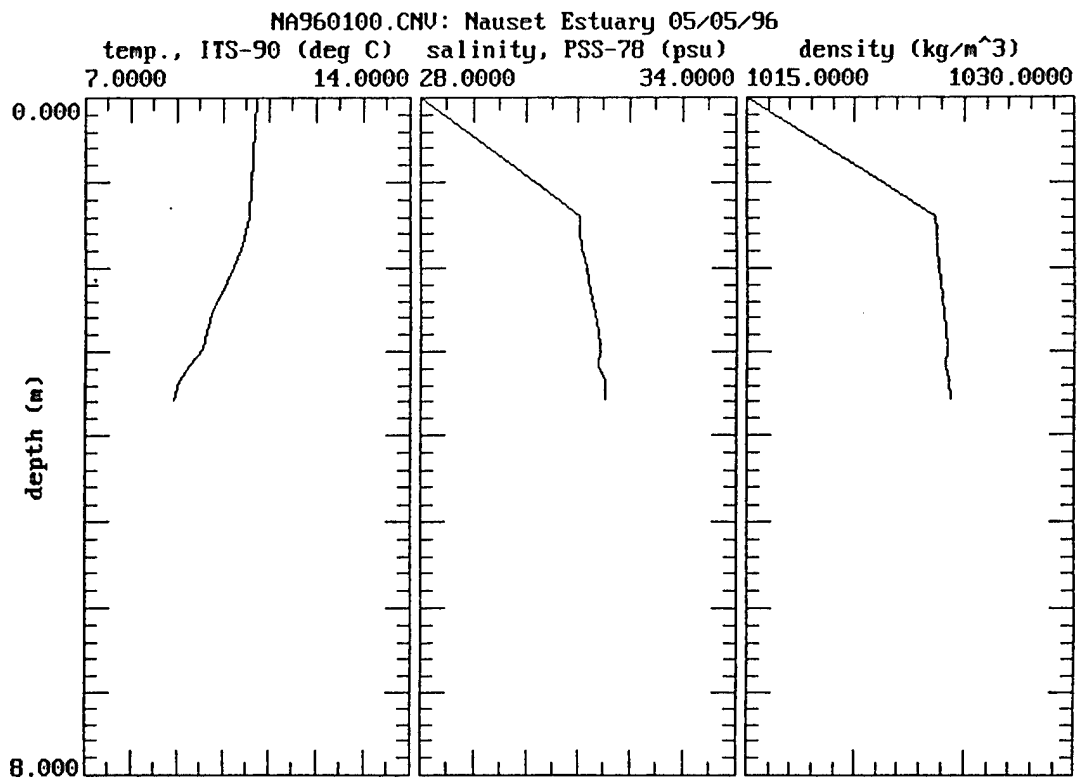
APPENDIX IV

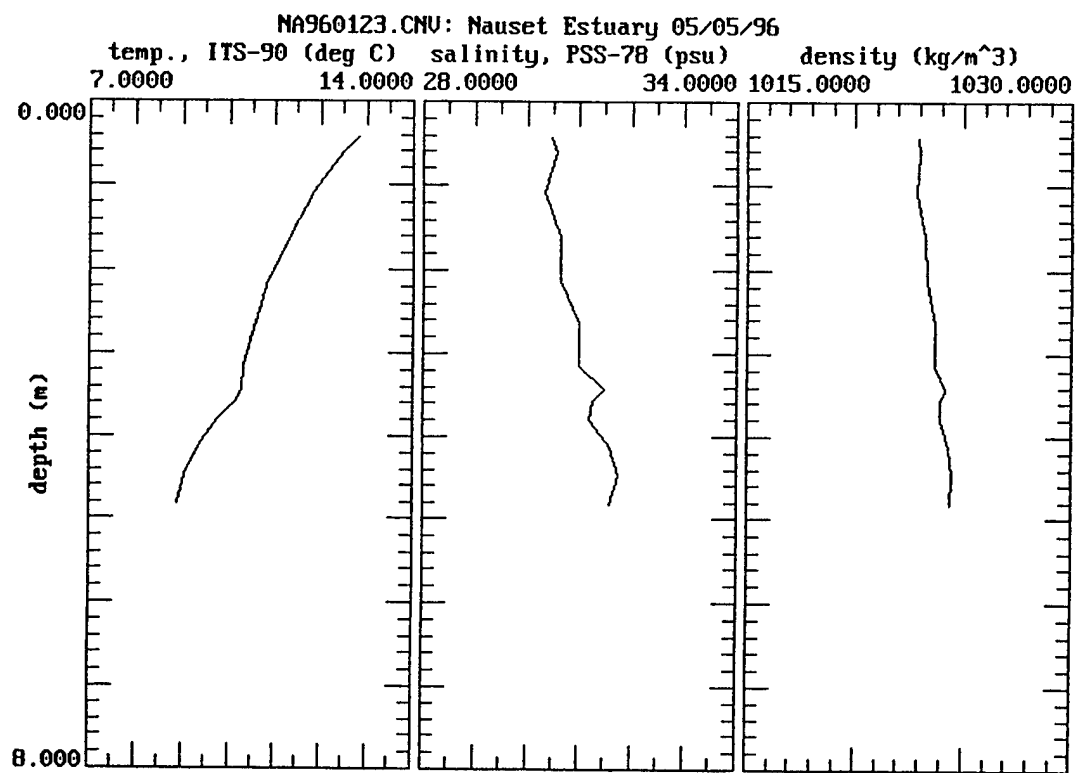
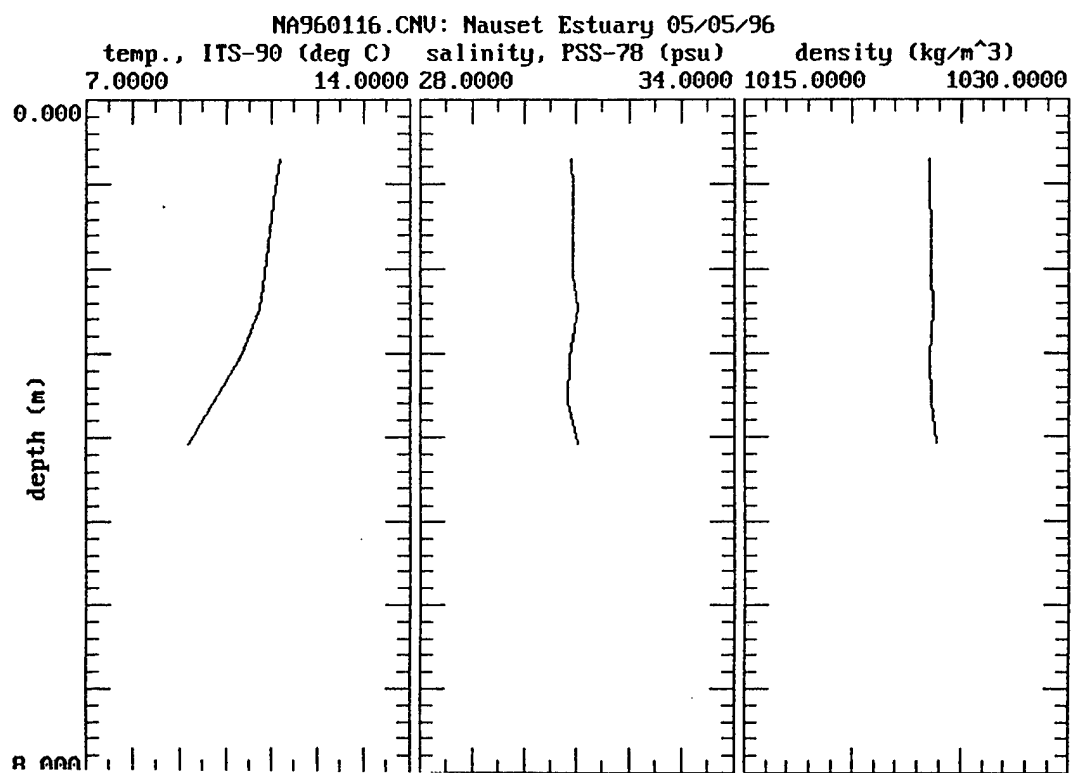
CTD Profiles

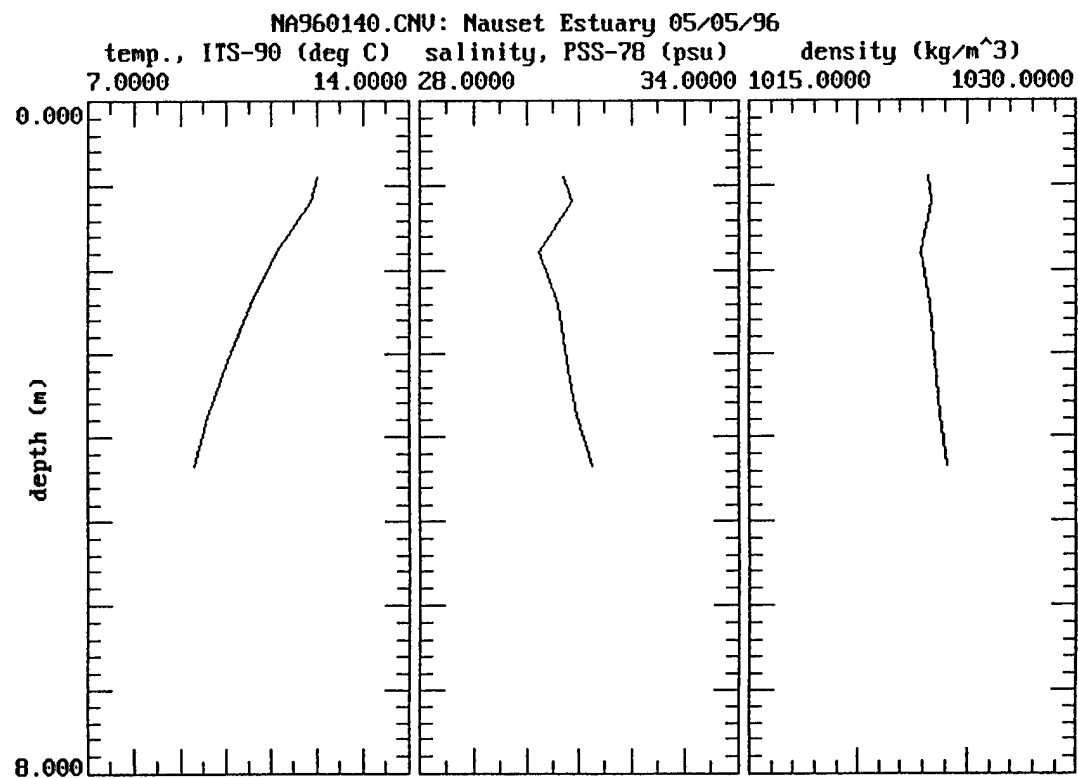
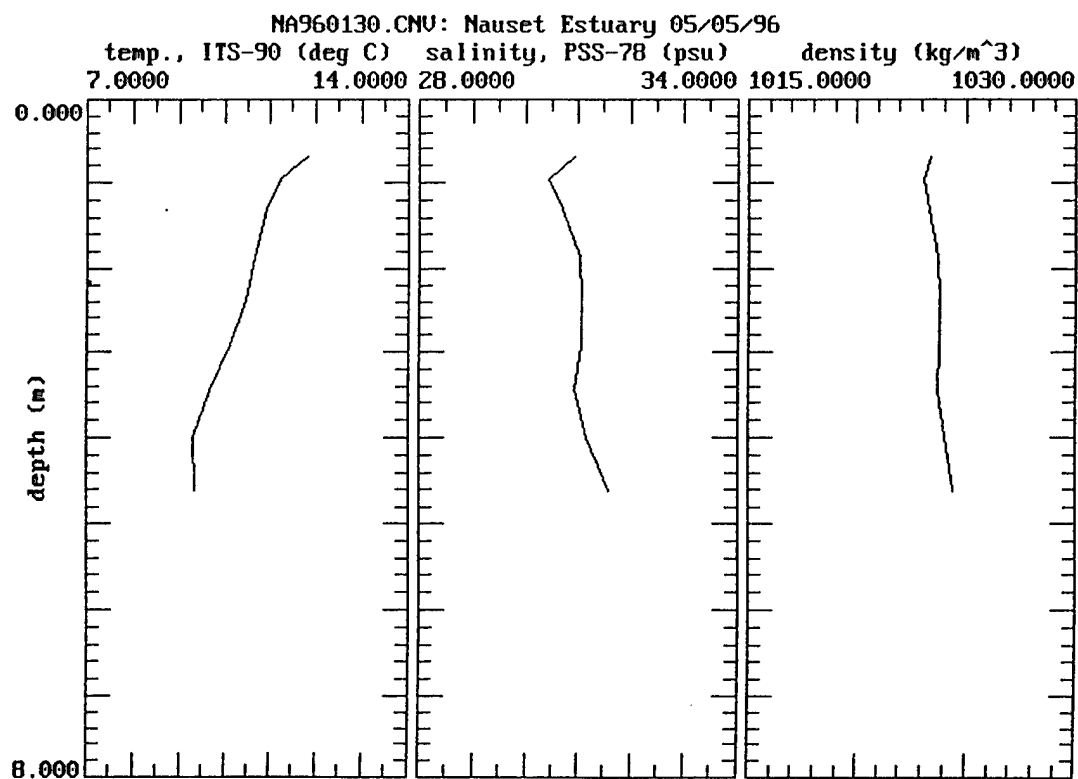
Table IV.1
Station A CTD data files

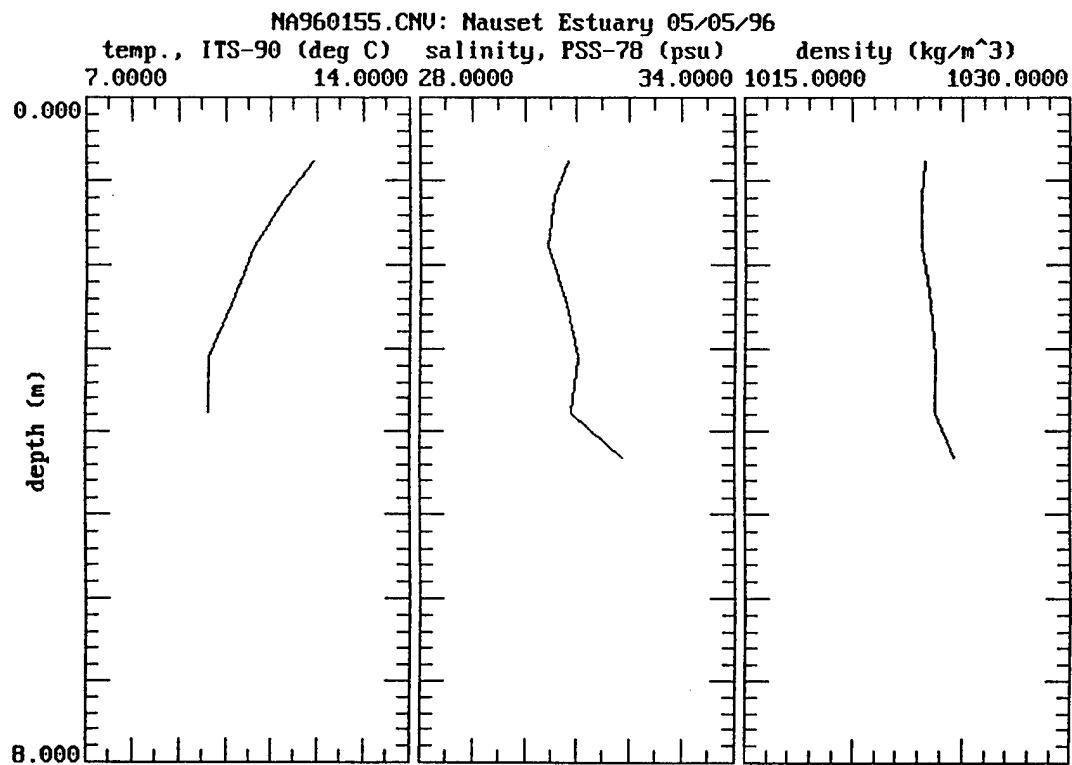
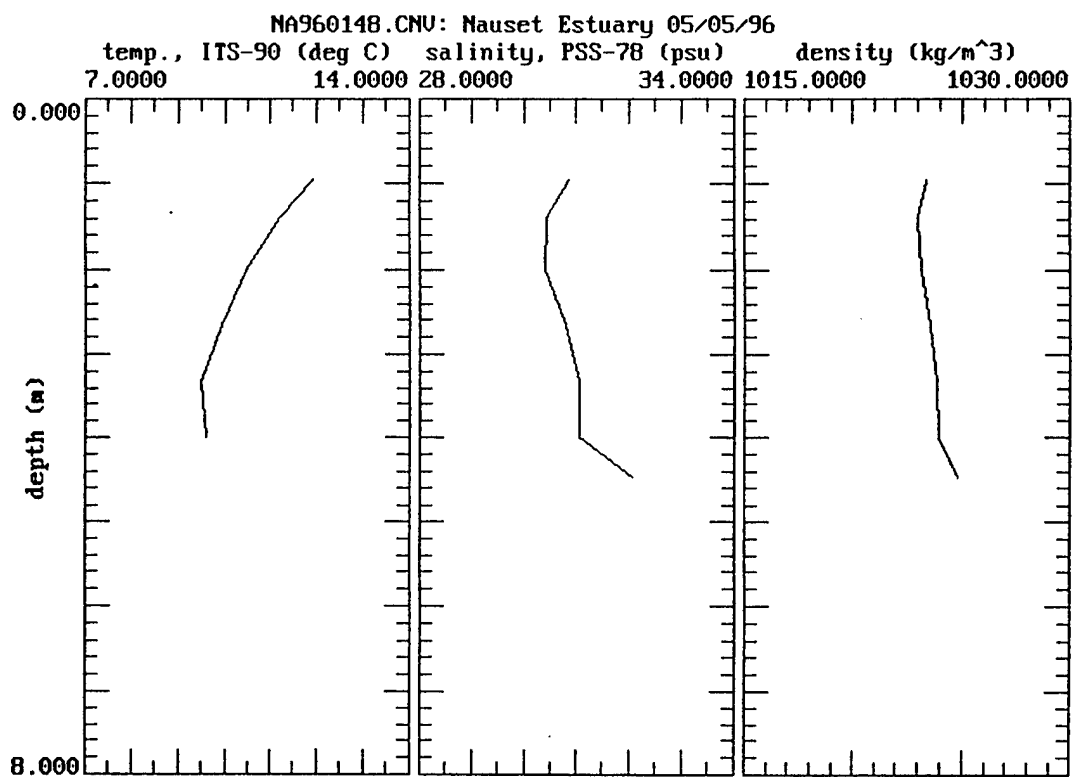
4 May 1996

Plot	Time (EST)
NA960100	07:01:51
NA960108	09:58:01
NA960116	12:34:56
NA960123	13:42:54
NA960130	14:42:50
NA960140	16:23:04
NA960148	17:03:13
NA960155	17:43:12
NA960161	18:46:21









NA960161.CNV: Nauset Estuary 05/05/96

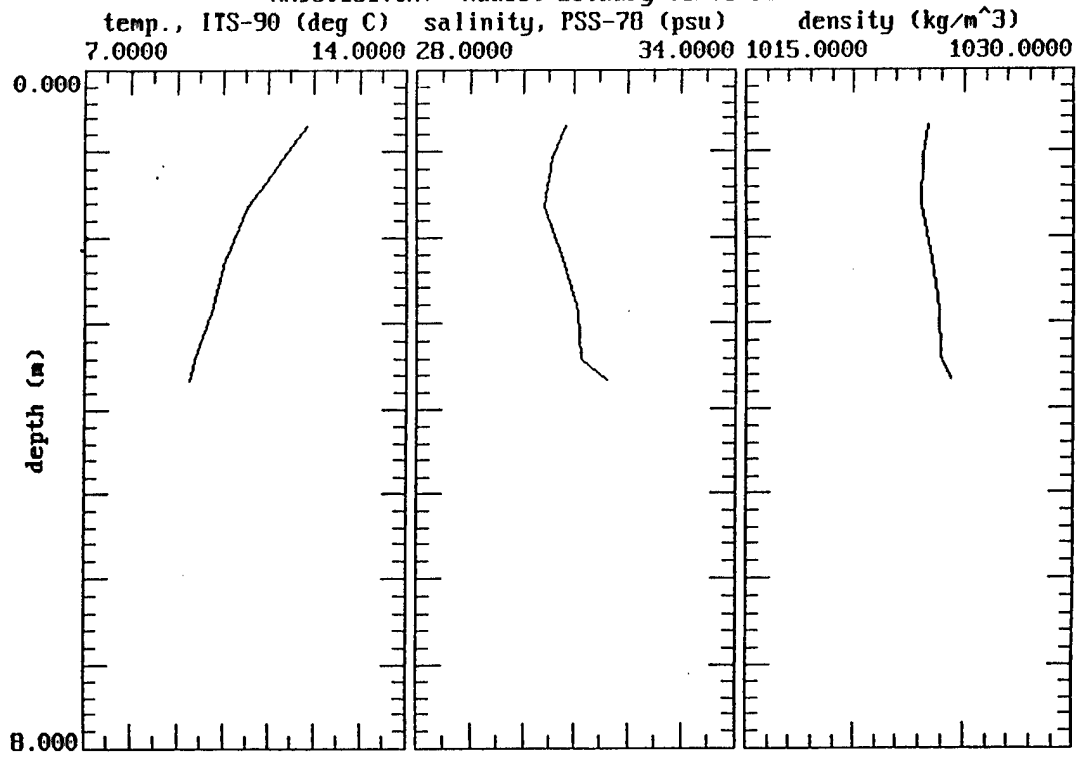
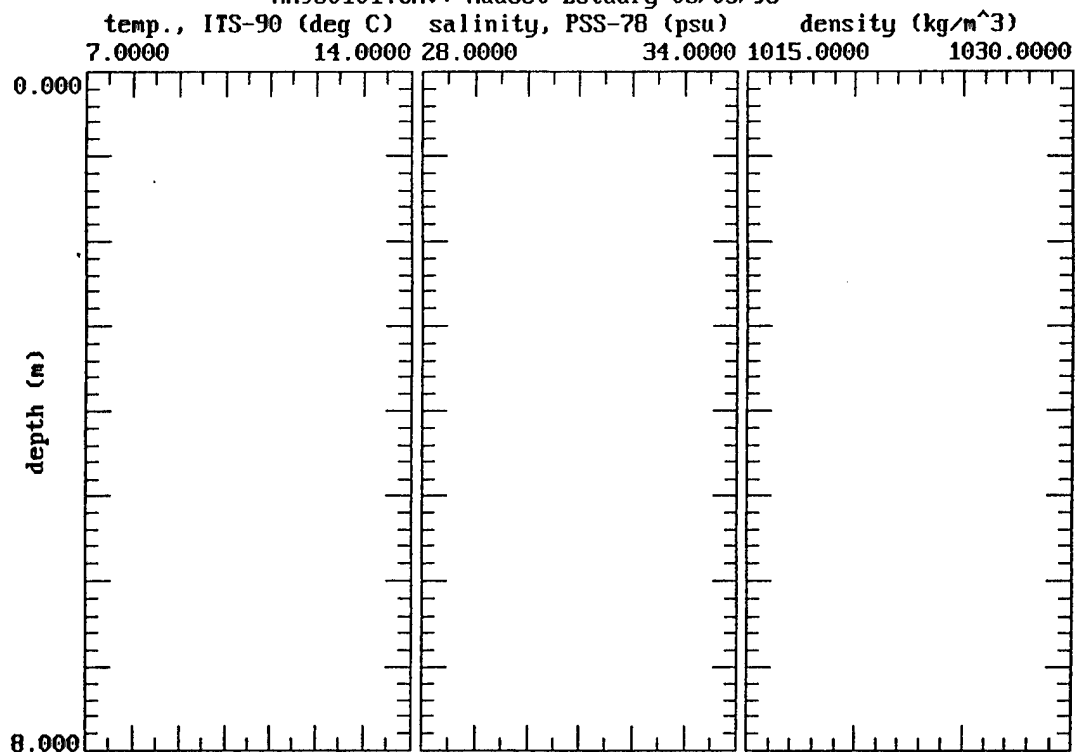


Table IV.2
Station B CTD data files

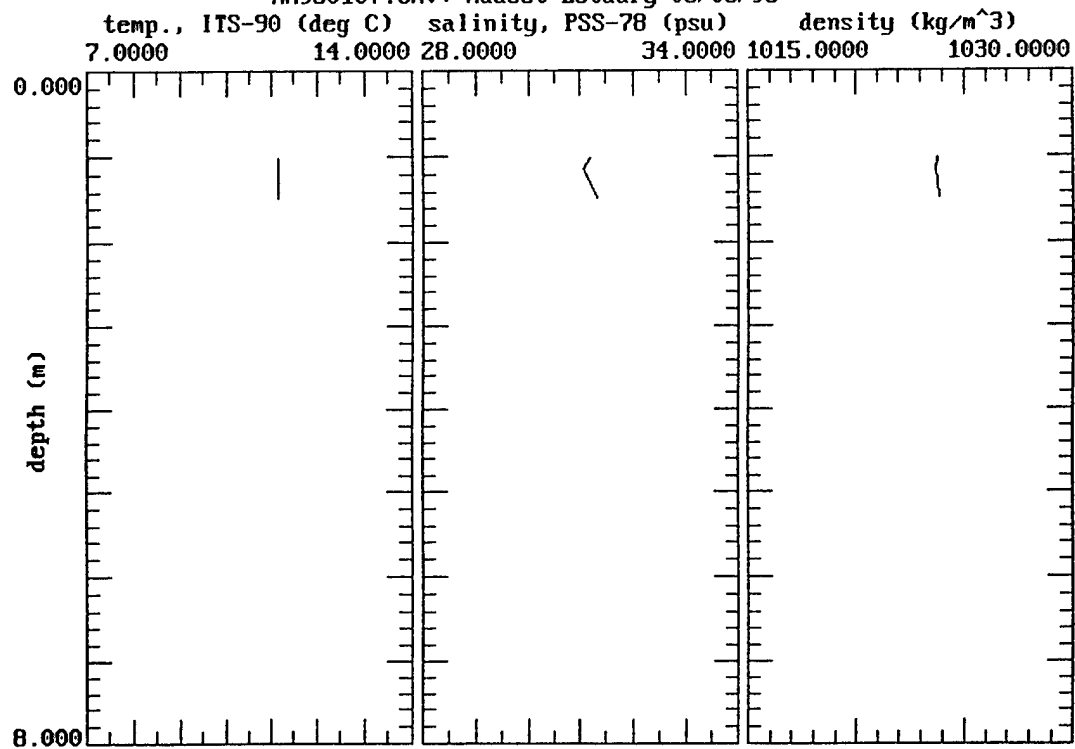
4 May 1996

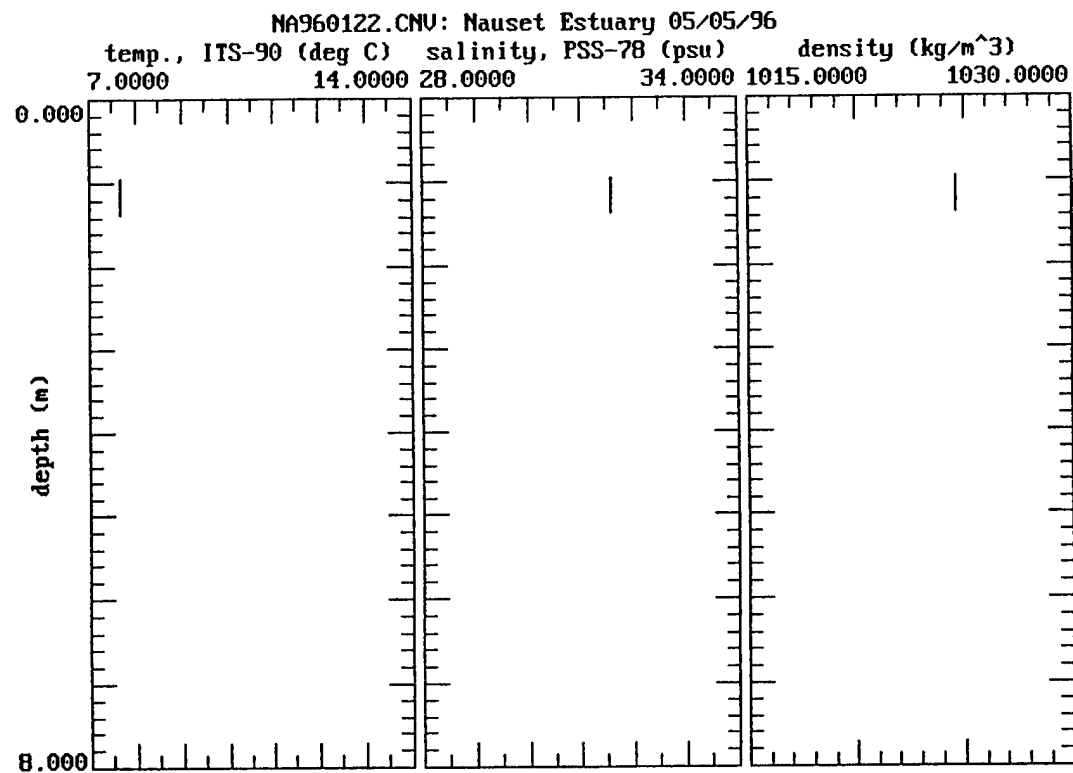
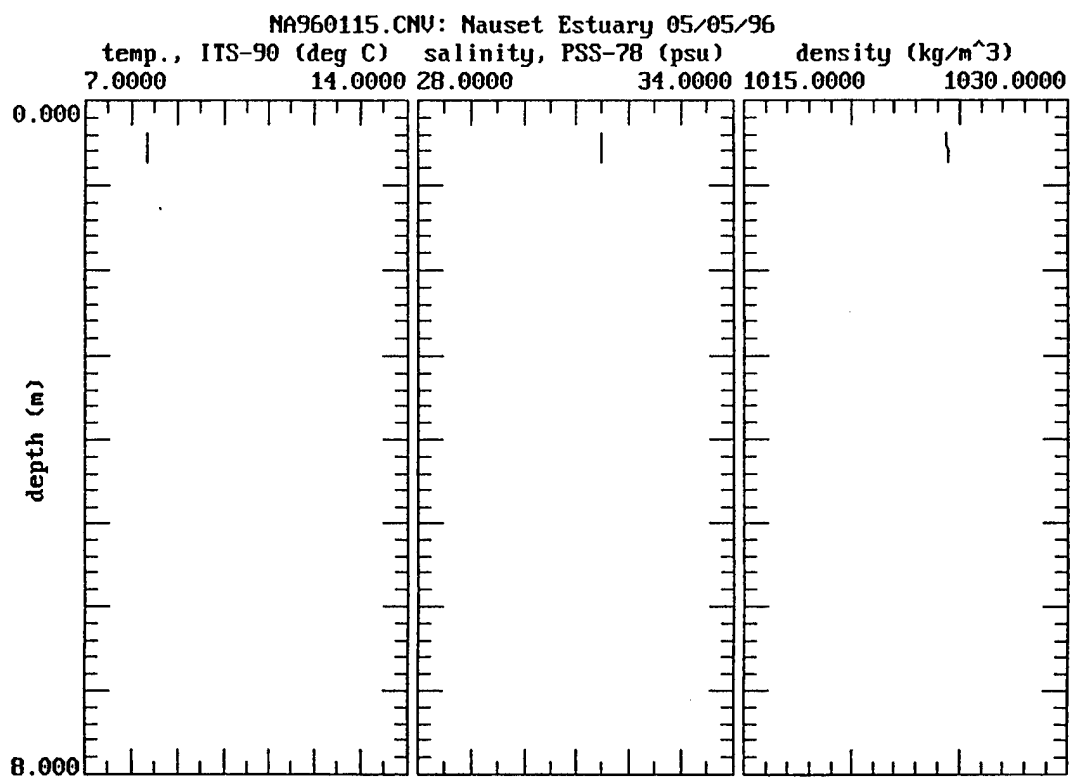
Plot	Time (EST)
NA960101	07:30:13
NA960107	09:39:02
NA960115	12:14:47
NA960122	13:35:00
NA960129	14:36:28
NA960139	16:15:38
NA960147	16:59:02
NA960154	17:38:31
NA960160	18:35:28

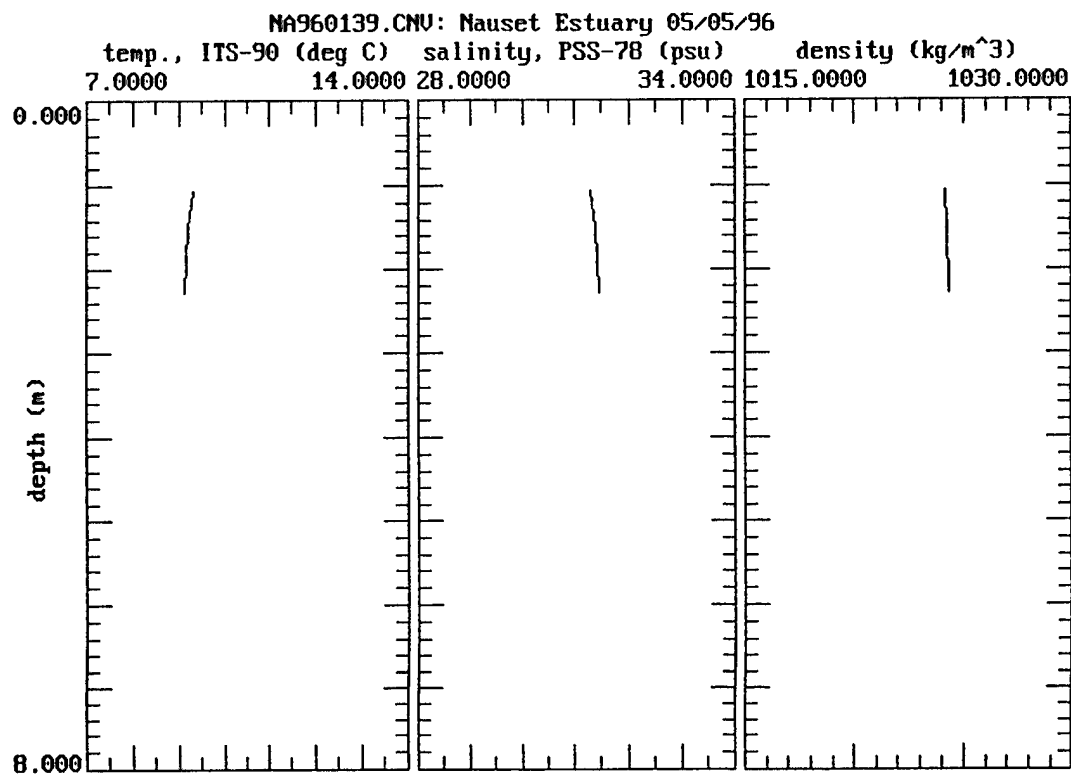
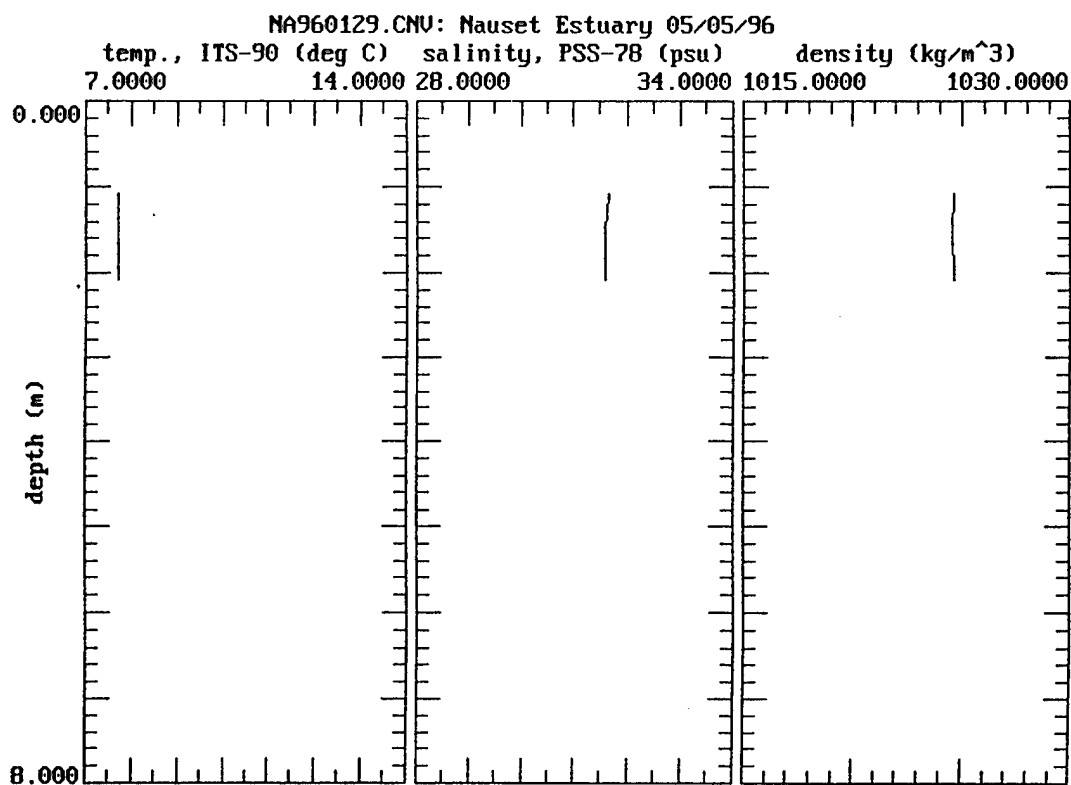
NA960101.CNU: Nauset Estuary 05/05/96

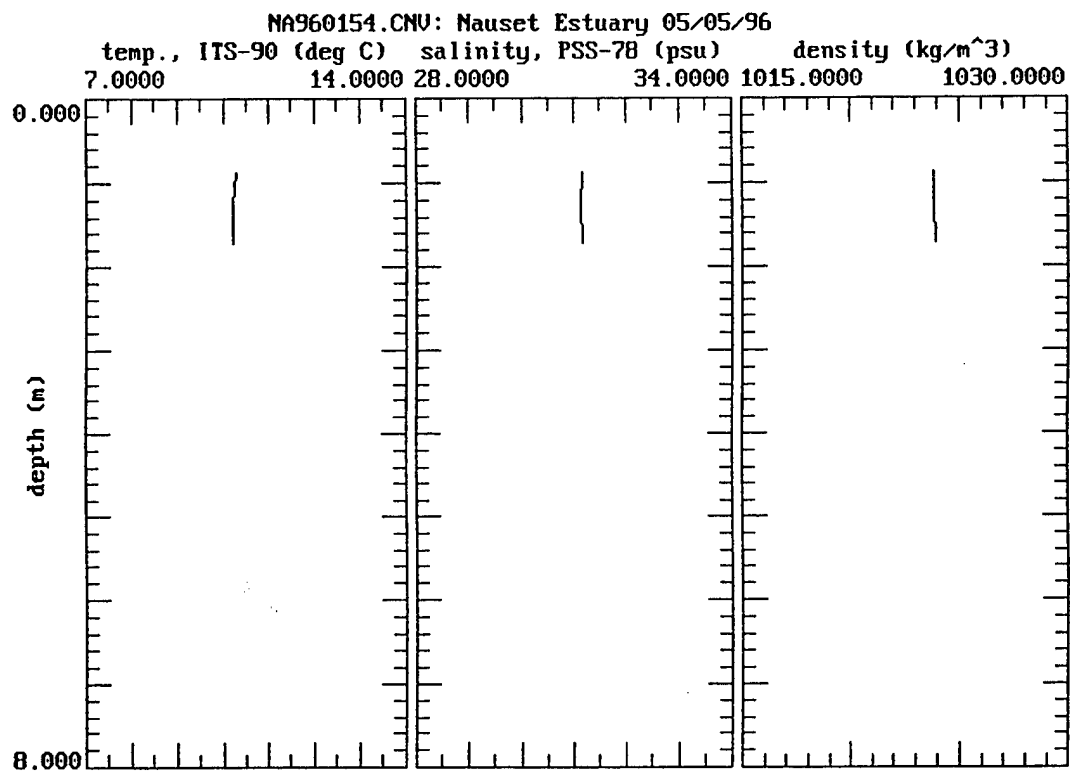
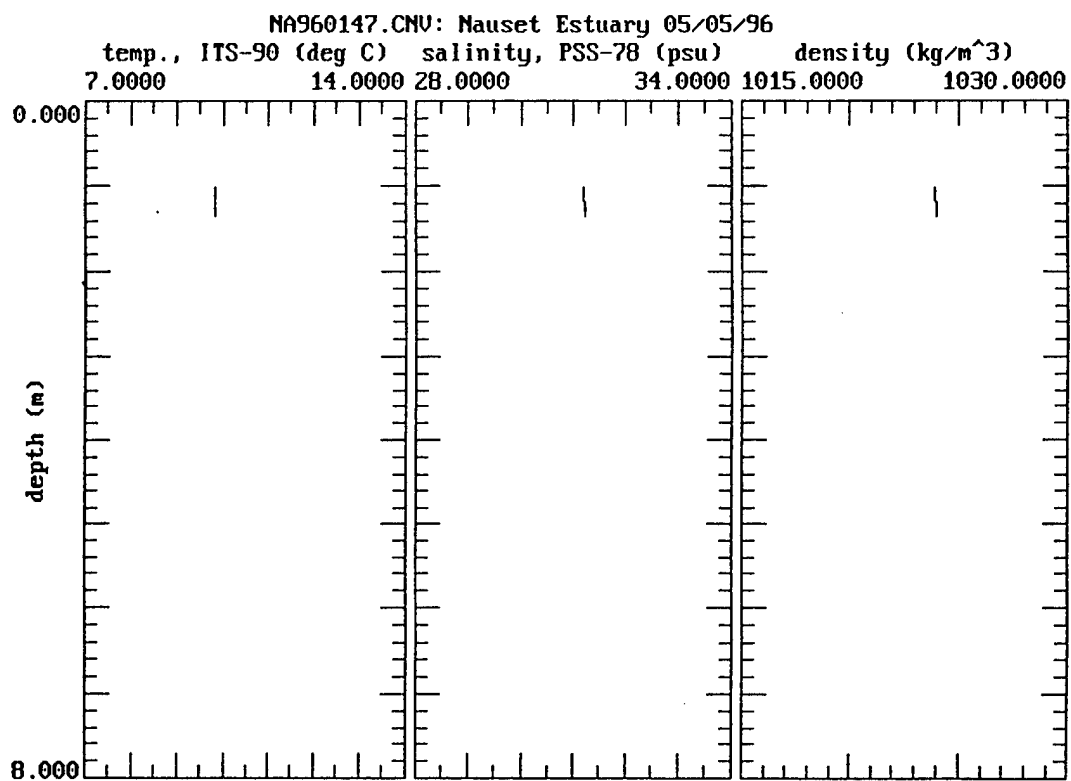


NA960107.CNU: Nauset Estuary 05/05/96









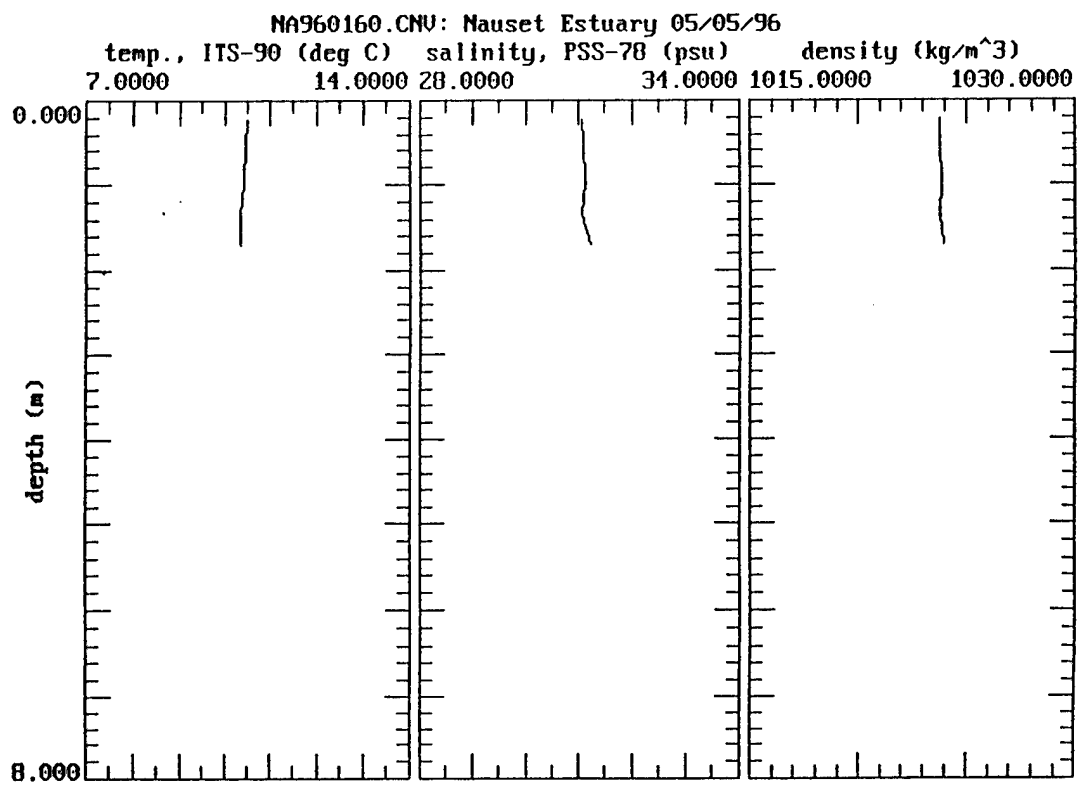
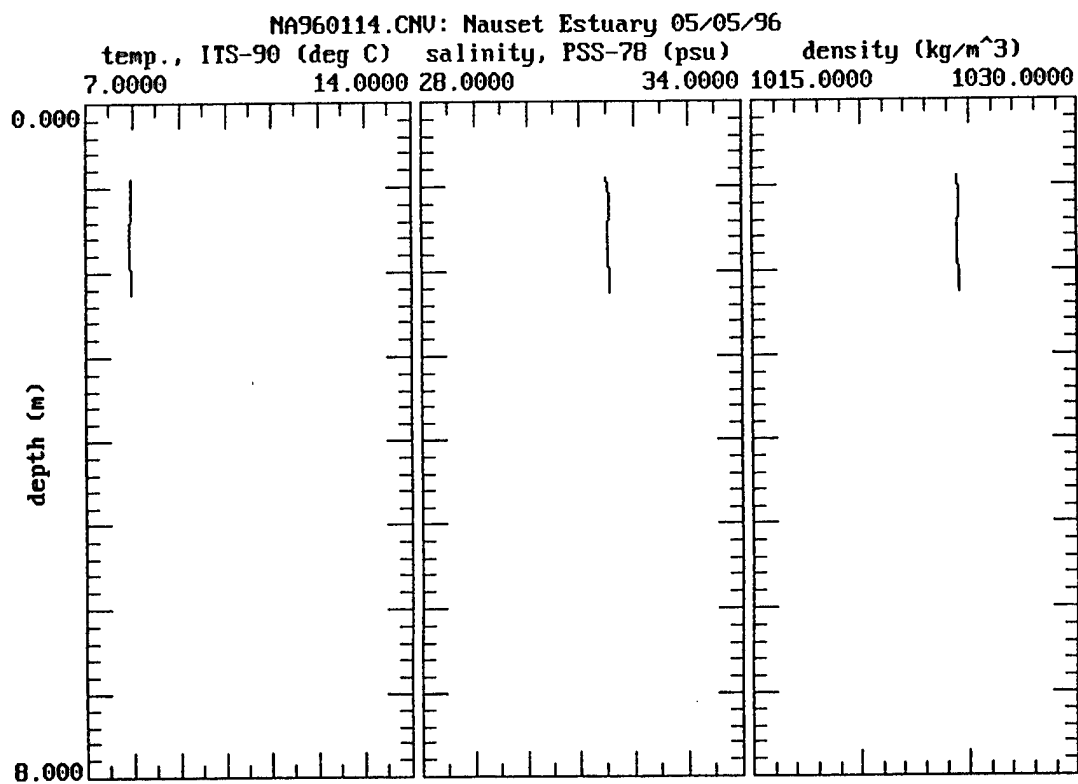
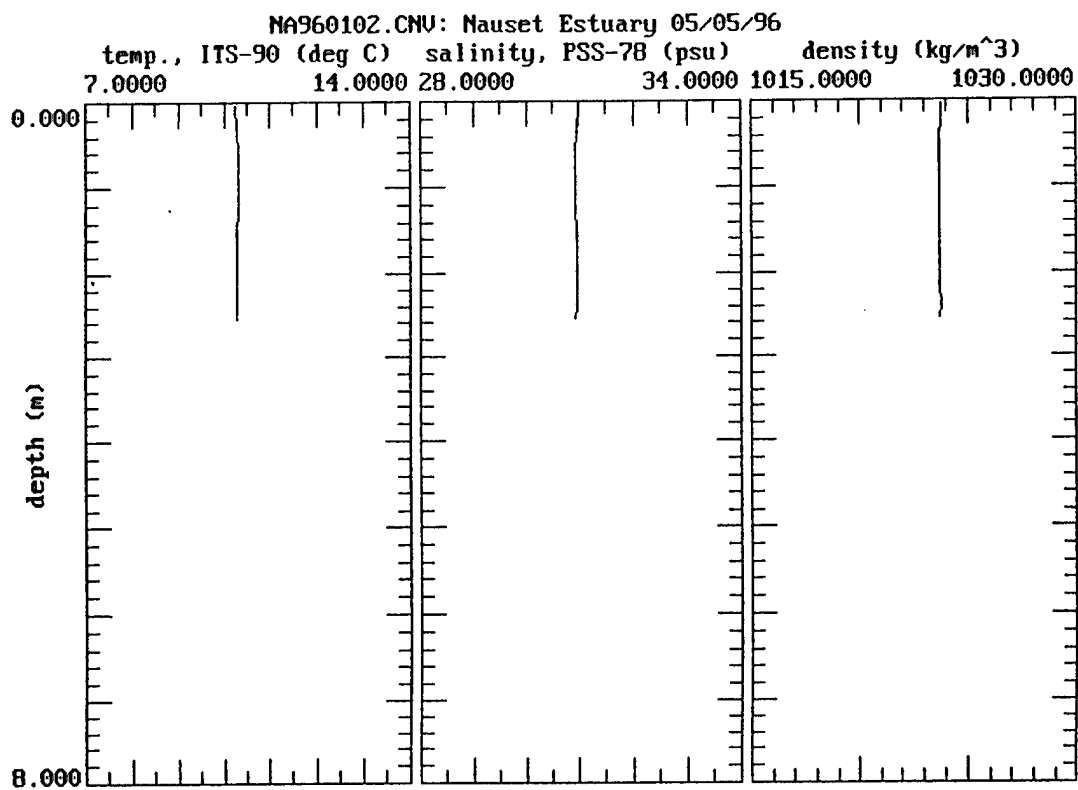
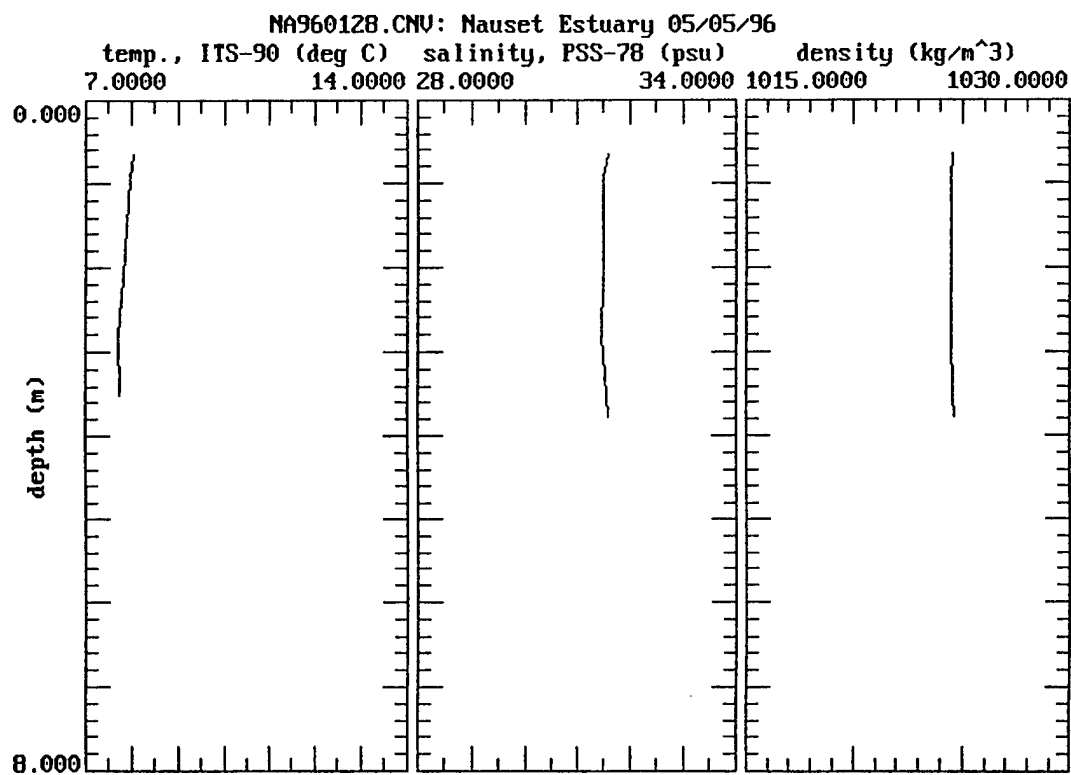
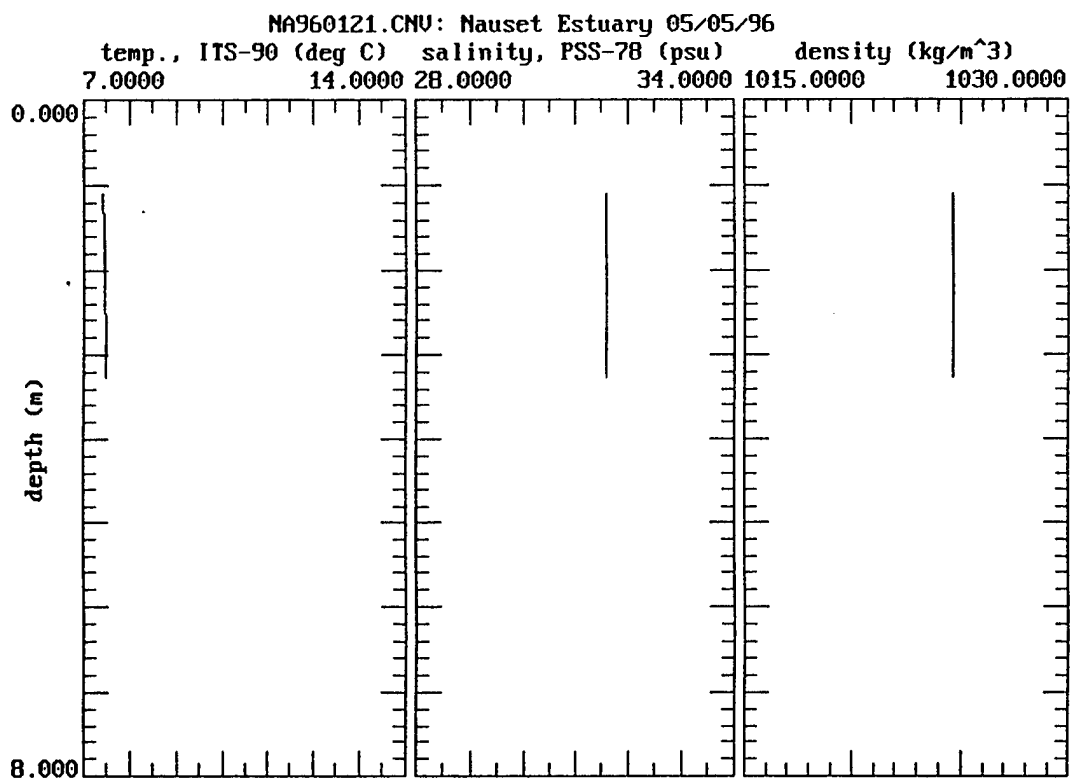
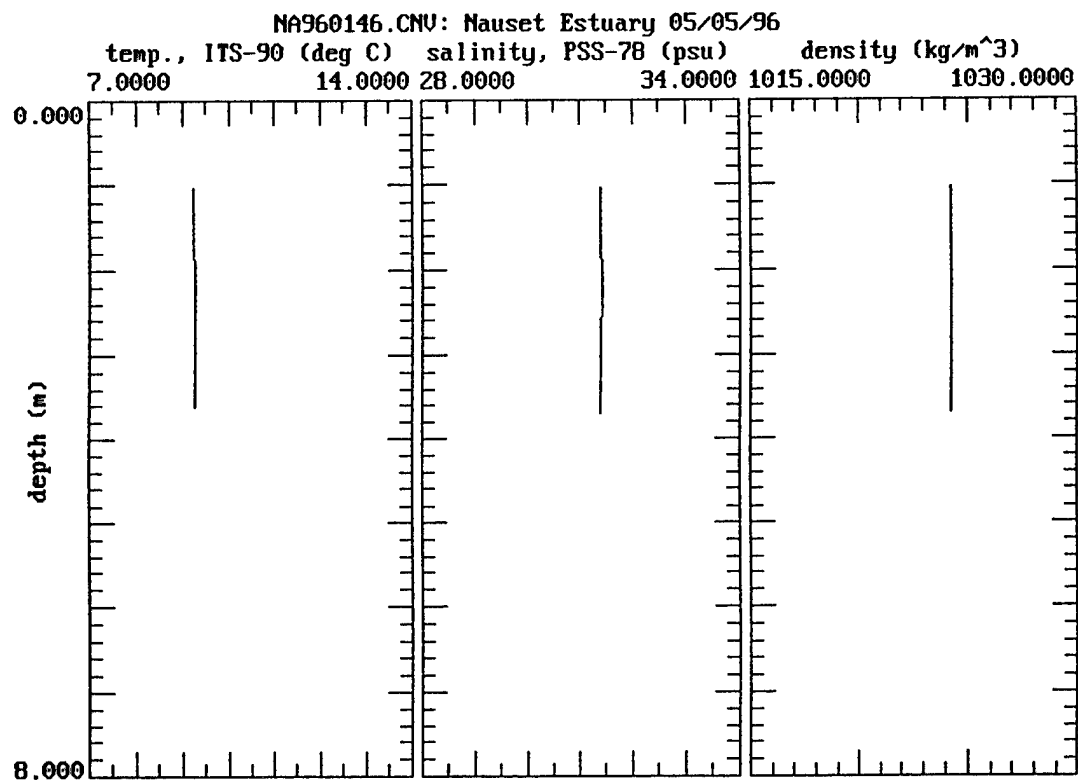
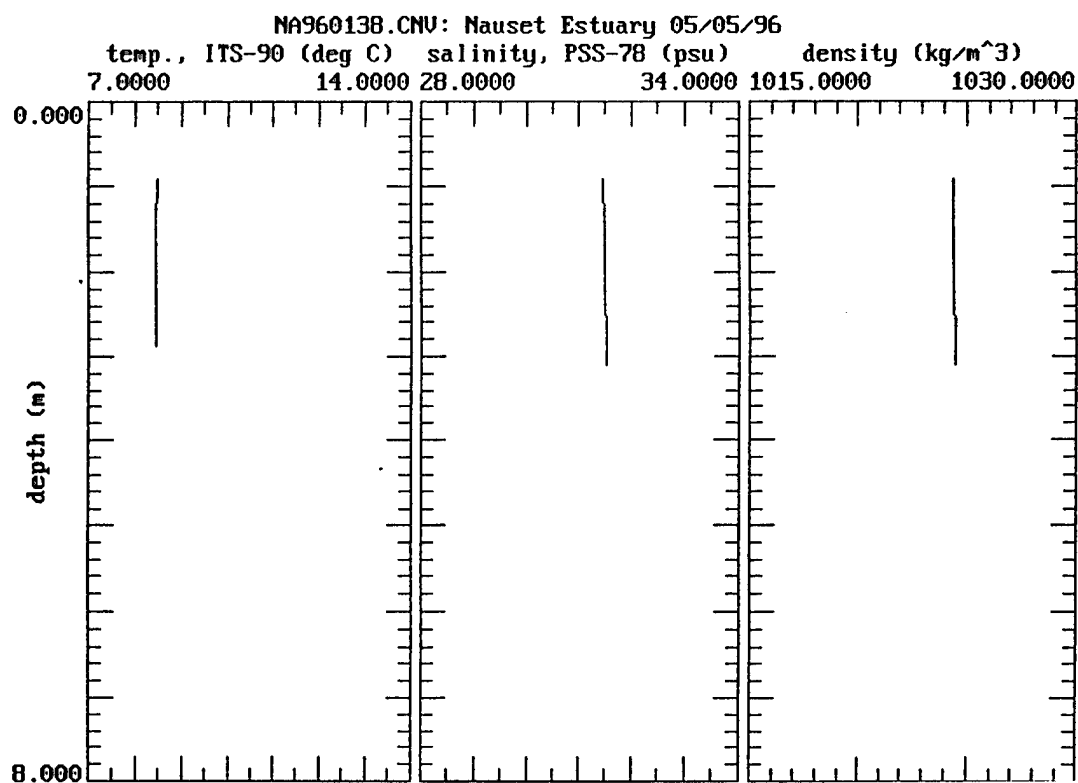


Table IV.3
Station C CTD data files
4 May 1996

Plot	Time (EST)
NA960102	07:41:31
NA960114	11:57:24
NA960121	13:29:19
NA960128	14:30:57
NA960138	16:11:41
NA960146	16:55:13
NA960153	17:34:44
NA960159	18:31:54







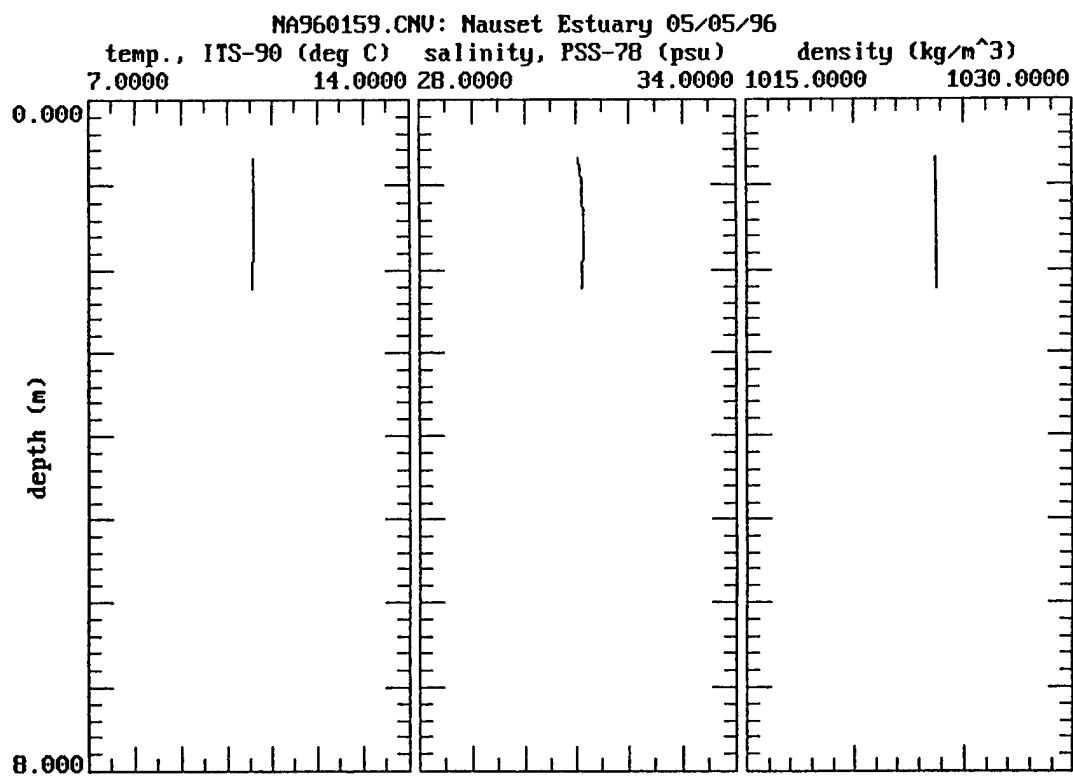
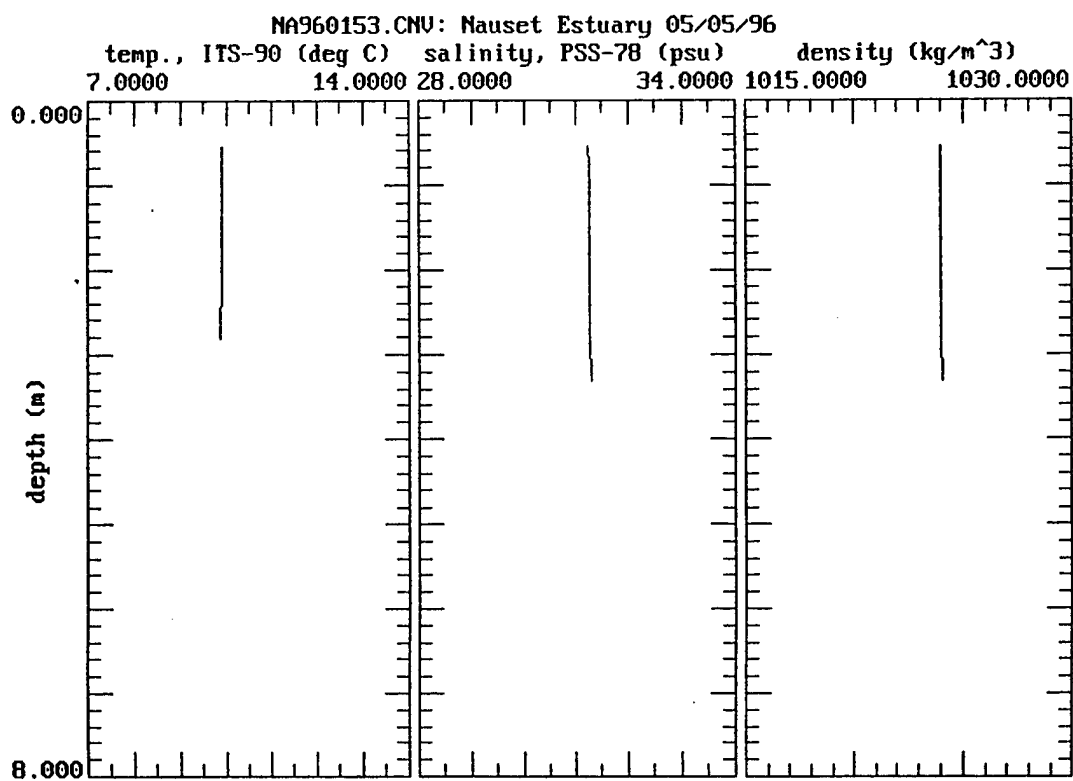
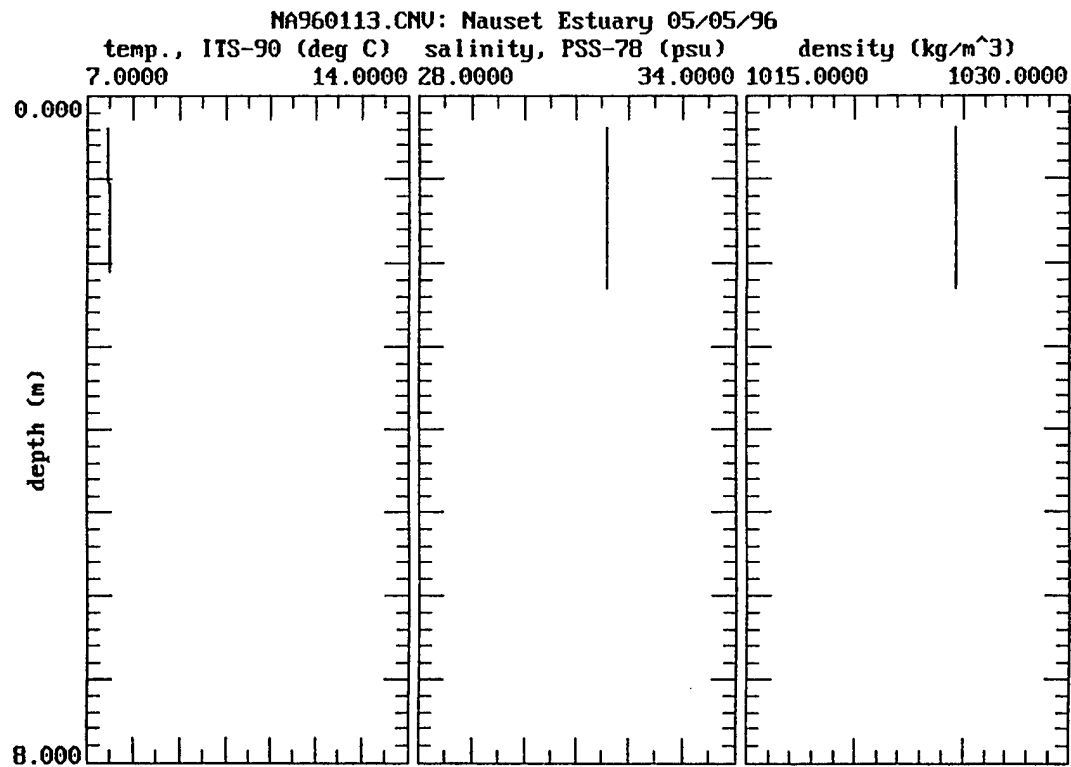
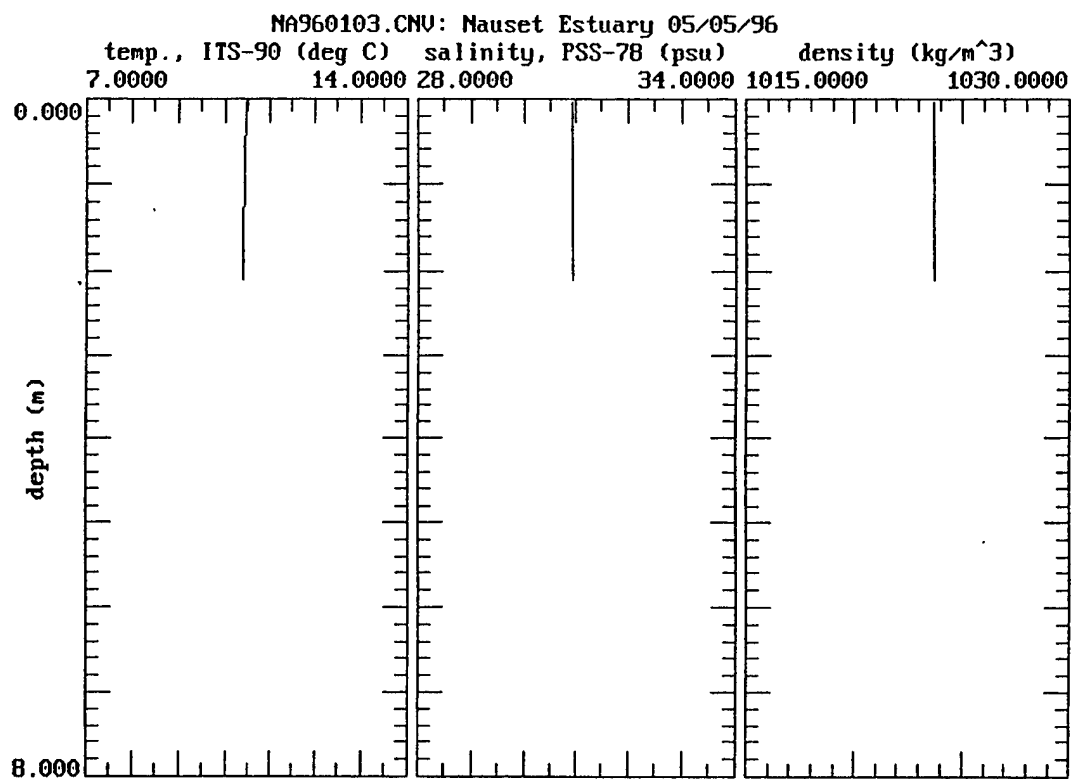
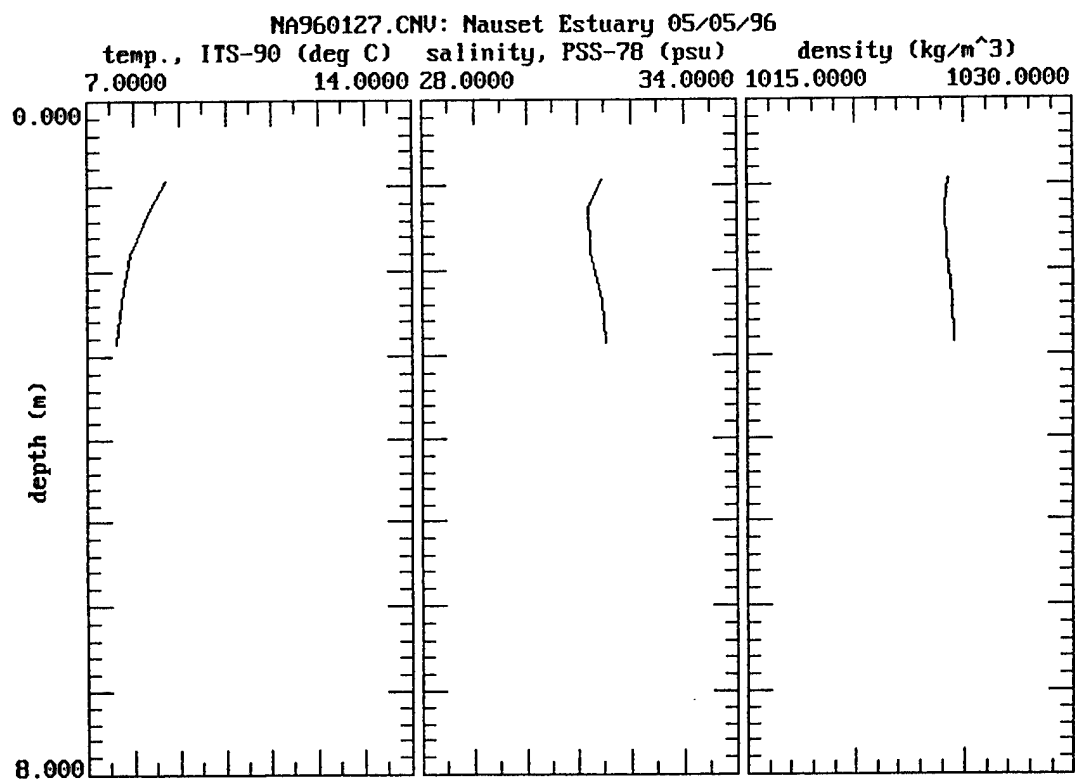
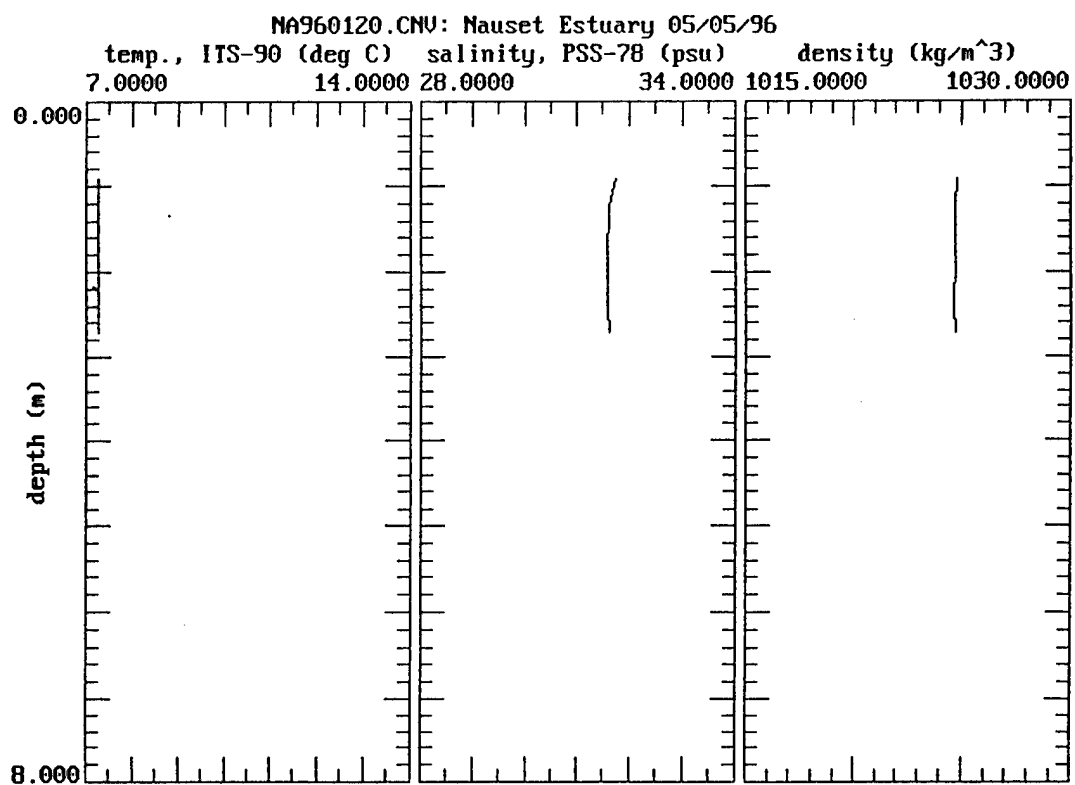
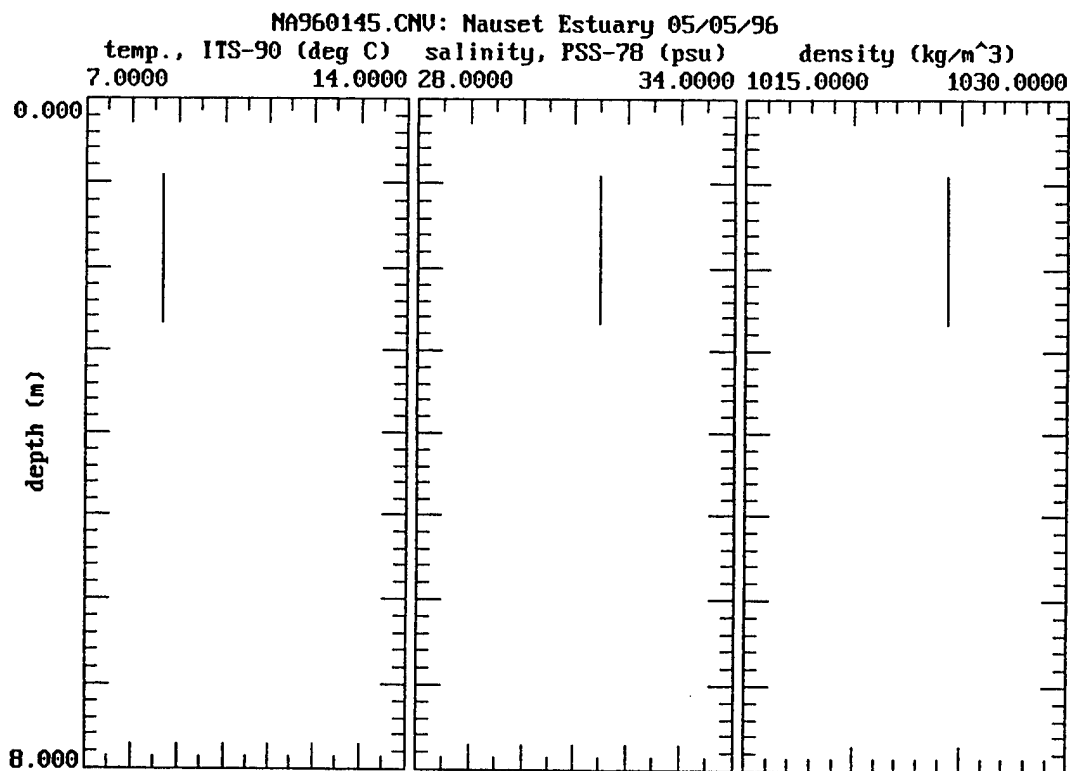
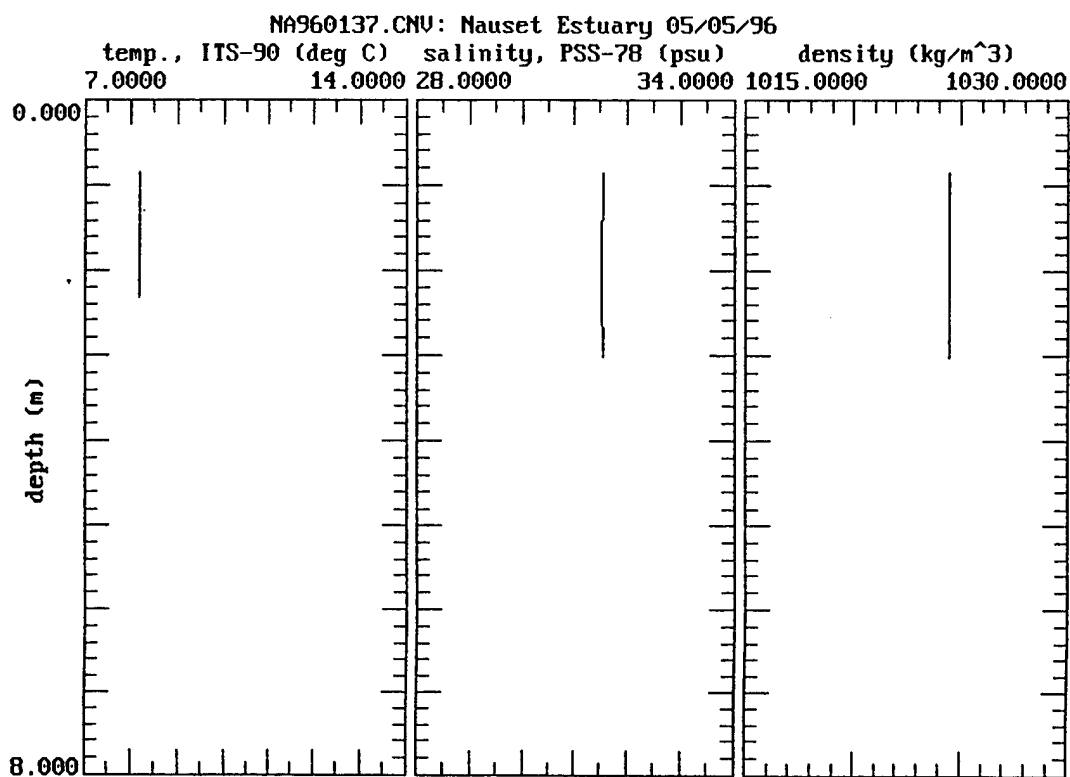


Table IV.4
Station D CTD data files
 4 May 1996

Plot	Time (EST)
NA960103	07:53:30
NA960113	11:44:10
NA960120	13:25:01
NA960127	14:24:50
NA960137	16:06:38
NA960145	16:51:14
NA960152	17:26:36
NA960158	18:23:21







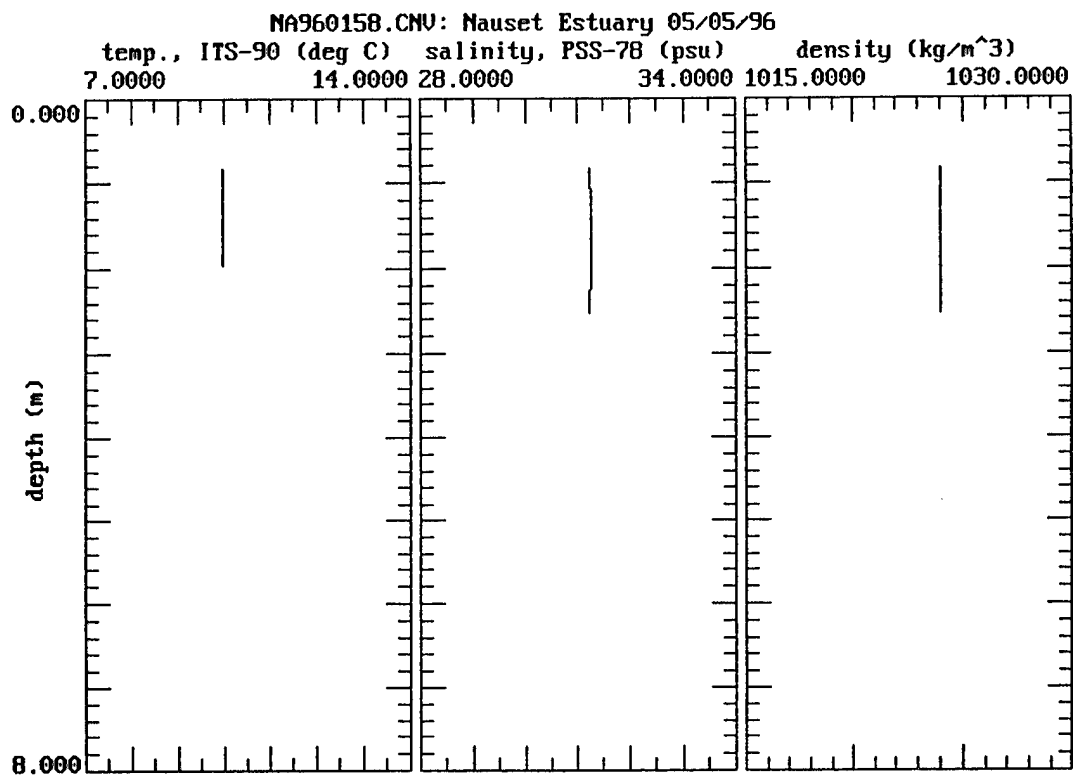
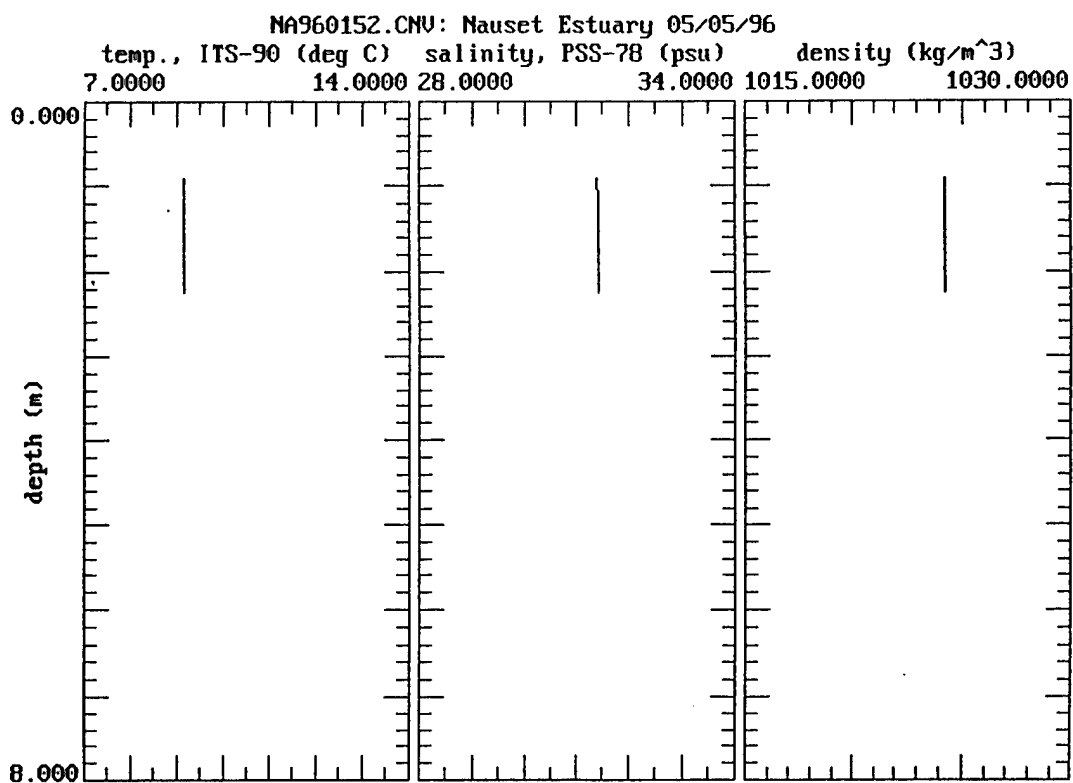
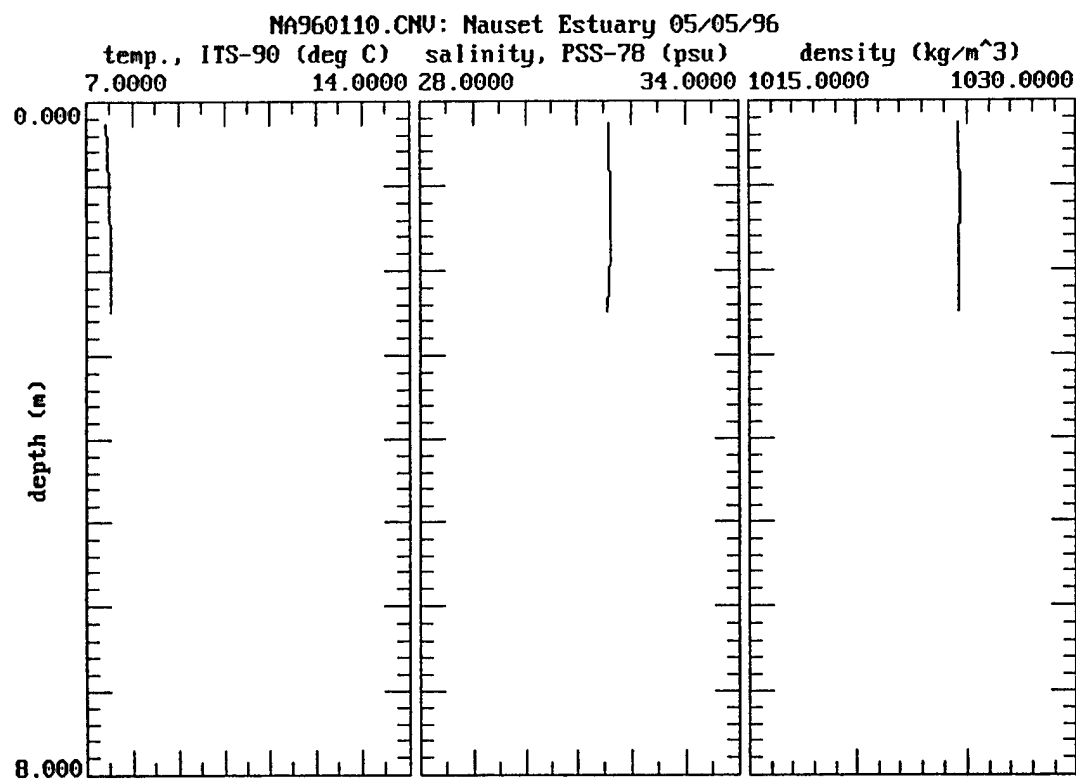
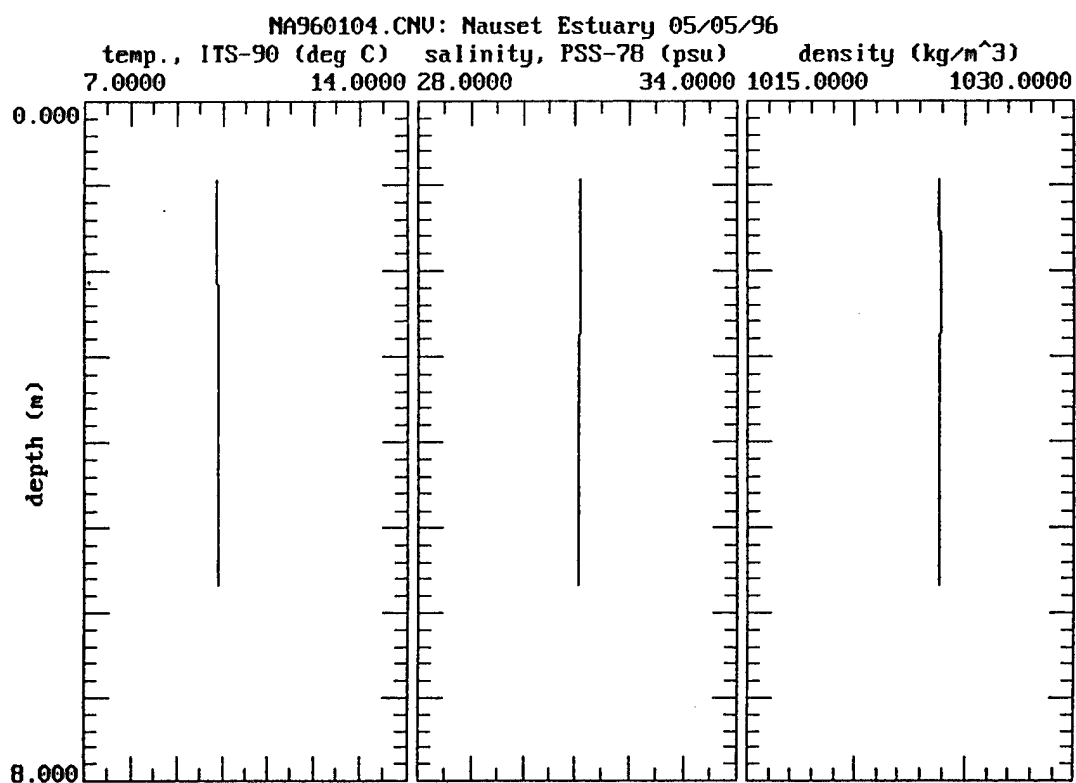
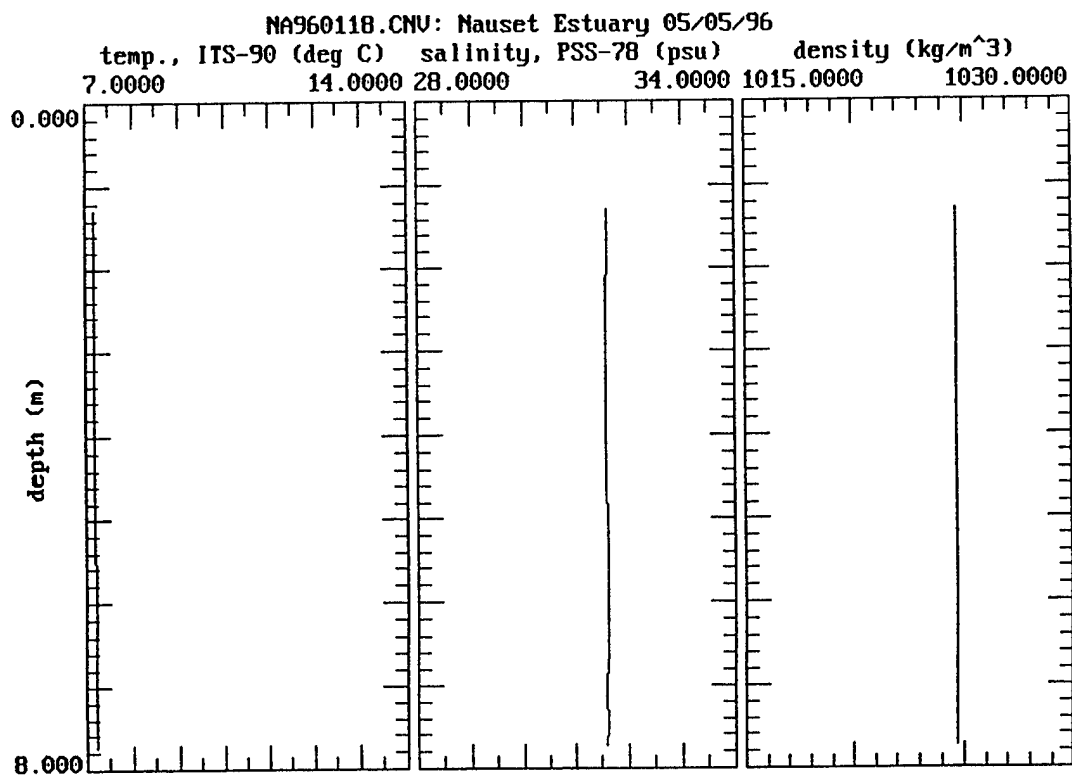
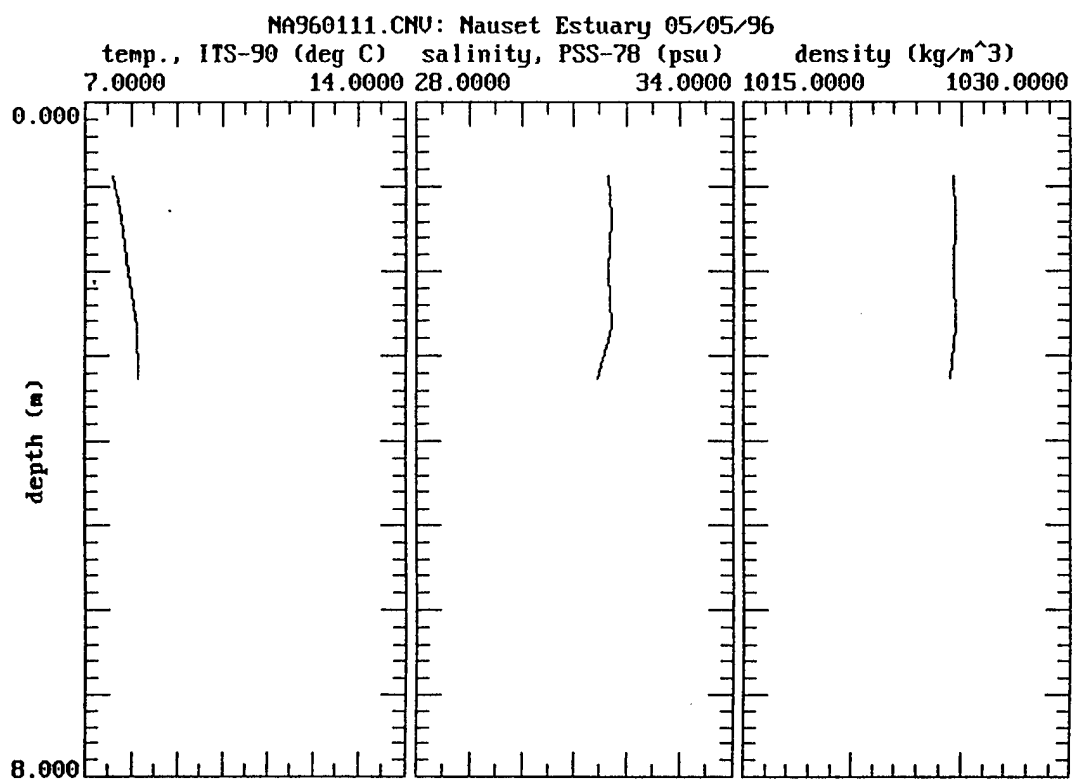
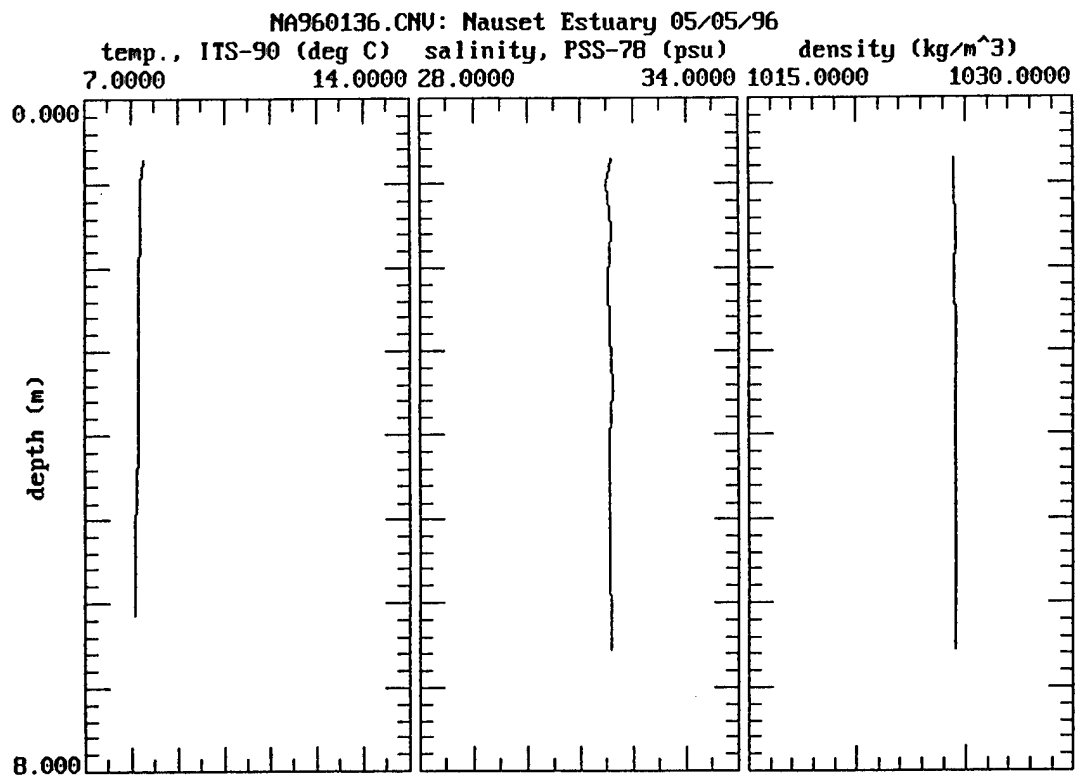
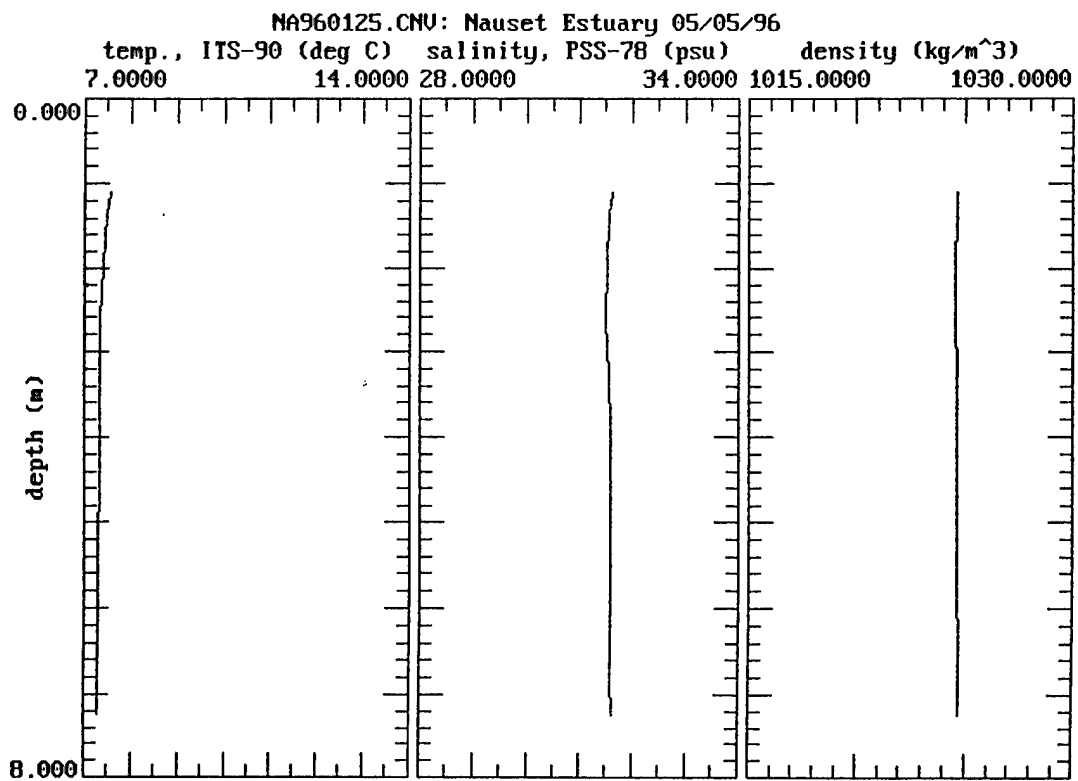


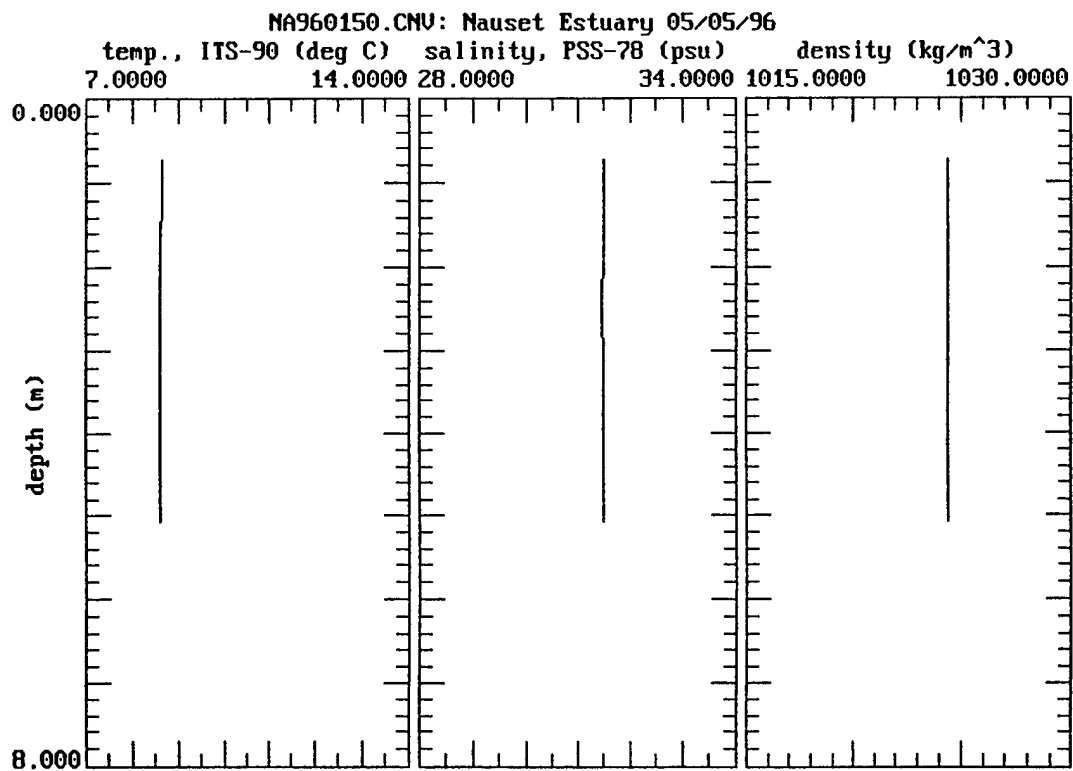
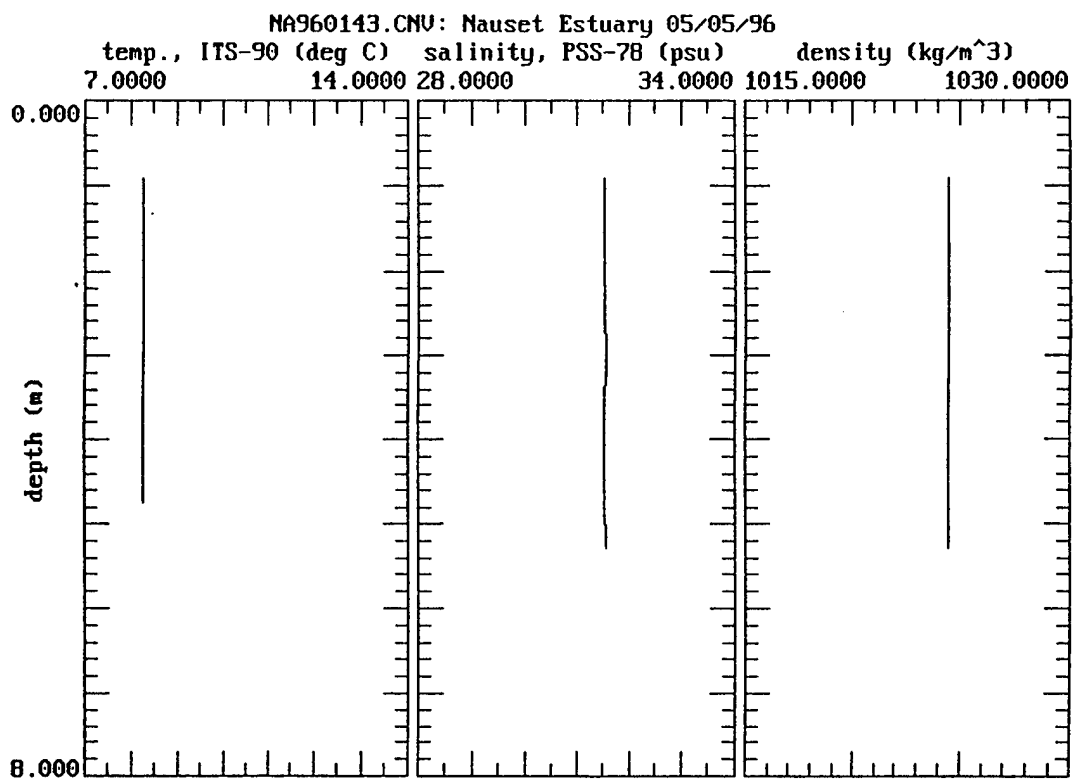
Table IV.5
Station E CTD data files
4 May 1996

Plot	Time (EST)
NA960104	08:05:46
NA960110	11:29:57
NA960111	11:31:14
NA960118	13:15:02
NA960125	14:03:38
NA960136	16:01:07
NA960143	16:42:55
NA960150	17:17:06
NA960157	18:18:47









NA960157.CNU: Nauset Estuary 05/05/96

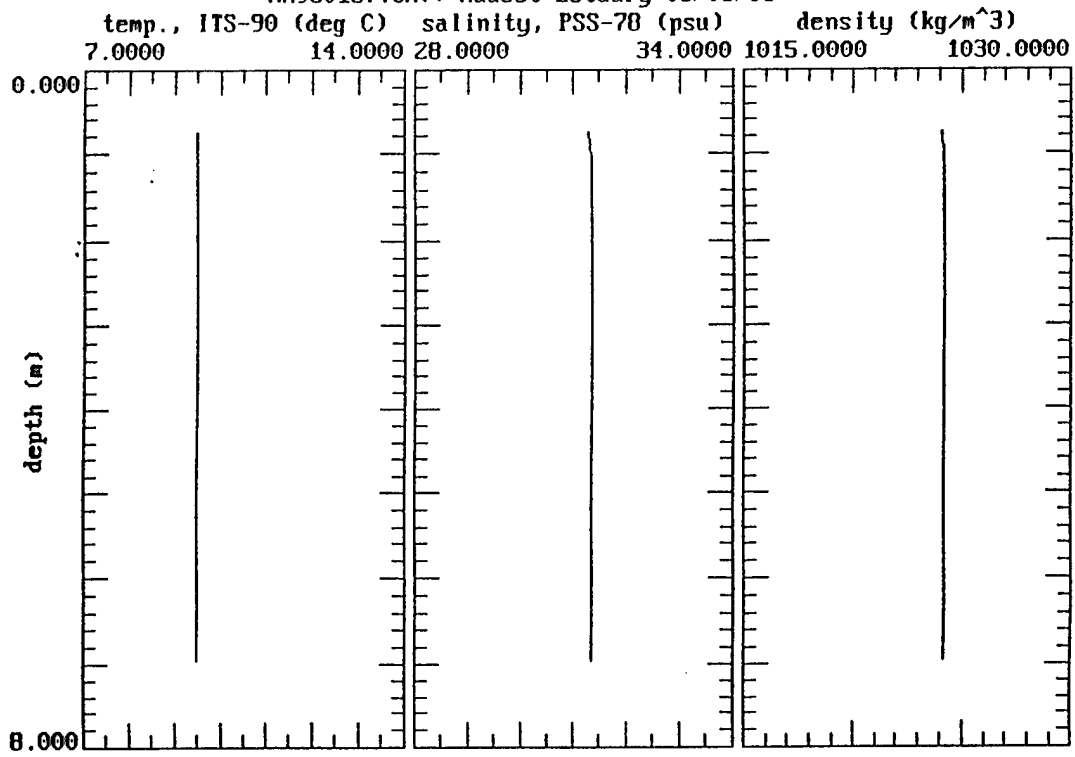
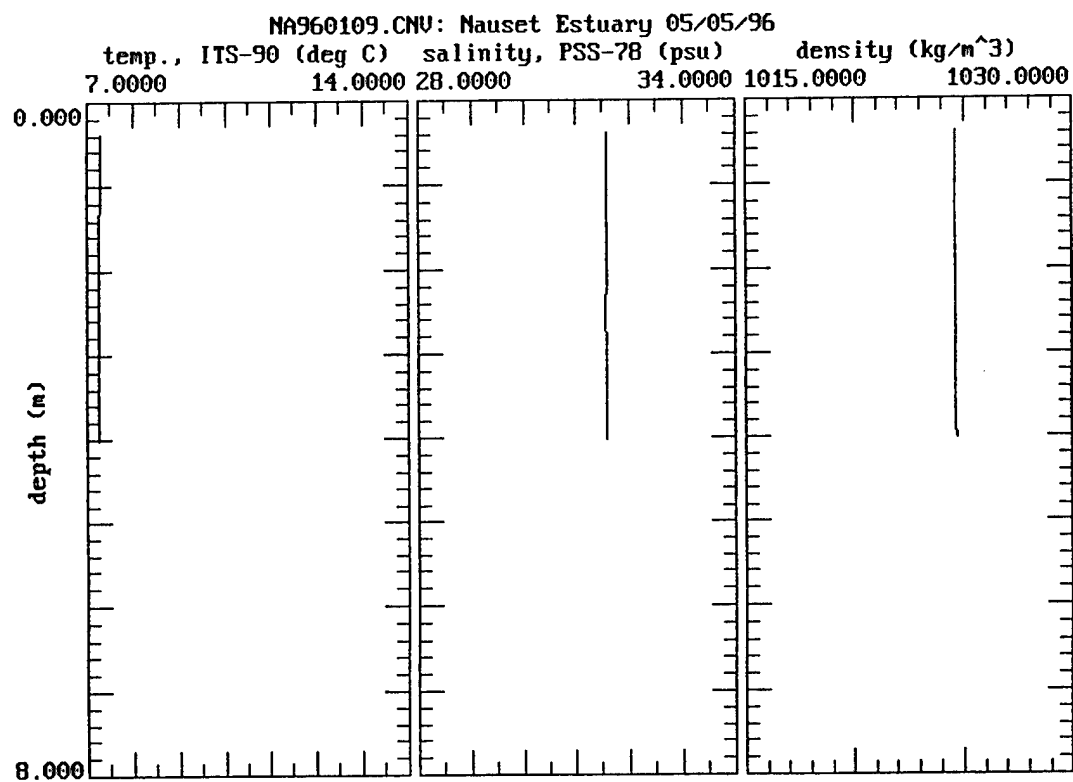
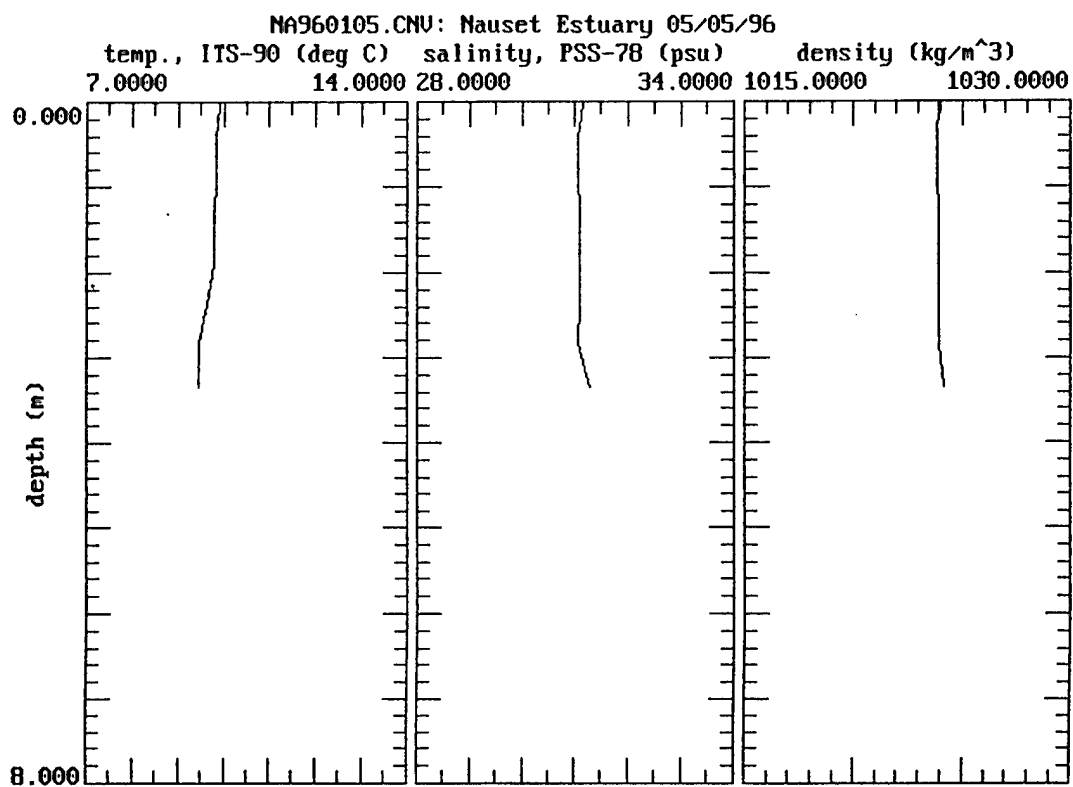
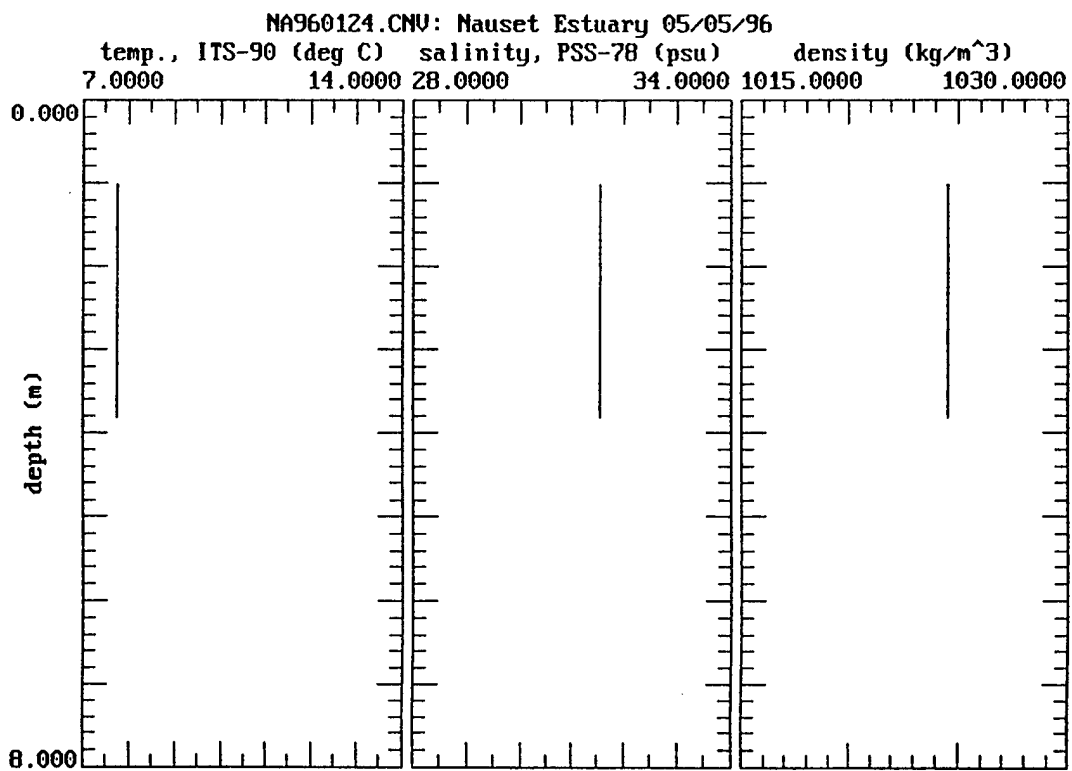
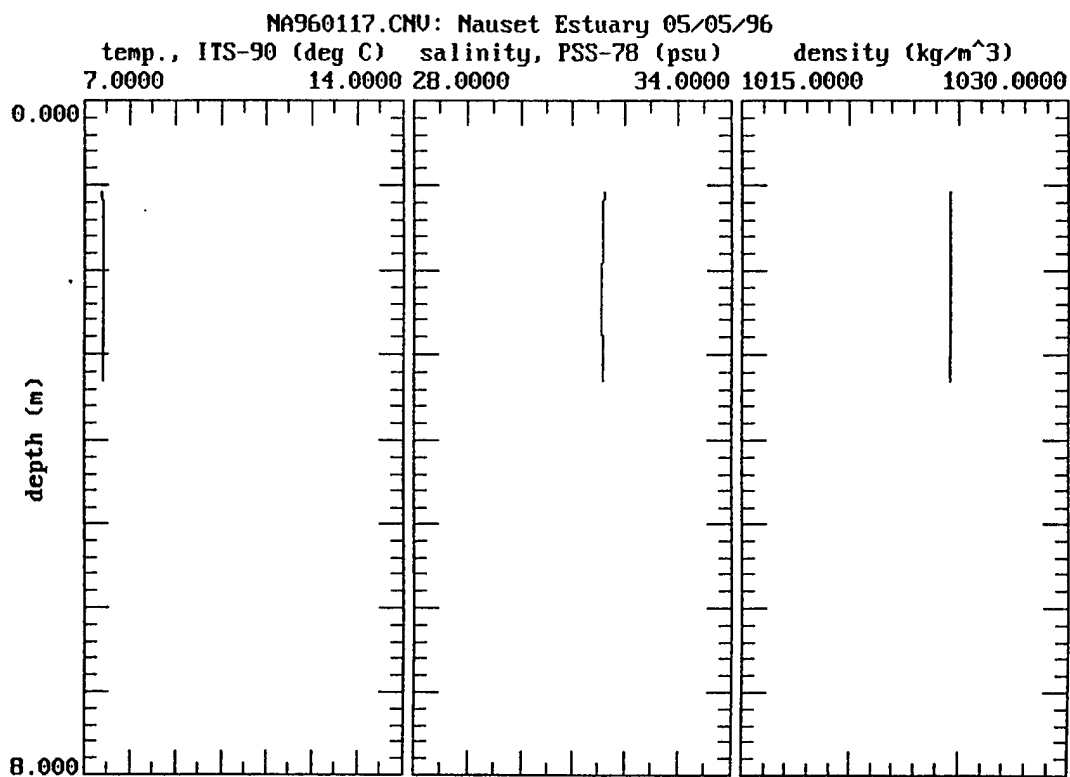
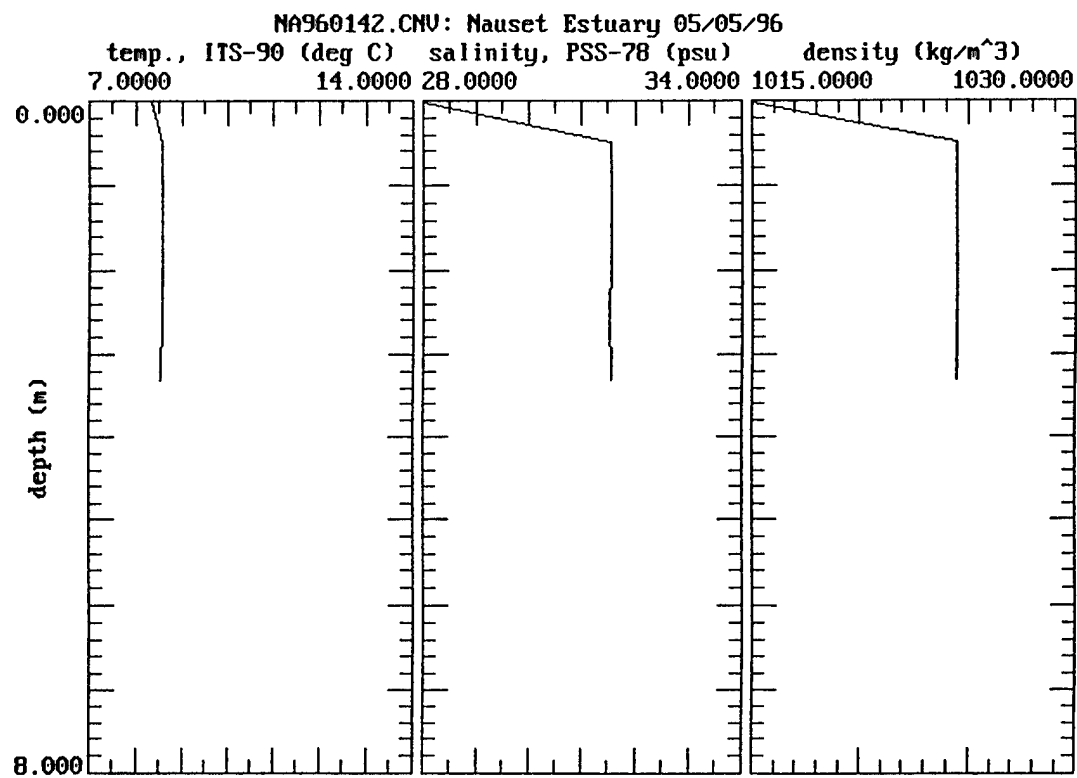
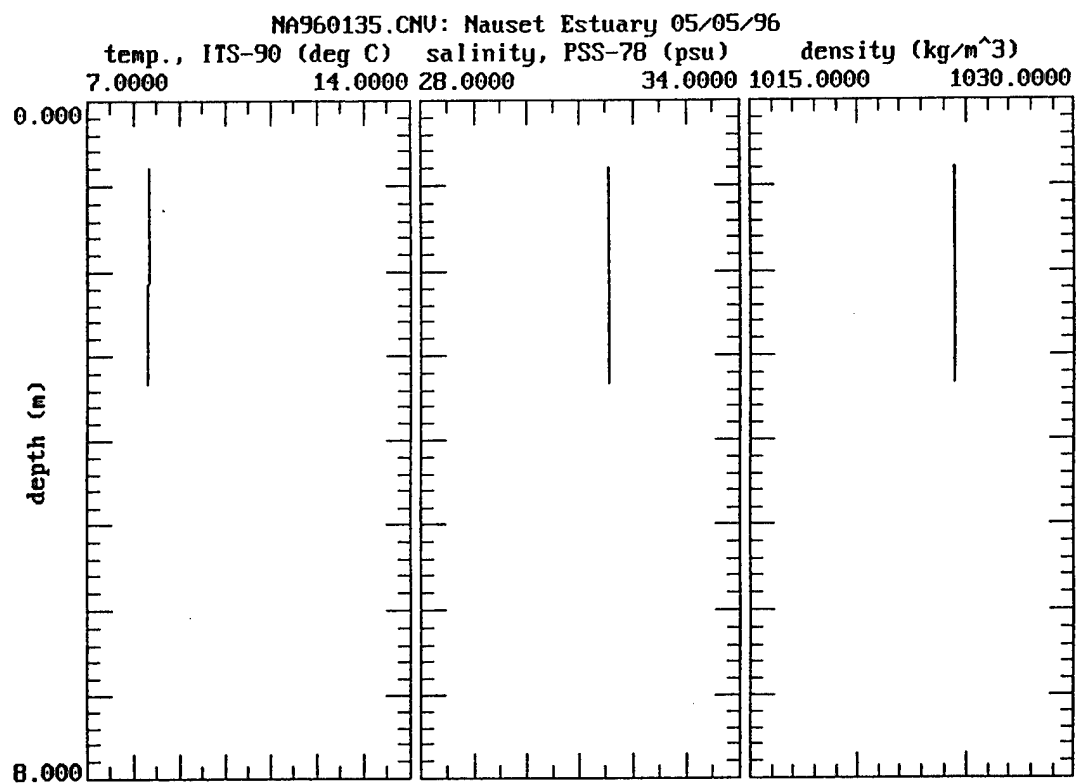


Table IV.6
Station F CTD data files
4 May 1996

Plot	Time (EST)
NA960105	08:21:56
NA960109	11:22:06
NA960117	13:08:22
NA960124	13:58:49
NA960135	15:51:25
NA960142	16:37:21
NA960149	17:13:31
NA960156	17:57:08







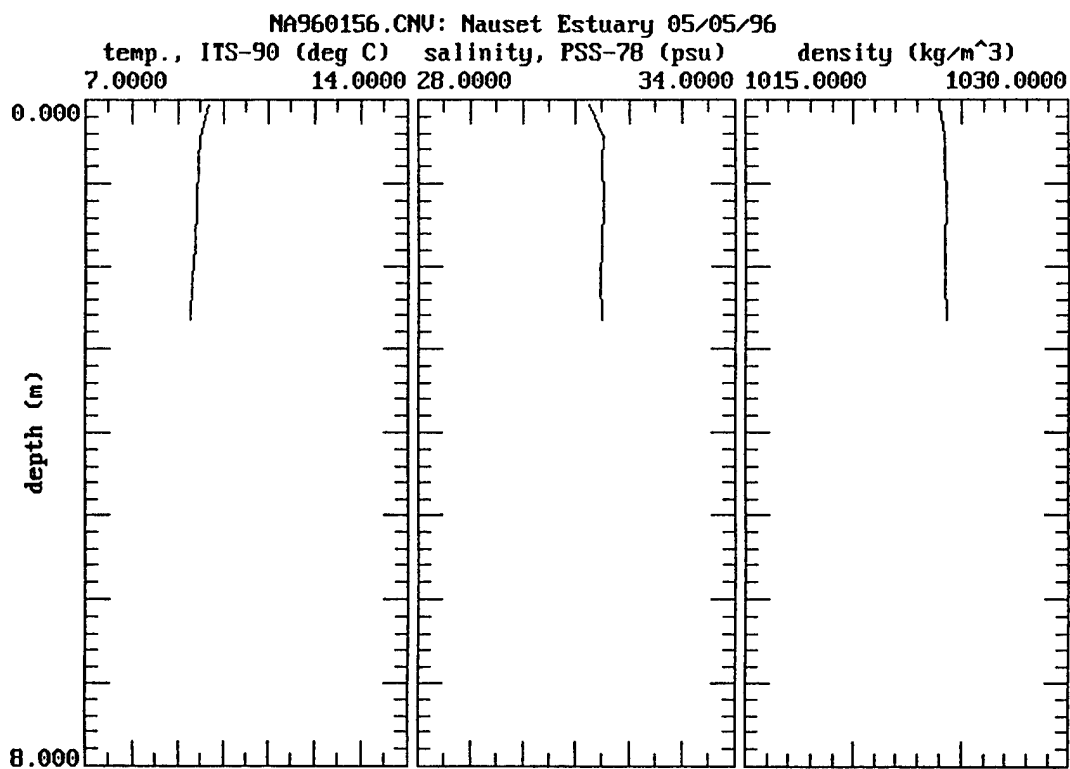
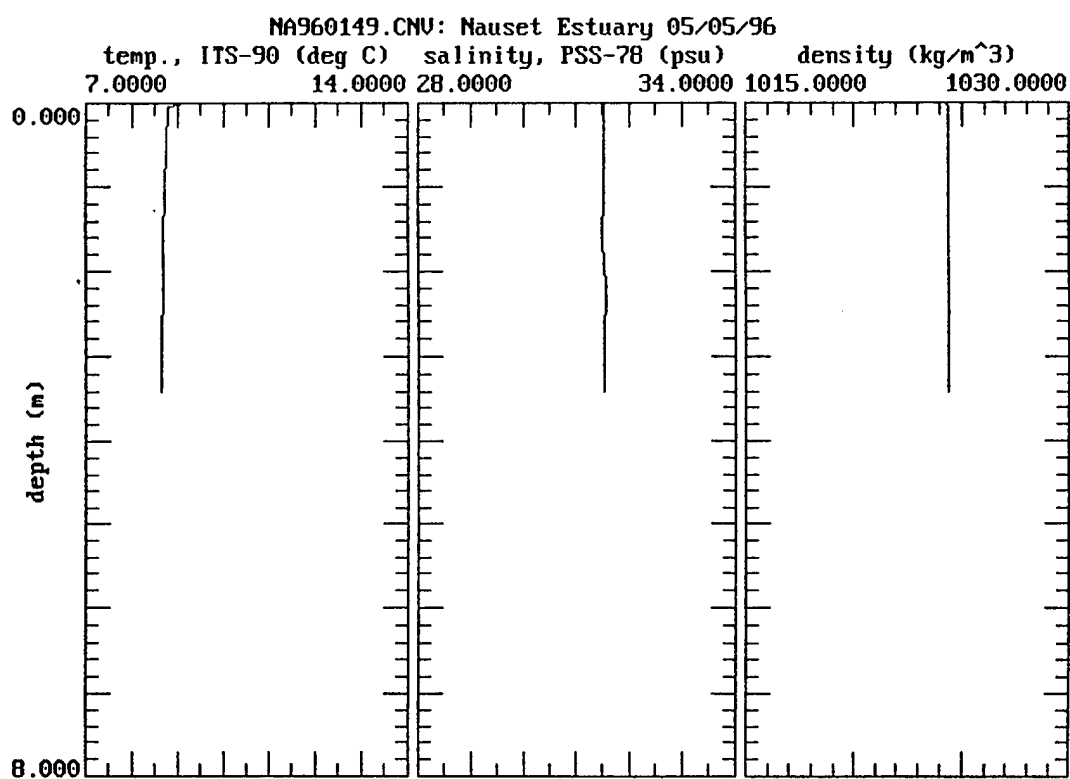
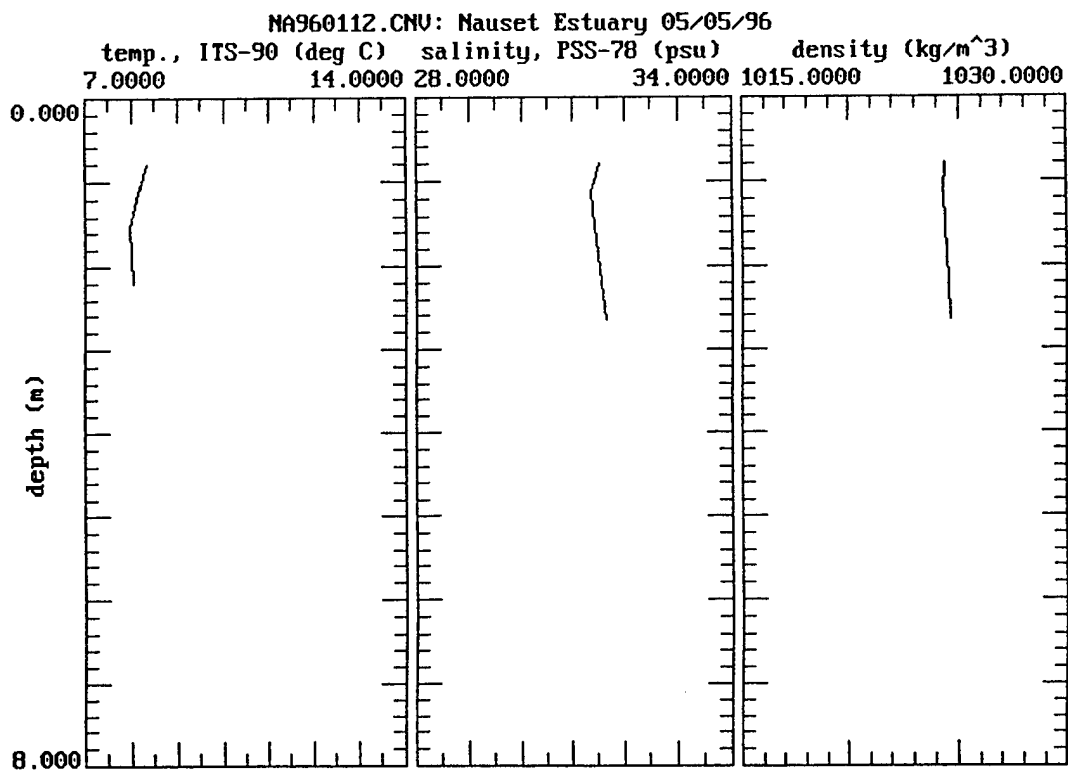
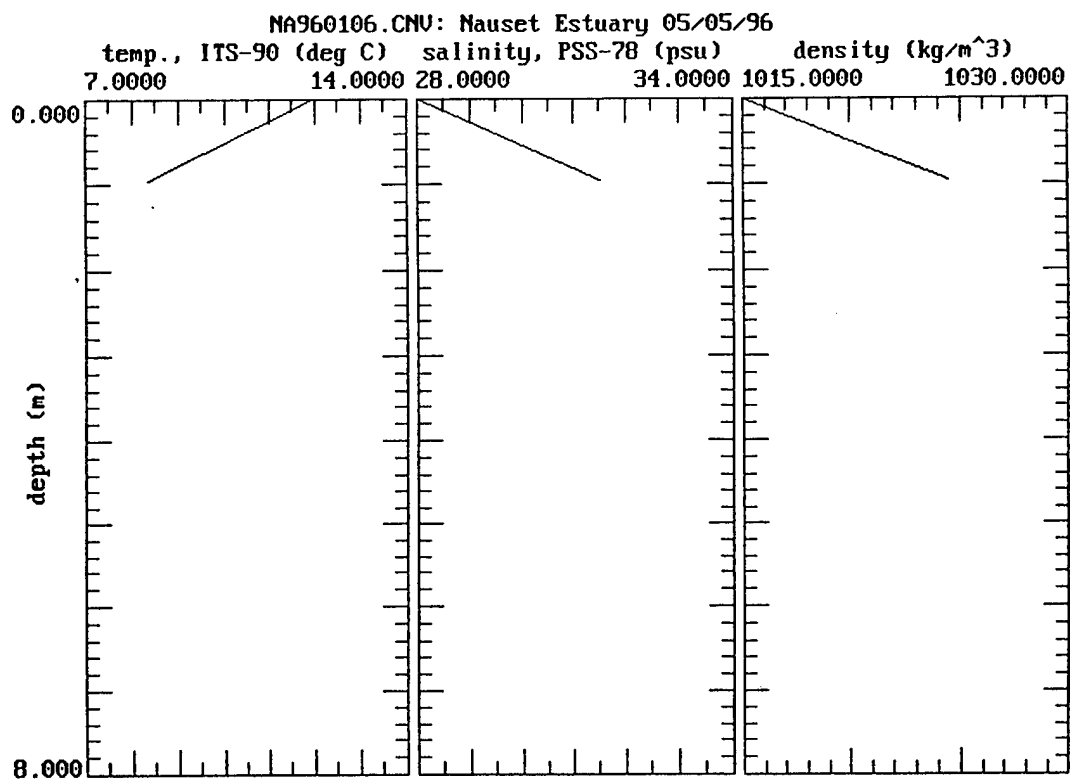
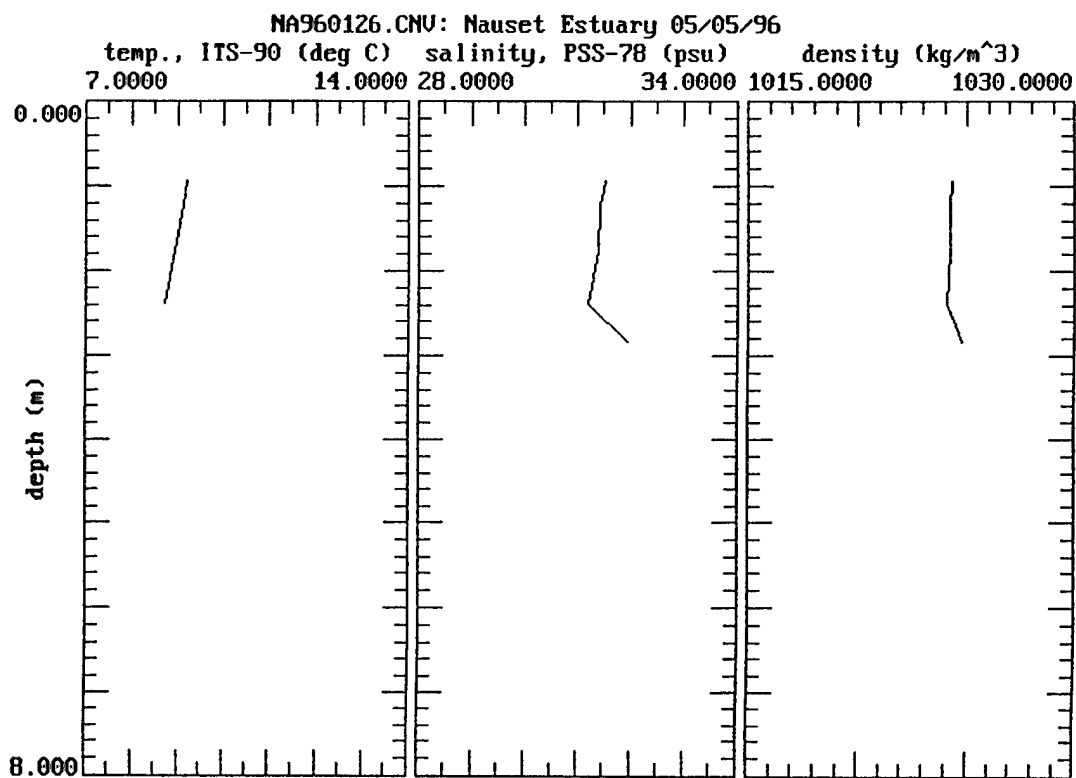
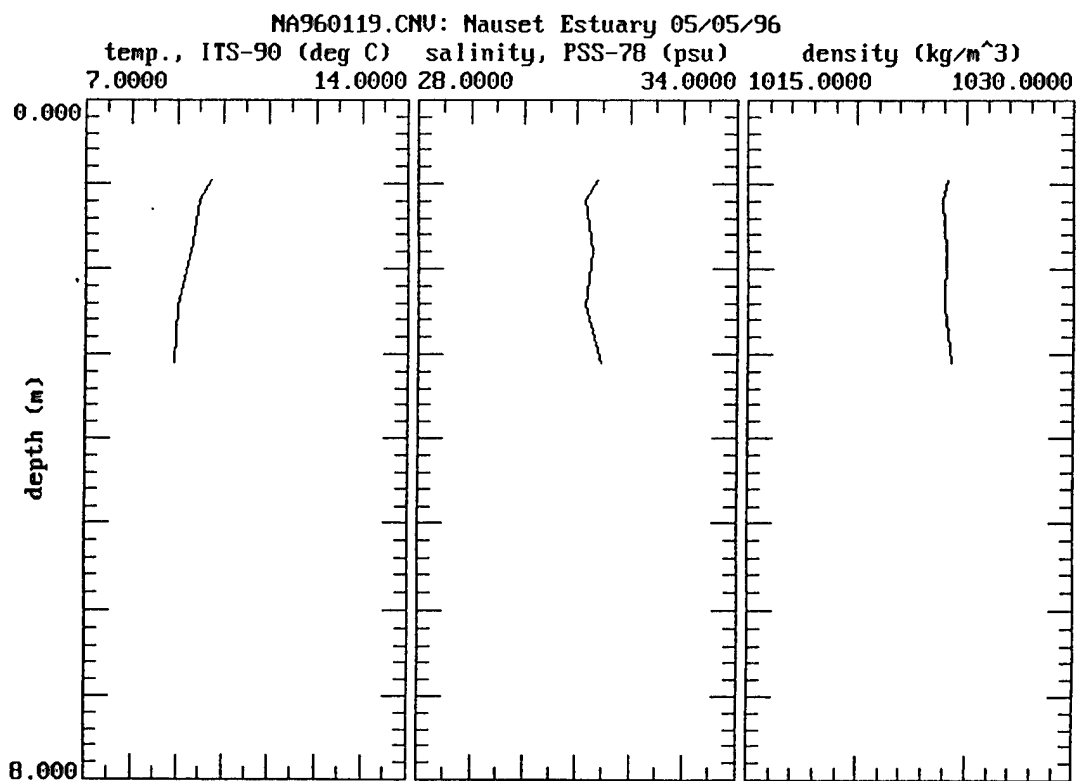
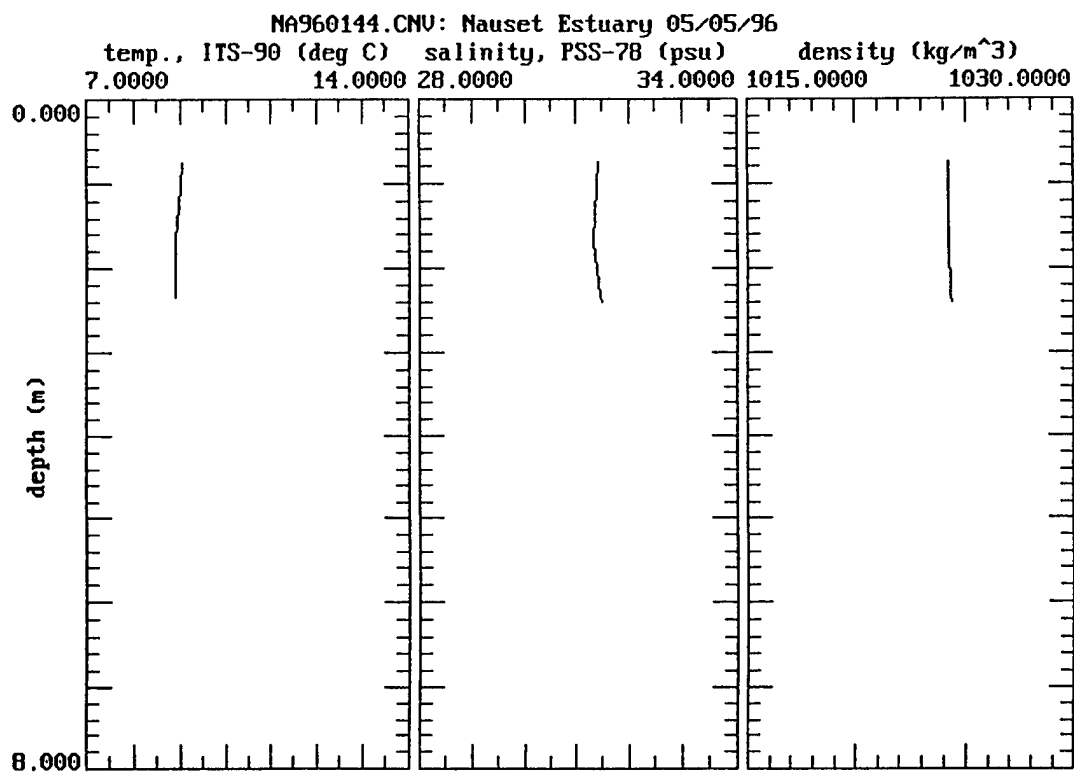
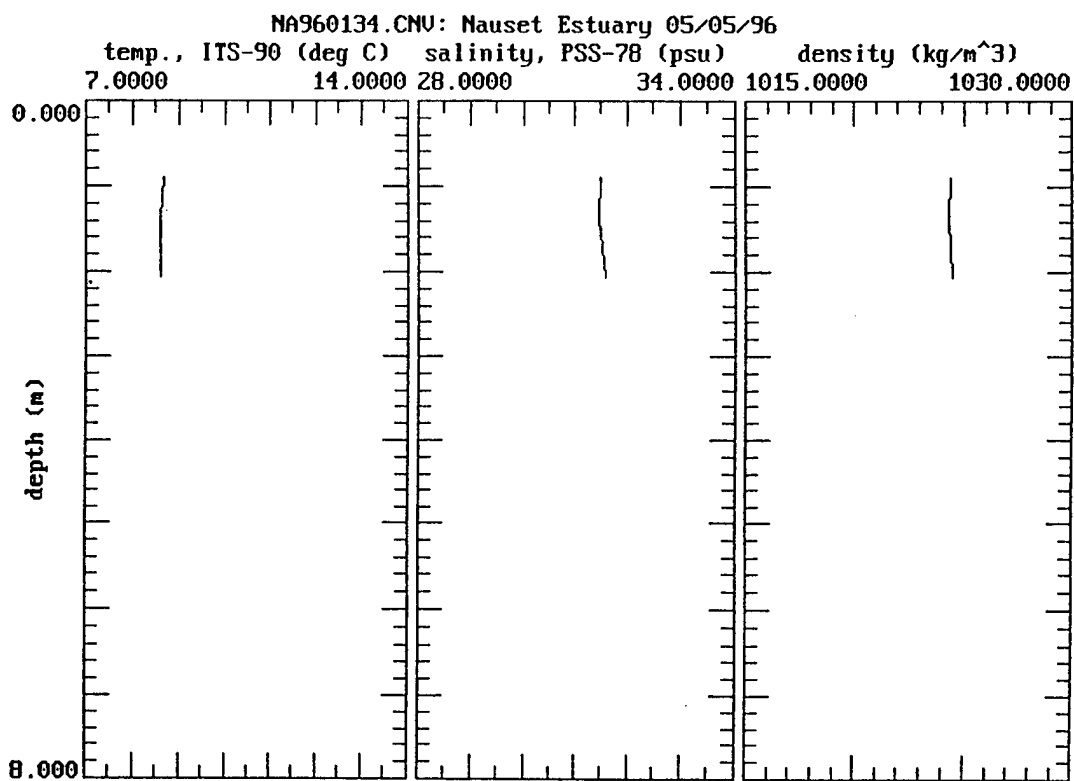


Table IV.7
Station G CTD data files
 4 May 1996

Plot	Time (EST)
NA960106	08:34:53
NA960112	11:37:12
NA960119	13:19:44
NA960126	14:09:50
NA960134	15:39:54
NA960144	16:46:57
NA960151	17:21:05







NA960151.CNV: Nauset Estuary 05/05/96

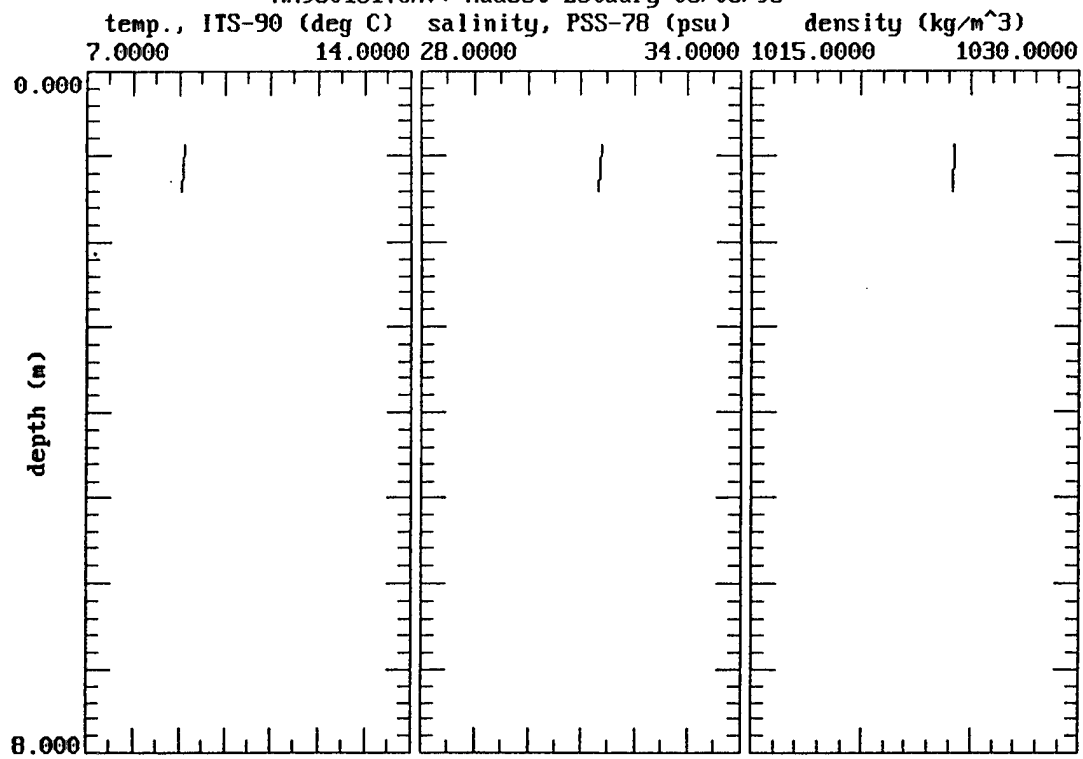
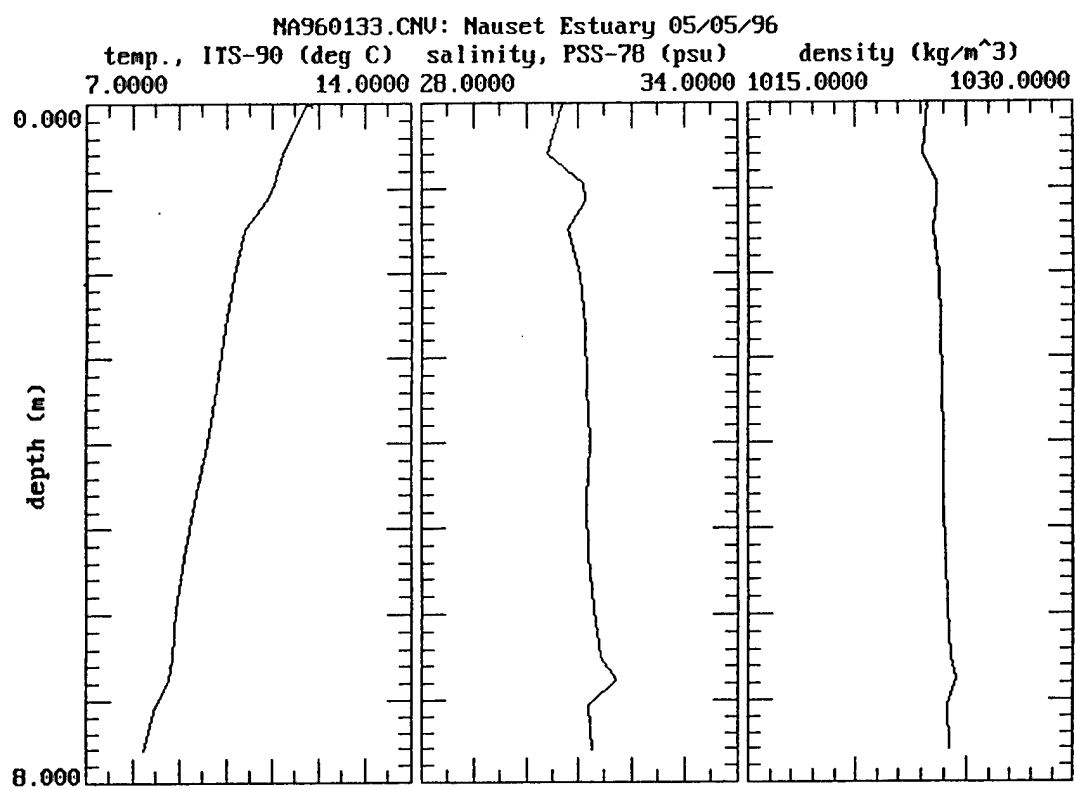


Table IV.8

Mill Pond CTD data files

4 May 1996

Plot	Time (EST)
NA960133	15:25



DOCUMENT LIBRARY

Distribution List for Technical Report Exchange – February 1996

University of California, San Diego
SIO Library 0175C
9500 Gilman Drive
La Jolla, CA 92093-0175

Hancock Library of Biology & Oceanography
Alan Hancock Laboratory
University of Southern California
University Park
Los Angeles, CA 90089-0371

Gifts & Exchanges
Library
Bedford Institute of Oceanography
P.O. Box 1006
Dartmouth, NS, B2Y 4A2, CANADA

Commander
International Ice Patrol
1082 Shennecossett Road
Groton, CT 06340-6095

NOAA/EDIS Miami Library Center
4301 Rickenbacker Causeway
Miami, FL 33149

Research Library
U.S. Army Corps of Engineers
Waterways Experiment Station
3909 Halls Ferry Road
Vicksburg, MS 39180-6199

Institute of Geophysics
University of Hawaii
Library Room 252
2525 Correa Road
Honolulu, HI 96822

Marine Resources Information Center
Building E38-320
MIT
Cambridge, MA 02139

Library
Lamont-Doherty Geological Observatory
Columbia University
Palisades, NY 10964

Library
Serials Department
Oregon State University
Corvallis, OR 97331

Pell Marine Science Library
University of Rhode Island
Narragansett Bay Campus
Narragansett, RI 02882

Working Collection
Texas A&M University
Dept. of Oceanography
College Station, TX 77843

Fisheries-Oceanography Library
151 Oceanography Teaching Bldg.
University of Washington
Seattle, WA 98195

Library
R.S.M.A.S.
University of Miami
4600 Rickenbacker Causeway
Miami, FL 33149

Maury Oceanographic Library
Naval Oceanographic Office
Building 1003 South
1002 Balch Blvd.
Stennis Space Center, MS, 39522-5001

Library
Institute of Ocean Sciences
P.O. Box 6000
Sidney, B.C. V8L 4B2
CANADA

National Oceanographic Library
Southampton Oceanography Centre
European Way
Southampton SO14 3ZH
UK

The Librarian
CSIRO Marine Laboratories
G.P.O. Box 1538
Hobart, Tasmania
AUSTRALIA 7001

Library
Proudman Oceanographic Laboratory
Bidston Observatory
Birkenhead
Merseyside L43 7 RA
UNITED KINGDOM

IFREMER
Centre de Brest
Service Documentation - Publications
BP 70 29280 PLOUZANE
FRANCE

REPORT DOCUMENTATION PAGE	1. REPORT NO. WHOI-97-11	2.	3. Recipient's Accession No.
4. Title and Subtitle Tidal Circulation and Flushing Characteristics of the Nauset Marsh System		5. Report Date July 1997	
		6.	
7. Author(s) David G. Aubrey, George Voulgaris, Wayne D. Spencer		8. Performing Organization Rept. No. WHOI-97-11	
9. Performing Organization Name and Address Woods Hole Oceanographic Institution Woods Hole, Massachusetts 02543		10. Project/Task/Work Unit No.	
		11. Contract(C) or Grant(G) No. (C) (G)	
12. Sponsoring Organization Name and Address Town of Orleans, the National Park Service and the Andrew W. Mellon Foundation		13. Type of Report & Period Covered Technical Report	
		14.	
15. Supplementary Notes This report should be cited as: Woods Hole Oceanog. Inst. Tech. Rept., WHOI-97-11.			
16. Abstract (Limit: 200 words) <p>Various interested bodies (i.e., National Park Service, Cape Cod Commission, and the Town of Orleans) charged with management of the Nauset Marsh system on Cape Cod, Massachusetts, commissioned a study of the estuarine circulation within the Nauset system. Recent significant morphological changes in the system have changed mixing processes and residence times for the embayment. This study specifically addressed the differing water circulation and residence times arising from a migrating single inlet (dominant condition) and dual inlet (1992-1996) situations. These residence times are to be used by the Cape Cod Commission to identify nitrogen-sensitive sub-embayments based on various assumptions of build-out and nutrient loading. The Nauset Marsh system has experienced considerable development in recent years; proper management of this resource area requires knowledge of the consequences of such development.</p> <p>This study provides a defensible basis for evaluating nutrient loading and potential eutrophication arising from development in the watershed around Nauset embayment. However, since morphological changes occur on a rapid basis in this area, the issue of residence time should be re-examined periodically. For instance, rapid onshore migration of the southern barrier beach is threatening closure of the south channel, a condition which could adversely affect water quality in Nauset Harbor in the near future. A process should be established to examine the sensitivity of residence times for rapidly changing morphology.</p>			
17. Document Analysis a. Descriptors tidal flushing water quality numerical modeling b. Identifiers/Open-Ended Terms c. COSATI Field/Group			
18. Availability Statement Approved for public release; distribution unlimited.		19. Security Class (This Report) UNCLASSIFIED	21. No. of Pages 124
		20. Security Class (This Page)	22. Price